A thesis submitted to the University of Strasbourg in order to obtain a PhD degree in Life Sciences (Molecular and cellular aspects of biology)

Tissue-specific pathologies induced by two RNA viruses in *Drosophila melanogaster*

Stanislava CHTARBANOVA

Public defense
September 19th 2011

Committee members

Prof. Francis JIGGINS (external reviewer)
Prof. Mika RÄMET (external reviewer)
Prof. Philippe GEORGEL (internal examiner)
Prof. Jean-Luc IMLER (invited member)
Dr. Charles HETRU (PhD advisor)

UNIVERSITÉ DE STRASBOURG

Tissue-specific pathologies induced by two RNA viruses in *Drosophila melanogaster*

Stanislava Chtarbanova

August 1, 2011

A thesis submitted to the University of Strasbourg

Abstract

Insects are exposed in their environment to many viruses, and these infections can have a significant economical (bee, silk worm) or medical (transmission of arboviruses such as Chikungunya and Dengue by *Aedes* mosquitoes) impact. Despite the significant advances made in recent years on antiviral immunity of insects, little is known about the pathophysiological mechanisms involved in the susceptibility to viral infections. In the course of this PhD thesis, I used the fruit fly *Drosophila melanogaster* as a model system to study the pathology induced by two RNA viruses: the *Drosophila* C virus (DCV, *Dicistroviridae*) and the Flock House virus (FHV, *Nodaviridae*).

It was previously shown that ATP-sensitive potassium channels (K_{ATP}) regulate survival in certain viral infections in *Drosophila* and mammals. In fruit flies mutation of the gene encoding the regulatory subunit of K_{ATP}, *dSUR*, is associated with reduced survival and increased viral load following FHV, but not DCV infection. This result indicates that K_{ATP} channels control FHV replication in *Drosophila*. dSUR is highly expressed in the *Drosophila* heart and I showed that FHV infects this organ. Using a combination of genetic and pharmacological approaches we showed that the K_{ATP} channels activity is related to the major antiviral mechanism, that is RNA interference. These results suggest that the efflux of potassium regulates an important component of antiviral innate immunity in the heart of *Drosophila*. Together with work performed on mice by a group of colleagues in the USA, my results indicate that cardiac K_{ATP} channels play an important and conserved role during evolution in the control of infections by mechanisms that remain to be identified.

I next compared the transcriptional response of flies infected with DCV and FHV using genome-wide microarrays. I observed that DCV infection leads to the strong repression of several hundred of genes, predominantly expressed in the midgut of the fly. Many genes repressed by the DCV are also repressed under conditions of starvation, suggesting that infected flies stop feeding. However, DCV-infected flies continue to feed and gain weight compared to uninfected controls. This gain of weight is due to decreased excretion, associated with an accumulation of the food in the crop and the anterior part of the midgut. My data indicate that viral infection triggers intestinal obstruction in the anterior midgut of the fly, most probably at the level of the cardia. The results obtained during my PhD strongly suggest that the pathology induced by DCV results from the presence of the virus in a particular tissue, rather than from the adverse effect of the host's immune response.

Overall, my PhD work reveal the complexity of host-virus interactions in *Drosophila* and shows that DCV and FHV, which appear very similar at first sight, induce very different, organ-specific pathologies in *Drosophila*.

Aknowledgements

It is a pleasure to thank the many people around me who made this thesis possible.

In the first place, I would like to express my deepest gratitude to Prof. Jules Hoffmann and Prof. Jean-Marc Reichhart for accepting me in the laboratory and giving me the opportunity to work in such a good scientific environment.

I gratefully acknowledge my principal supervisor, Prof. Jean-Luc Imler. This thesis would not have been possible without your guidance, support and patience. Thank you very much for all valuable advices and contributions of time and ideas during the years I spent in your group. I appreciated a lot your support during the writing of this thesis.

I would like to sincerely acknowledge my second supervisor Dr. Charles Hetru for his support, encouragement and advice in the course of my PhD work in the laboratory.

The members of Jean-Luc's group have contributed immensely to my time in the lab and the group has been a source of friendships and collaboration. I had the grat pleasure to work with Ioannis and share with him many intersting discussions. Thank you so much for your encouragements, kindness and friendship! I would like to express my thanks to Safia, Cordula, Steffi, Dele, Barbara, Estelle and Miriam for their support, help, generosity and friendship. I wish you all the best for the future.

I would like to thank all the people who have been very helpful during the writing of my thesis including the current members of the group: Vincent, Karim, Olivier, Akira and Carine. I wish you all the best for the future and a lot of luck with your projects.

I appreciated the friendship and support of Magda, Ola, Sunny and Elie and their indispensable help during the writing of my thesis. I am grateful in every possible way to Eva, François, Jelena, Nicolas, Basti, Laurent, Ayyaz, Tochiko and all the other people from UPR9022 for their help and encouragements!

I would like to thank my family for all their love and support. And most of all for my loving, supportive and patient husband. During the final stages of this Ph.D. I immensly appreciated his encouragements. Thank you!

Contents

Abbreviations

ABC	ATP-binding cassette
AGO	Argonaute
AKH	Adipokinetic hormone
AMP	Antimicrobial peptide
Aub	Aubergine
cDNA	Complementary DNA
COP	Coat protein complex
CrPV	Cricket paralysis virus
DAP	meso-diaminopimelic acid
DAV	*Drosophila* A virus
DBV	*Drosophila* Birnavirus
DCV	*Drosophila* C virus
DD	Death domain
DFV	*Drosophila* F virus
DH31	Diuretic hormone-31
dILP	*Drosophila* Insulin-like peptide
DPV	*Drosophila* P virus
DNA	Desoxy ribonucleic acid
DREDD	Death related ced-3/Nedd2-like
dsRNA	double-stranded RNA
DTV	*Drosophila* Totivirus
DUOX	Dual oxidase
DXV	*Drosophila* X virus
FADD	Fas-associated Death Domain
FHV	Flock House virus
EB	Enteroblast
EC	Enterocyte
EE	Enteroendocrine cell
GNBP	Gram-negative binding protein
GPCR	G-protein-coupled receptors
ISC	Intestinal stem cell
IFN	Interferon
IIV 6	Invertebrate iridescent virus 6

IκB	Inhibitor of κB
IMD	Immune deficiency
IRAK	Interleukin-1 receptor-associated kinase
IRES	internal ribosomal entry site
JNK	JUN NH_2-terminal kinase
Jak	Janus kinase
Kir	Inwardly rectifying potassium channels
LTR	Long terminal repeat
MDA-5	Melanoma differentiation-associated gene 5
MyD88	Myeloid differentiation primary response gene (88)
NBD	Nucleotide binding domain
NF-κB	Nuclear factor kappa-light-chain-enhancer of activated B cells
ORF	Open reading frame
PAMP	Pathogen associated molecular pattern
PCR	Polymerase chain reaction
PGN	Peptidoglycan
PGRP	Peptidoglycan recognition protein
PI3K	Phosphatidylinositol 3-kinase
PRR	Pattern recognition receptor
qRT-PCR	Quantitative real time PCR
RdRP	RNA dependent RNA polymerase
RIG-I	Retinoic acid-inducible gene I
RLR	RIG-I-like receptor
RNA	Ribonucleic acid
RNAi	RNA interference
ROS	Reactive oxygen species
SIGMAV	Sigma virus
SINV	Sindbis virus
siRNA	Small interfering RNA
SOG	Subesophagial ganglion
STAT	Signal transducers and ativators of transcription
SUR	Sulfonylurea receptor
TAB2	TAK1-associated binding protein 2
TAK-1	TGF-β activated kinase 1
TIR	Toll/IL-1 receptor
TLR	Toll-like recptor
TNF	Tumor necrosis factor
TOR	Target of rapamycin
TotM	Turandot M
upd	Unpaired
VACV	Vaccinia virus
vir-1	Virus-induced RNA1

VSR	Viral suppressors of RNAi
VSV	Vesicular stomatis virus

Part I

Introduction

Viral diseases are a constant threat and a major cause of mortality worldwide. As obligate intracellular pathogens, viruses ultimately rely on strategies, requiring further infection and replication within naive host cells, that allow high levels of viral production and facilitate transmission. At the same time, viruses must deal with the host immune response and develop counter-mechanisms, which guarantee the success of infection. Viral infections of insects might have serious consequences for humans. Viruses can be pathogenic to beneficial insects such as the honeybee *Apis melifera* or the silkworm *Bombyx mori*, causing important economical losses. Viruses can also be transmitted to humans by insect vectors such as mosquitoes. For example, the arthropod-borne virus (arbovirus) West Nile, since its first appearance in 1999 in the United States, is responsible for the largest epidemic of human encephalitis in the US. This flavivirus transmitted by the *Culex* mosquitoes continues to be one of the most frequent causes of meningoencephalitis in North America today [Debiasi, 2011]. Therefore, the study of antiviral defenses in animals remains a priority.

To counteract infection, hosts rely on their immune defenses and it is of crucial importance for them to react immediately within the hours following infection. The innate immune system is the first line of defense against pathogenic invaders in all animal kingdom and is based on the recognition of Pathogen-Associated Molecular Patterns (PAMPs) by germline-encoded receptors, called Pattern Recognition Receptors (PRRs) [Medzhitov and Janeway, 1997]. The adaptive immune system appeared with the early-jawed vertebrates. It is characterized by genetic rearrangements of the genes encoding antigen receptors, clonal expansion of lymphocytes and production of antibodies. This allows the recognition of virtually any antigen. The adaptive immune system also has the capacity to remember the pathogens that the organism has already encountered and can mount faster and stronger response against them upon re-exposure [Janeway, 2005].

The fruit fly *Drosophila melanogaster* is a favorite model organism for studying

different biological processes. For the past two decades *Drosophila* has proved its utility as an experimental model organism to study innate immune mechanisms and has allowed researchers to make significant progress in this field. The key discovery of antimicrobial activity in the hemolymph of insects after challenge with pathogenic microorganisms led to the identification of new classes of antibiotics such as the antimicrobial peptides [Steiner et al., 1981]. Subsequently, the study of the regulation of antimicrobial peptides production allowed the discovery of molecules of immune signaling pathways conserved along evolution, such as Toll and the Toll-like receptors (TLRs) [Hoffmann, 2003], (Figure 1).

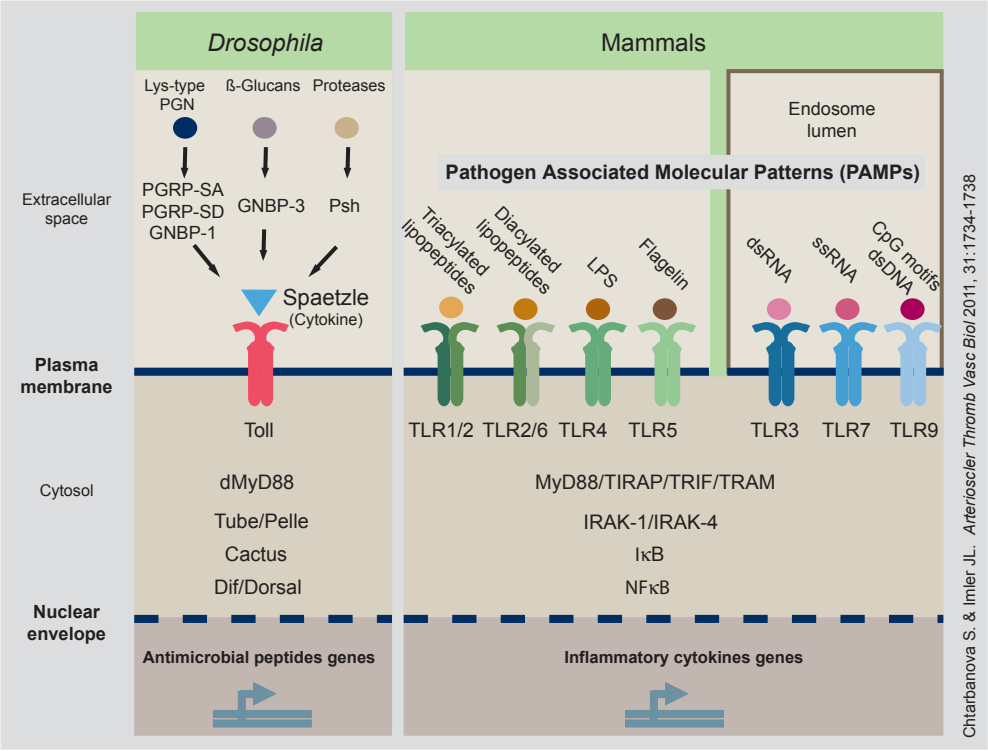

Figure 1: Schematic representation of Toll/TLR pathways in *Drosophila* and mammals . Toll and TLRs activate an evolutionary conserved signaling pathway involving the TIR domain adapters DmMyD88/MyD88, the death domain (DD) kinases Pelle/IRAK, the inhibitors Cactus/IκB and the Rel family transcription factors Dif/NF-κB . Mammalian TLRs are activated upon direct binding of microbial molecular patterns, whereas *Drosophila* Toll is activated by the cytokine Spaetzle. Detection of microbial molecular patterns or virulence factors by different sets of sensors in *Drosophila* activates a proteolytic cascade leading to Spaetzle activation.

In contrast to the large amount of information available for infection with extracellular pathogens such as bacteria and fungi, the interaction of *Drosophila*

with viruses has only been addressed recently. Several research groups in the world, including the group of Prof. Jean-Luc Imler in Strasbourg initiated the studies on antiviral defenses in flies. The availability of different viruses infecting *Drosophila* facilitated this research and a fly infection model was developed. Initial studies identified two major responses to positive-stranded RNA-viruses: the antiviral RNA interference (RNAi) [Galiana-Arnoux et al., 2006, van Rij et al., 2006, Wang et al., 2006, Zambon et al., 2006] and the inducible response contributing to the host defense [Dostert et al., 2005, Zambon et al., 2005]. However, the pathophysiology of the viral infections, as well as the host response that control the outcome of the infection remain poorly characterized.

My PhD work has focused on the understanding of the pathology caused by viral infection in the fruit fly *Drosophila melanogaster*. In the first part of this thesis, I will introduce the *Drosophila* model for viral infection, describe our current knowledge on antiviral immunity and homeostatic mechanisms contributing to the control of infections. The second part is dedicated to material and methods that were used to perform the research. In the third part, I will summarize the results I obtained during my thesis. Finally, in the fourth part I will discuss the relevance of this work and its contribution to the understanding of the complex host-virus interactions.

Chapter 1

Drosophila models of viral infection

In this chapter I will describe the viruses used to decipher the mechanisms of antiviral immunity in *Drosophila melanogaster*, including natural pathogens, as well as viruses isolated from other hosts and used to infect the fly. These viruses provide interesting experimental system allowing to analyse how the fly recognizes and controls infection caused by viral pathogens belonging to different families and having different RNA or DNA genomes. I will pay a particular attention to the dicistrovirus DCV and the nodavirus FHV, which were the major infectious agents used in the course of my PhD work.

1.1 *Drosophila* viruses: natural pathogens of the fly

1.1.1 *Drosophila* C virus (DCV)

Drosophila C virus (DCV) is the best-characterized *Drosophila* virus. DCV was originally reported in 1972 in a laboratory stock that exhibited unusually high mortality rates [Jousset et al., 1972]. DCV was later found in several laboratory stocks, as well as populations of *Drosophila* in the wild [Plus et al., 1975a,

Gateff et al., 1980]. DCV is a small, non-enveloped RNA-containing virus that shares many properties with picornaviruses. It belongs to the *Dicstroviridae* family, genus *Cripavirus*. DCV particles have icosahedral shape with 25-30 nm of diameter. The DCV genome is a single molecule of RNA of positive polarity and 9264 nt of length, which is attached at its 5' end to a small genome-linked protein (VPg), and polyadenylated at its 3' end [Jousset et al., 1977, King and Moore, 1988], (Figure 1.1). The DCV genome contains two open reading frames (ORFs). The translation of both ORFs is dependent on two internal ribosomal entry sites (IRES) located at the 5' end for ORF1 and in the intergenic region for ORF2, respectively. ORF1 codes for non-structural proteins, including a suppressor of the host antiviral RNA interference, called DCV-1A, a helicase, a protease, the VPg protein and the viral RNA-dependent RNA polymerase (vRdRp). ORF2 codes the virion capsid proteins (VP1-4). The virus-encoded protease generates these proteins from larger polyprotein precursors [Bonning and Miller, 2010].

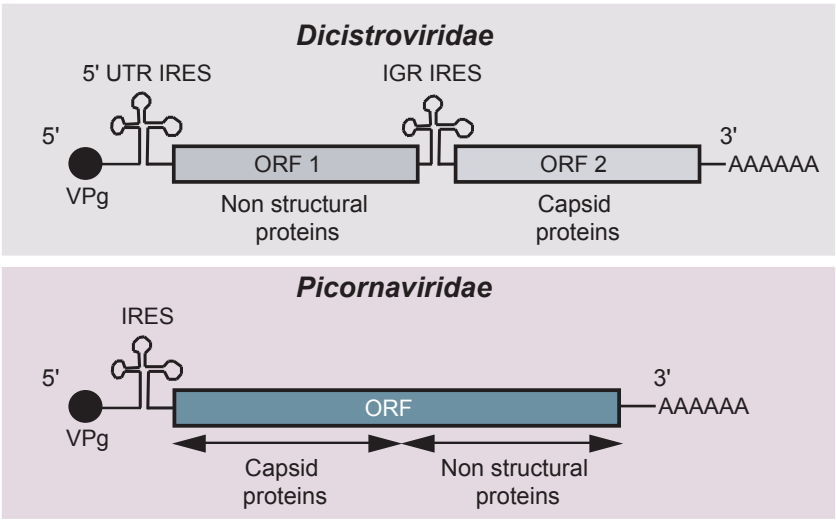

Figure 1.1: Dicistroviral and picornaviral genome organization . The genomic single stranded RNA of positive polarity is linked to the viral VPg protein at its 5' end and polyadenilated at its 3' end.The dicistroviral genome contains two ORFs encoding non-structural proteins (ORF1) and capsid proteins (ORF2). Translation of viral proteins is dependant on two IRES sites. For picornaviruses, a single ORF encodes capsid and non-structural proteins, which translation is initiated by a 5' IRES.

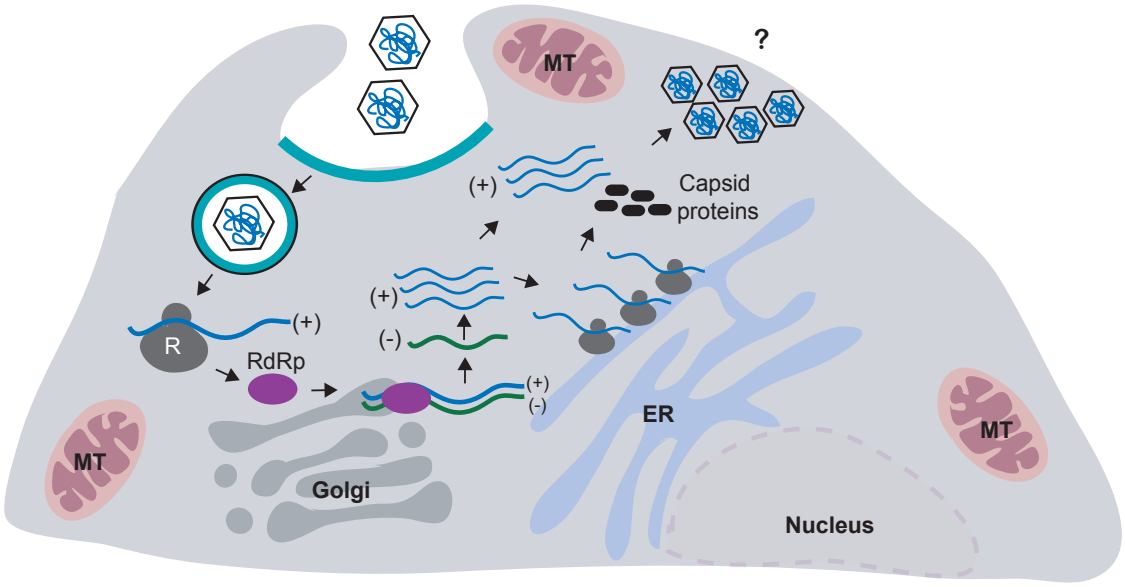

Figure 1.2: Dicistroviral replication cycle . Viral particles enter the cell via clathrin-mediated endocytosis. After uncoating, the genome RNA of positive polarity (+) is translated and the viral replicase associates with Golgi-derived vesicles. On these vesicles replication occurs via double-stranded RNA intermediates. The negative strand (-) serves as template for the production of (+) strands. Capsid proteins are translated from the accumulating (+) strands. Virions are assembled and accumulate in paracrystaline arrays in infected cells.The release of the newly formed virus occurs trough unknown mechanism. **MT**: mitochondria, **ER**: endoplasmic reticulum, **R**: ribosome, **RdRp**: viral RNA-dependant RNA polymerase.

The replication of DCV starts by the uptake of the viral particles by the host cell through clathrin-mediated endocytosis [Cherry and Perrimon, 2004]. After entry and uncoating, the virus genome is translated, and then replicated. The positive-strand RNA viral genome is used as a template for viral proteins synthesis and is highly sensitive to the availability of ribosomes within the host's cell [Cherry et al., 2005]. Typically, positive-strand viral RNA replication occurs in association with membrane rearrangements of the cell, called replication factories [Novoa et al., 2005]. For example, the picornavirus Poliovirus (PV) reorganizes the endoplasmic reticulum (ER), Golgi apparatus, and lysosomal membranes into 50-500 nm of diameter vesicles, associated with RNA replication. The PV-induced vesicles are linked to the coat protein complex II (COPII), which mediates the anterograde transport from ER to Golgi in the cell [Rust et al., 2001]. The replication of the picorna-like virus DCV was shown to take place in Golgi ap-

paratus derived vesicles, involving the fatty acids biosynthesis pathway and the host coat protein complex I (COPI), but not COPII [Cherry et al., 2006], (Figure 1.2). Following RNA replication, the DCV genome and viral proteins assemble into virus particles. However, the exact mechanism of DCV particles assembly and their release from infected cells remain poorly characterized.

1.1.2 SIGMA virus (SIGMAV)

SIGMAV is a rhabdovirus, belonging to the same family as the Vesicular Stomatitis virus (VSV) (see subsection 1.2.3) and Rabies virus (RV). SIGMAV is an enveloped, bullet-shaped virus, carrying a single, negative-stranded RNA genome. SIGMAV occurs naturally in several *Drosophila* species, and is maintained in fly populations via vertical transmission. In natural populations, infected eggs show reduced viability and a slight reduction of flies survival over winter is observed [Fleuriet, 1981]. After exposure to CO_2, SIGMAV-infected flies remain irreversibly paralyzed and die, whereas non-infected flies recover from the CO_2 exposure, once they are put back to fresh air. The CO_2-sensitive phenotype is possibly due to the preferential neurotropism of the virus [Ammar el et al., 2009]. Interestingly, in natural populations of *Drosophila*, several polymorphic host *loci* were identified to confer resistance to SIGMAV. The best-characterized gene is *ref(2)P*. This gene does not appear essential for development, however it is required for male fertility. Flies containing permissive alleles of *ref(2)P* are more susceptible to infection than flies deficient for the gene, suggesting that SIGMAV uses the permissive allele to infect *Drosophila* [Carre-Mlouka et al., 2007]. *Ref(2)P* encodes the orthologue of the evolutionary conserved polyubiquitination binding protein p62.

1.1.3 *Drosophila* X virus (DXV)

The name DXV reflects the enigmatic origin of this virus. Originally, DXV was identified as a contaminant in a series of experiments with SIGMAV. In uninfected group of 72 control flies, two of them turned to be sensitive to CO_2. Electron microscope analysis revealed that they were not infected with the bullet-shaped SIGMAV, but rather contained icosaedral viral particles [Teninges et al., 1979]. DXV is non-enveloped virus, with a capsid diameter of 70 nm, belonging to the *Birnaviridae* family. Its genome is bipartite and contains two molecules of double stranded RNA.

1.1.4 *Drosophila* F virus (DFV)

DFV is a reovirus, identified in laboratory stocks and natural populations of *Drosophila melanogaster*. DFV is a non-enveloped virus forming large viral particles (diameter of 60-70 nm) [Plus et al., 1975a, Gateff et al., 1980]. Its genome is composed of several fragments of double-stranded RNA [Huszar and Imler, 2008]. The replication cycle of DFV as well as the pathology associated with the infection are poorly understood.

1.1.5 Unclassified *Drosophila* viruses

Drosophila A virus

DAV was originally isolated from *Drosophila melanogaster* and classified as picorna-like virus, without detailed charcterization of the viral genome and virion structure [Plus et al., 1976, Jousset et al., 1972]. Recent studies showed that DAV virion of 30 nm of diameter contains a positive-stranded RNA genome, encoding two ORFs. The first ORF codes for RdRP, which ressembles the tetravirus and birnavirus RdRP. The second ORF encodes the capsid protein,

which assembles in a unique way. DAV was described as "unusual" RNA virus [Ambrose et al., 2009].

Drosophila P virus (DPV)

DPV was identified in laboratory stocks, as well as wild populations of flies, mostly from tropical areas. DPV was shown to kill much slower then DCV, when injected to the flies [Jousset et al., 1972, Plus et al., 1975b]. The virus, which is serologically related to iota virus isolated from *Drosophila immigrans*, can be transmitted vertically through the female germ-line. DPV has not been characterized molecularly at this stage, nor is its replication cycle is known. At this stage, DPV cannot be classified.

Nora virus

In the fruit fly *Drosophila melanogaster*, Nora virus causes persistent infection in laboratory stocks and natural populations [Habayeb et al., 2006]. Nora virus is vaguely related to dicistroviruses and its genome is composed of a single-stranded RNA of positive polarity, polyadenylated at its 3' end [Ekstrom et al., 2011]. Nora virus was proposed as a model virus to study interactions between the host and persistent pathogen. Flies with low viral titers are able to clear the infection, however the exact mechanism of this control is not known [Habayeb et al., 2009]. Nora is highly enriched in the intestine of infected flies and is transmitted via feces. Infected stocks do not show any pathological effects in laboratory conditions, suggesting that Nora is very well adapted to its host [Habayeb et al., 2009]. However, the presence of persistent Nora virus infection flies might affect the viability of flies in the wild, or in stress conditions. Clearly, it will be very interesting to study the mechanisms regulating the persistence of Nora in *Drosophila*, but also its possible contribution to the pathology caused by other infectious agents.

1.1.6 Virus discovery by deep sequencing in *Drosophila*

Recent studies have proposed a deep-sequencing-based method to discover new viruses in invertebrate organisms such as flies, nematods and mosquitoes [Wu et al., 2010a]. In the case of *Drosophila*, small RNA libraries were constructed from cultured S2 cells, then sequenced and assembled into contigs. Interestingly, the analysis of contigs identified virus-derived small RNAs from previously undescribed viruses, belonging to different families. The cultured cells were persistently infected with *Drosophila* Totivirus (DTV) and *Drosophila* Birnavirus (DBV), which genomes are composed of dsRNA and are proposed to belong to the *Totiviridae* and *Birnaviridae* families, respectively.

The deep sequencing analysis show that it remains possible to discover unknown RNA-containing viruses in *Drosophila*. So far however, no DNA viruses were isolated from *Drosophila*. Electron microscope analysis revealed the presence of viral particles forming agregates in the nucleus of enterocytes in several of our laboratory stocks (Figure 1.3). This virus has not been isolated and characterized yet. However, it is likely that it may correspond to invertebrate parvovirus, or densovirus, a family, which has not been identified in flies yet.

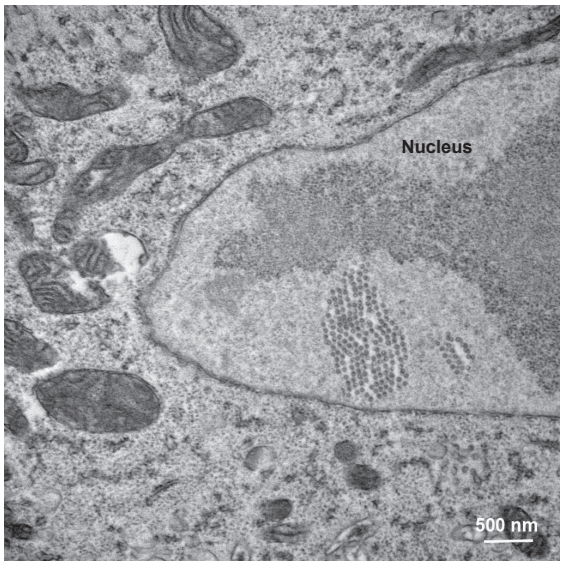

Figure 1.3: Presence of viral particles in the nucleus of *Drosophila* enterocyte
.

1.1.7 *Gypsy* and endogenous retroviruses

Retrotransposons are mobile genetic elements that replicate by reverse transcription of an RNA intermediate and integrate into the genome of host cells. Retrotransposons have been found in eukaryotes and can be divided in two families: long terminal repeat (LTR) retrotransposons and non-LTR retrotransposons. In *Drosophila*, LTR-retrotransposons typically posses 2 ORFs very similar to *gag* and *pol* genes of retroviruses. However, some LTR-retrotransposons also contain an *env*-like gene. Such retrotransposons, also known as endogenous retroviruses, belong to the *Errantiviridae* family. They are generally transmitted vertically from mother to the offspring. *Gypsy* is the best-characterized errantivirus [Bucheton, 1995], and its spreading trough *Drosophila* genome is controlled by the *flamenco* locus [Prud'homme et al., 1995]. The mechanisms that control the mobile genetic elements in *Drosophila* somatic and germline cells is addresses in section 2.1.1.

1.2 Non-*Drosophila* viruses able to infect the fruit fly

Viruses isolated from other host organisms yet able to infect *Drosophila* can be utilized as good tools for studying the basic mechanisms of antiviral immune defense and host-pathogen interactions.

1.2.1 Flock House virus (FHV)

FHV was originally isolated in 1983 from third instar larvae of the grass grub *Costelytra zaelandica*, near the Flock House Agricultural Research Station in New Zealand [Scotti et al., 1983]. The very simple genome organization of this virus and its capability to replicate in a broad range of insect hosts

[Dasgupta et al., 2003, Dasgupta et al., 2007], make FHV a highly attractive and tractable system for studies on a variety of basic aspects of virology and insect immunity. FHV belongs to the *Nodaviridae* family, genus *Alphanodavirus* and it is a small (about 35 nm in diameter) non-enveloped RNA virus, with bipartite positive-stranded genome. The two RNA molecules: RNA1 (3,1 kb) and RNA2 (1,4 kb) are co-packaged into a single virion and their combined length constitutes one of the smallest genomes of all animal viruses. The 5' end of the two RNA molecules is capped, but not polyadenylated. RNA1 contains one ORF for the synthesis of the highly multifunctional protein A. Protein A contains a N-terminal transmembrane domain, targeting the outer mitochondrial membrane, a RdRp domain necessary for the amplification of both genomic RNA strands, as well as the subgenomic RNA (RNA3) [den Boon et al., 2010]. The 3' end of RNA1 produces a subgenomic RNA (RNA3) in infected cells. RNA3 codes the protein B2, a potent supressor of RNA interference in the infected host (see below). Finally, RNA2 encodes the precursor of the capsid protein α [Venter and Schneemann, 2008]. The genomic organization of FHV is shown on (Figure 1.4).

Like all RNA viruses, FHV replication occurs in replication factories, which assemble on mitochondria of infected cells (Figure 1.5). Three-dimensional imaging by electron microscope tomography revealed that FHV induces the formation of $\cong$50 nm diameter spherule-like vesicles between the inner and outer mitochondrial membranes. Protein A and the newly synthesized RNAs accumulate inside these vesicles. Each replication complex sequesters the replicase protein A and negative-sense RNAs (RNA (-))that serve as templates for the production of abundant positive-strand genomes (RNA (+)). RNA (+) are then exported to the cytoplasm of the cell for translation and encapsidation into virions [Kopek et al., 2007]. The efficient replication of FHV RNAs and the formation of new viral particles are highly dependant on the expression of B2. The B2 role in the suppression of the host defense mechanism RNA interference will be discussed in detail in

subsection 2.1.3. Studies in cultured *Drosophila* S2 cells suggested a role of the heat-shock protein 90 (HSP-90) in the establishment of FHV RNA replication complexes [Kampmueller and Miller, 2005]. However, additional studies demonstrated that Hsp90 is neither required for the post-translational modification of this protein nor for its subcellular targeting [Castorena et al., 2007]. Instead, Hsp90 was shown to be required for the efficient translation of protein A by a yet unidentified mechanism.

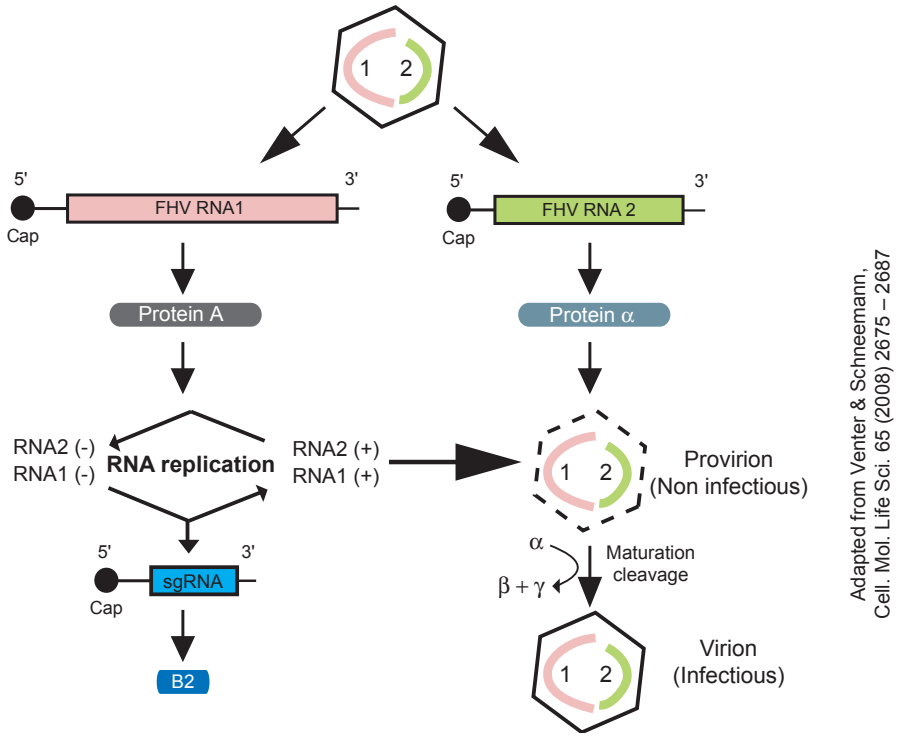

Figure 1.4: FHV genome organization and replication strategy .

Subsequent to their synthesis in the mitochondrial spherules, the two genomic RNAs of FHV are incorporated together into provirion particles formed by the single protein α. The production of mature virions is dependant on the autocatalytic cleavage of protein α into proteins β and γ, which confer physicochemical stability to the viral particle [Venter and Schneemann, 2008]. Studies in *Drosophila* DL-1 cells showed that infection with FHV leads to caspase-dependant cell death [Settles and Friesen, 2008]. Virus-induced apoptosis might represent adaptive

strategy for the release of infectious particles and their dissemination to neighboring cells [Best, 2008].

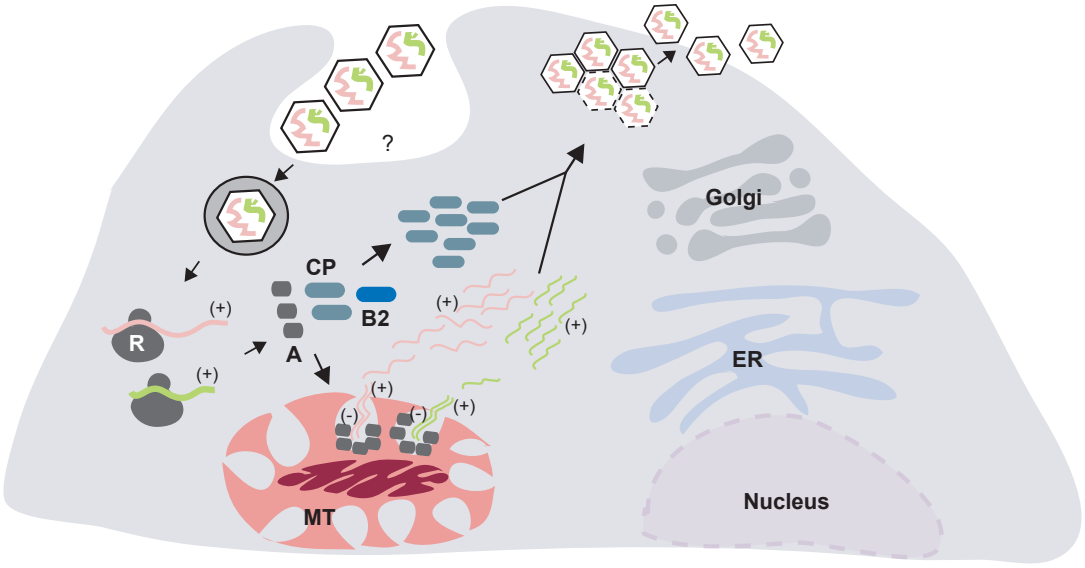

Figure 1.5: FHV replication cycle . Schematic representation of FHV infection cycle. Viral particles enter the cell via unknown receptor. After uncoating, the genome RNAs (+) are translated into protein A, capsid protein and B2. Protein A replicase associates with mitochondria into the virus-induced spherules and sequester the (-) starnded RNAs, which serve as template for the production of (+) strands. The capsid proteins and the newly synthesized (+) RNAs form provirions and infectious particles. The newly formed virus is then released from the cell. **MT**: mitochondria, **ER**: endoplasmic reticulum, **R**: ribosome, **A**: protein A, CP: capsid protein

1.2.2 Sindbis virus (SINV)

SINV is an arbovirus, originally discovered in the mosquito *Culex univittatus* in 1952 in Egypt. SINV is a member of a large group of viruses of medical and economical importance: the Alphaviruses, belonging to the *Togaviridae* family. Alphaviruses are transmitted by mosquitoes and mainly infect vertebrate hosts, including humans. SINV is enveloped virus and contains a single molecule of positive-stranded RNA of 11,7 kb, capped at its 5' end and polyadenylated at its 3' end [Strauss and Strauss, 1994]. SINV was shown to cause neuronal infection in mice and serves as model system for the study of the pathogenesis of alphavirus-induced encephalomyelitis [Griffin, 1976, Jackson et al., 1987]. After injection

of viral suspension, SINV is able to replicate within *Drosophila* and depending on the injected dose could also kill or not its host [Galiana-Arnoux et al., 2006, Saleh et al., 2009].

1.2.3 Vesicular Stomatitis virus (VSV)

VSV is an arbovirus that primarily infects rodents, cattle, swine and horses causing acute disease. VSV can also infect humans and other species, including flies. VSV is member of the *Rhabdoviridae* family and its genome is a single-stranded RNA molecule of negative polarity. VSV is a good model virus for studying the properties of rhabdoviruses and its potential as vaccine vector has been addressed [Lichty et al., 2004]. For example inocculataion of VSV expressing the influenza hemaglutinin (HA) protein was shown to prevent mice from influenza challenge [Roberts et al., 1998].

1.2.4 Cricket paralysis virus (CrPV)

CrPV was originally isolated from the Australian field crickets *Telleogrylus oceanicus* and *Teleogryllus commodus*. Some early-instar nymphae of these species, which developed a paralysis of hind legs, became uncoordinated and died [Reinganum C, 1970]. CrPV belongs to the *Dicistroviridae* family and its genome organization shares high homology with that of DCV (see Figure 1.1). CrPV contains two IRESs that mediate cap-independent protein syntheis and provide a remarkable example of molecular mimicry [Costantino et al., 2008]. Recent studies in cultured *Drosophila* S2 cells showed that CrPV infection at higher temperature (37°C instead of 25°C) resulted in increased viral RNA and protein production [Cevallos and Sarnow, 2010]. Although the virus was isolated from crickets, it has a wide range of hosts including insects belonging to the orders

Diptera, *Hymenoptera*, *Lepidoptera* and *Orthoptera*. CrPV replicates in cultured *Drosophila* cells and is pathogenic when injected into flies [Wang et al., 2006].

1.2.5 DNA viruses

DNA viruses such as baculoviruses, ascoviruses or iridoviruses can also infect insects. As was mentioned before, no DNA viruses were isolated from *Drosophila* so far. Attempts were made to infect flies with DNA viruses. The baculovirus *Autographa californica* multinucleopolyhedrovirus (Ac*M*NPV) was shown to efficiently enter cultured *Drosophila* DL-1 cells. However, the entry of the virus and the early gene expression triggers apoptosis, making these cells non-permissive for the virus [Lannan et al., 2007]. *Drosophila* cultured DL-1 cells were shown to be infectable with the DNA virus Vaccinia virus (VACV), which belongs to the *Poxviridae* family [Moser et al., 2010]. Interestingly, recent studies showed that the IIV6 iridovirus replicates efficiently in flies, as shown by the accumulation of iridescent hues, arising from the quasicrystalline arrangements of virus particles in the host [Teixeira et al., 2008, Kemp, 2011]. In the absence of DNA viruses naturally infecting *Drosophila*, IIV6 can potentially open new avenues for studying antiviral immunity against DNA viruses in the invertebrate *Drosophila melanogaster* model.

Chapter 2

Drosophila antiviral immunity

Most of the studies on *Drosophila* immunity were mainly focused on anti-bacterial and anti-fungal defenses. In the case of such infections, the innate response is dominated by a strong humoral response, in which a cocktail of potent antimicrobial peptides (Cecropins, Defensins) is secreted into the insect hemolymph by cells of the fat body (a functional equivalent of the mammalian liver). The genetic and molecular analysis of the induction of genes encoding these antimicrobial peptides resulted in the discovery of the two signaling pathways, Toll and IMD (**Im**mune **d**eficiency) [Lemaitre et al., 1995, Lemaitre et al., 1996], which activate the transcription factors of the NF-κB family (Dif and Relish, respectively). The Toll pathway is preferentially activated by fungi and Gram-positive bacteria and regulates the expression of a group of antimicrobial peptides including Drosomycin. The IMD pathway is preferentially activated by Gram-negative bacteria, and regulates the expression of antibacterial peptides including Diptericin (Figure 2.1) [Ferrandon et al., 2007]. These two signaling pathways are activated after recognition of conserved microbial patterns absent in the host, such as β-glucans or peptidoglycans abundantly present in the fungal or bacterial cell walls, respectively. Upstream of the Toll pathway, the protease Persephone can also detect microbial viru-

lence factors, such as proteases used by bacteria or fungi during the infection [El Chamy et al., 2008, Gottar et al., 2006]. The Toll and IMD pathways have many similarities with the signaling pathways activated by the Toll-like receptors and the cytokines interleukin-1 (IL-1) and tumor necrosis factor (TNF) in mammals. The discovered conservation of mechanisms of antibacterial and antifungal innate immunity during evolution stimulated the interest for antiviral immunity in *Drosophila*.

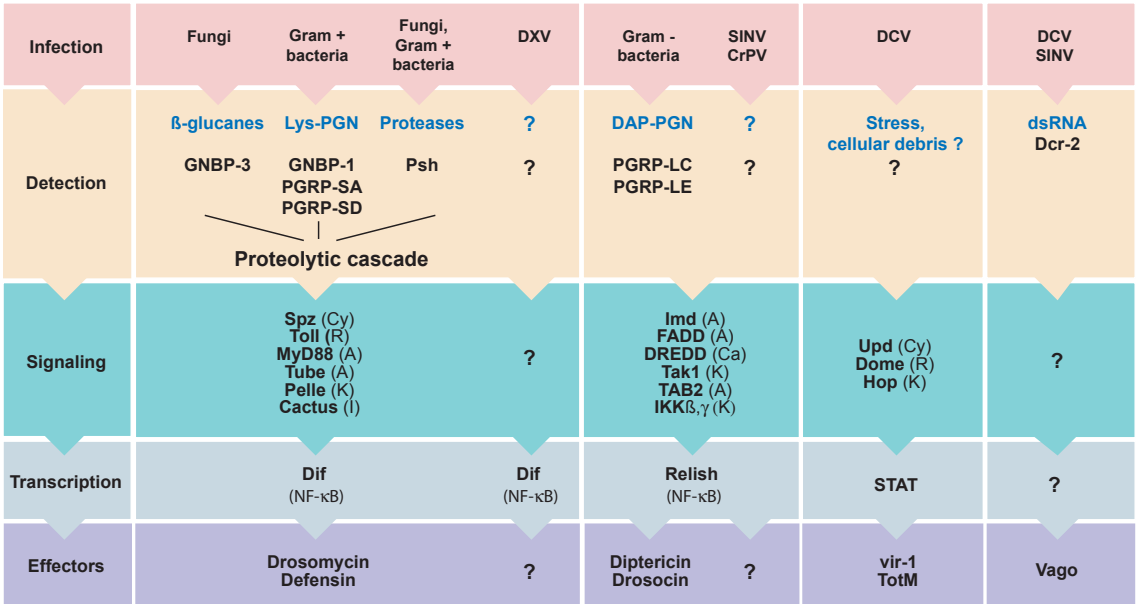

Figure 2.1: The inducible immune response pathways in *Drosophila* . The different steps of the response: from infection to the production of effector molecules (left column). Detected microbial inducers are shown in blue. Lys PGN and DAP-PGN: Lysine-type and diaminopimelic acid-type peptidoglycan, respectively. Cy: cytokine, R: receptor, A: adaptor molecule, K: kinase I: inhibitor, Ca: caspase.

As mentioned previously, the fruit fly is a host for numerous viruses, representing different families. The diversity of their genome organization (single positive- or negative-stranded RNA, double-stranded RNA or DNA) provides an interesting experimental system for the analysis of insect-virus interactions and the antiviral defense mechanisms. The studies performed on *Drosophila* with all these viruses suggest that there are two types of response to viral infection: the sequence-specific degradation of the viral RNA by the mechanism of RNA inter-

ference (RNAi) and the inducible response, characterized by the induction of a large number of genes which products may counter viral infection.

2.1 RNA interference: sequence-specific antiviral defense mechanism

In the early 1990, plant scientists have been confronted to gene silencing phenomena (reviewed in [Matzke and Matzke, 2004]), which remained enigmatic until the discovery of RNA interference (RNAi) in the roundworm *Caenorhabditis elegans* [Fire et al., 1998]. The break-through study of Andrew Fire and Creg Mello on the mechanism of RNAi, which is triggered by double-stranded RNA has revolutionized biology. The mechanism of RNAi was correlated with the production of small interfering RNAs (small RNAs) that will guide the cleavage of mRNA [Hamilton and Baulcombe, 1999, Zamore et al., 2000, Parrish et al., 2000]. This highly specific control mode is based on the base pairing between small RNAs and their targeted nucleic acids [Tomari and Zamore, 2005].

This field was extensively studied during the past decade and small RNAs were found to regulate different biological processes including host defense in organisms as diverse as plants, insects and mammals. In the model organism *Drosophila melanogaster* RNAi is based on a family of molecules called Argonaute, which interact with small RNAs and use them as a guide to identify complementary sequences in target RNAs and inhibit their translation or induce their degradation [Ding and Voinnet, 2007]. In *Drosophila*, there are five such proteins: Argonaute (AGO) -1, -2, -3, Piwi and Aubergine. They define the three pathways of RNA interference, characterized by the nature of small RNAs they guide: micro RNAs (miRNAs), small interfering RNAs (siRNAs) from endogenous (endo-siRNAs) or exogenous origin (exo-siRNAs), and the Piwi-associated RNAs (piRNAs). In the following subsection I will summarize the different RNAi pathways in

Drosophila with particular focus on the role played by the siRNAs in the control of viral infections.

2.1.1 Biogenesis and mode of action of small RNAs: three major pathways

miRNA pathway

The miRNA pathway is present from plants to humans, and can finely modulate gene expression, especially during development. In *Drosophila*, miRNAs are generated from hairpin-forming transcripts of miRNA-coding genes. These transcripts, called primary miRNAs (pri-miRNAs), are first cleaved by the RNAse III enzyme Drosha in the nucleus to release the short hairpin precursor (pre-miRNAs). Pre-mi RNAs are then exported to the cytosol, where Dicer-1 (Dcr-1) processes them into miRNAs of 22-23 nt of length. Drosha in the nucleus, and Dicer-1 in the cytoplasm are assisted by the double-stranded RNA (dsRNA) binding proteins Pasha and Loquacious-PB (Loqs-PB), respectively. The generated miRNAs are loaded into the miRNA induced silencing complex (miRISC), containing the RNAse H-like enzyme AGO1. They will subsequently guide the miRISC complex to the target mRNA, typically to its 3'-untranslated region (3'UTR). This will lead to either translational inhibition in the case of imperfect complementarities between the mRNA and miRNA, or degradation of the target mRNA in the case of perfect sequence complementarities between the miRNA and its target [Ding, 2010] (Figure 2.2A). The miRNA pathway plays an essential role during animal development and mutations in genes coding for components of this pathway are lethal.

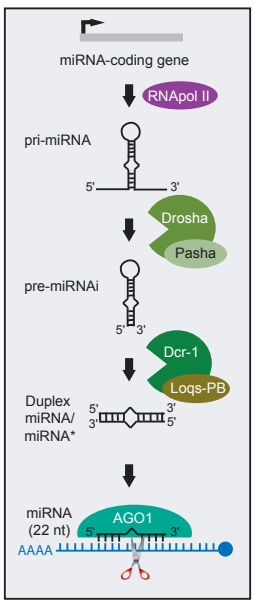

A miRNA pathway

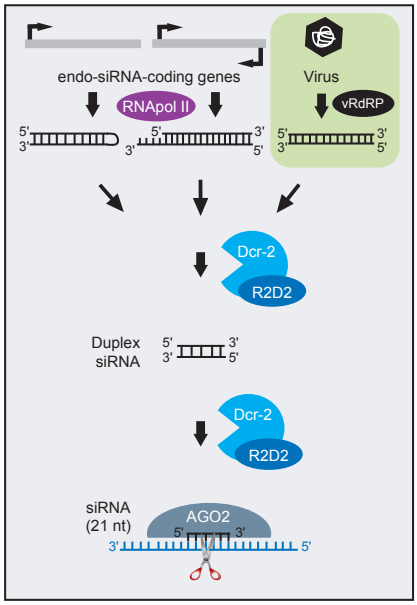

B siRNA pathway

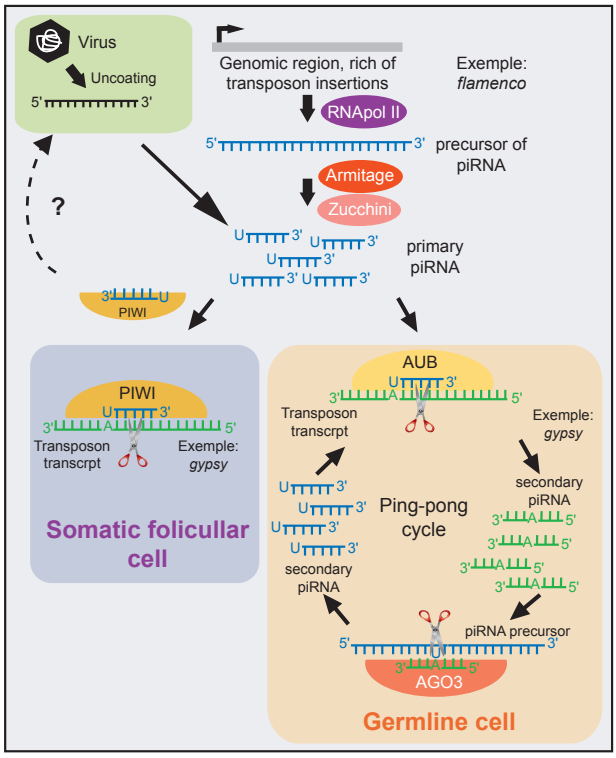

C piRNA pathway

Figure 2.2: RNA interference pathways in *Drosophila* . The mechanism of RNA interference is based on the five members of Argonaute family. These proteins are guided to their target RNA by small RNA (miRNA, siRNA and piRNA), and cleave it or inhibit its translation. The RNA that induces the mechanism and is target by it, may be of cellular origin (**A**) or viral origin (**B**, **C**). The dsRNA binding proteins Drosha, Loqs-PB and R2D2 are associated with the RNAse III enzymes Pasha, Dcr-1 and Dcr-2, respectively.

siRNA pathway

The siRNA pathway is activated by either endogenous or exogenous dsRNA and involves the enzymes Dcr-2 and AGO2. Endo-siRNAs are generated in somatic cells of *Drosophila* from transposons, structured cellular *loci* forming RNA hairpins, and overlapping regions of convergent transcripts. Deep sequencing analysis revealed that transposon-dervided endo-siRNAs map predominantly to LTR retrotransposons, but also to non-LTR retrotransposons and DNA transposons [Ghildiyal et al., 2008]. The double-stranded substrate for Dcr-2 might originate from the insertion of two transposons as inverted repeats in the genome, or the integration of a transposable element in a reverse orientation downstream of a cellular promoter, thus producing antisens transposon transcripts. Structured cellular loci are also source of endo-siRNAs and generate dsRNA structures via intramolecular basepairing. In *Drosophila* genome, several genes are in opposite orientation and generate overlapping transcripts, creating a dsRNA substrate for Dcr-2 [van Rij and Berezikov, 2009], (Figure 2.2B).

The exo-siRNAs are implicated in the degradation of viral nucleic acids and are often called virus-derived siRNAs (vsiRNAs). They are generated from the cleavage of dsRNA of viral origin by Dcr-2 with the help of the dsRNA-binding protein R2D2. The resulting siRNA duplexes of 21nt of long pair in a way that leaves a two nucleotide overhang at their 3' ends [Ghildiyal and Zamore, 2009]. One strand of the vsiRNA duplex, called the "guide" is loaded into AGO2 within the RISC complex and serves as a guide. Within this complex, AGO2 slices the target RNA. The cleavage site is situated between the positions 10 and 11 of the guide siRNA, counting from its 5' end [Sontheimer, 2005]. The vsiRNAs role in the control of viral infection is addressed in the section 2.1.2.

piRNA pathway

The piRNA pathway involves the action of the other three Argonaute proteins: Piwi, Aubergine (Aub) and AGO3. It mediates the silencing of mobile genetic elements within the germline, but also somatic cells in the ovary of *Drosophila* [Senti and Brennecke, 2010]. The biogenesis of piRNAs (26-28 nt of length) occurs through two distinct mechanisms. The first leads to the production of primary piRNAs, and the second corresponds to the “ping-pong” amplification cycle, generating secondary piRNAs. In the ovary, the follicular somatic cells express only Piwi, which binds piRNAs carrying a uridine at their 5’ ends (5’U). These piRNAs are generated from genomic regions, enriched in multiple transposon insertions (Figure 2.2C). piRNAs are processed from long RNA precursors, with the help of the helicase Armitage and the nuclease Zucchini, although the exact mechanism remains poorly understood in particular with regards to the formation of the 3’ end of the piRNA [Olivieri et al., 2010].

In the cells of the *Drosophila* germline, the expression of Aub and AGO3 contributes to the amplification loop of primary piRNAs by the “ping-pong” mechanism. Aub binds piRNAs with 5’U, whereas AGO3 preferentially binds piRNA containing an Adenosine at position 10. This observation from deep sequencing analysis of small RNAs associated with AGO3 and Aub led to the model of the "ping-pong" amplification, described below. The cleavage of transposon transcripts by Aub containing primary piRNAs generates secondary piRNAs carrying an A at position 10. The secondary piRNAs are then loaded on AGO3 and target complementary transposon transcripts. Their cleavage leads to the production of secondary piRNAs, identical to the primary piRNAs (Figure 2.2C).

The piRNA pathway controls the expression of the endogenous retrovirus *gypsy*, through the piRNAs produced from the locus *flamenco*. *flamenco* is located on the X chromosome and contains defective copies of *gypsy* and their transcription leads to the production of primary (soma and germline) and sec-

ondary (germline specific) piRNAs [Pelisson et al., 2007] (Figure 2.2C). Interestingly, recent deep sequencing studies identified piRNAs matching sequences from the DCV and FHV genomes in the OSS cell line, which is derived from *Drosophila* ovary somatic cells. This suggests that piRNAs are produced during viral infection in some tissues and play a role in the control of viral infection [Wu et al., 2010b].

2.1.2 Antiviral siRNA pathway

Null mutants for genes encoding the three essential components of the siRNA pathway, *Dcr-2*, *R2D2* and *AGO2* are susceptible to viral infections and succumb faster than wild type controls, with higher viral loads. This has been demonstrated for several RNA viruses with genomes double-stranded or single-stranded of either positive or negative polarity [Chotkowski et al., 2008, Galiana-Arnoux et al., 2006, Mueller et al., 2010, Sabin et al., 2009, van Rij et al., 2006, Wang et al., 2006, Zambon et al., 2006]. Recent studies in *Drosophila* showed that Dcr-2 also participates in the control of infection by the DNA virus IIV6 [Kemp, 2011]. This suggests that the siRNA pathway controls also DNA virus replication in flies, as previously reported in plants.

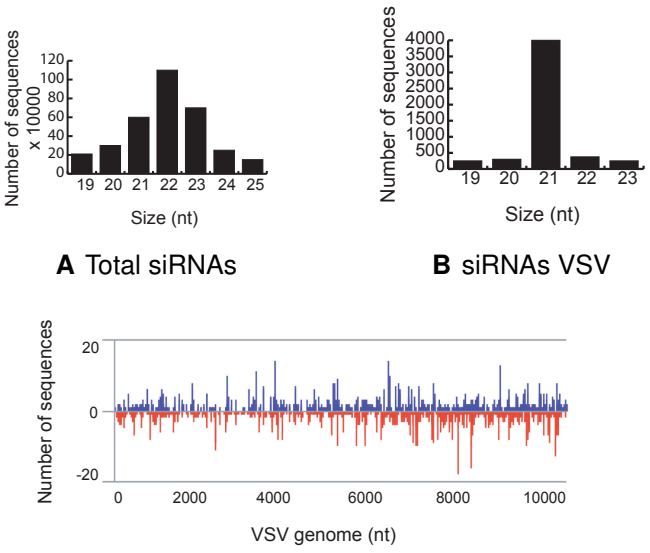

Figure 2.3: Production of siRNAs in *Drosophila* after infection with VSV . **A.** Size of total small RNAs. The size of the majority corresponds to 22-23 nt miRNAs. **B.** Size of small RNAs corresponding to the genome or antigenome of VSV. The peak at 21 nt correspond to the size of siRNAs produced by Dcr-2. **C.** Distribution of siRNAs along the sequence of the VSV. siRNAs corresponding to the genome are represented in red, while those corresponding to the antigenome are shown in blue.

Deep sequencing analysis of small RNAs produced during infection confirmed that they are mostly 21 nt long, as expected for products of the enzyme Dcr-2 [Aliyari et al., 2008, Flynt et al., 2009, Mueller et al., 2010, Wu et al., 2010b] (Figure 2.3A, 2.3B). These siRNA cover the entire viral genome and the ratio between the number of small RNA corresponding to the genome and antigenome is close to 1, confirming that they originate from double-stranded RNA, which may be formed during the replication of the virus (Figure 2.3C).

In concordance with that, it is possible to assemble contigs from sequences of siRNAs isolated from cells or flies, and to discover new latent or persistent viruses present in these samples. This interesting property allowed the development of novel approach, known as “virus discovery by deep sequencing and assembly of small RNAs” from plants or insects [Ding, 2010, Wu et al., 2010b]. The production of siRNAs is strongly reduced in Dcr-2 mutant flies, confirming the importance of this enzyme for the biogenesis of siRNAs [Mueller et al., 2010]. The siRNAs,

which are associated with AGO2, are protected from oxidative β-elimination, indicating that their 3' ends are methylated, presumably by the methylase Hen1 [Aliyari et al., 2008]. The biochemical data therefore confirm the genetic data, and suggest a model in which dsRNA formed during viral replication is recognized by Dcr-2, and then cleaved into siRNAs of 21nt. The siRNAs are then loaded into AGO2 in the RISC complex and guide AGO2 towards the viral RNAs. Through its slicer activity AGO2 cleave then the target viral RNA (Figure 2.4).

Dcr-2, R2D2 and AGO2 are the core components of the antiviral RNAi. One important question, which deserves to be addressed, is whether additional factors are involved in the control of the antiviral siRNA pathway. Recent studies identified the evolutionary conserved protein Ars2 as required for the efficient function of Dcr-2 in the processing of long dsRNA [Sabin et al., 2009]. Flies with reduced Ars2 expression succumbed more rapidly to infection with DCV, FHV, SINV and VSV.

In addition to its function as dsRNA binding protein in the endosiRNA pathway, the isoform PD of Loquacious (Loqs-PD) was suggested to play a role in the siRNA pathway activation from exogenous sources [Marques et al., 2010]. The injection of dsRNA against *bicoid* (*bcd*) in *Loqs* mutant embryos failed to silence *bcd* mRNA. However, the implication of Loqs-PD in the vsiRNA pathway has not been demonstrated yet.

Initially it was believed that systemic antiviral RNAi was present in plants and *C. elegans*, but not in *Drosophila* [Ding and Voinnet, 2007, Roignant et al., 2003]. Recent studies showed that cells lysed during infection may release dsRNAs which, when uptaken by uninfected cells, can induce the RNAi mechanism and confer protection against a subsequent challenge with this virus [Saleh et al., 2009] (Figure 2.4).

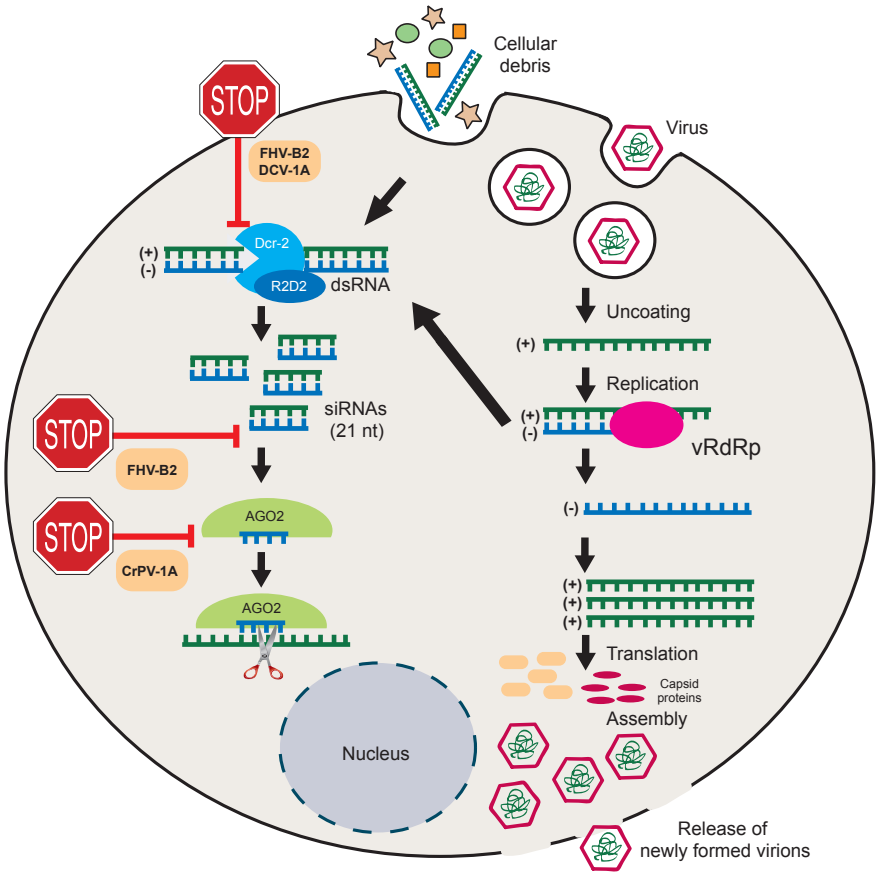

Figure 2.4: Control of viral infection by siRNA pathway . The viral suppressors of RNA interference (VSR) FHV-B2, DCV-1A and CrPV-1A act at different levels to disrupt the action of Dcr-2 and AGO2.

2.1.3 Viral suppressors of RNAi

Viruses defend themselves against the mechanism of RNA interference by expressing suppressors, named VSRs (for Viral Suppressor of RNAi). Originally VSRs were identified in plant viruses, but these suppressors are also present in the genomes of insect viruses. Up to now three of them were characterized: FHV-B2, DCV-1A and CrPV-1A (Figure 2.4).

An efficient way to counteract the siRNA-mediated silencing is to prevent the binding and the cleavage of dsRNAs by Dcr-2, and the subsequent production of small RNAs. The FHV-B2 and DCV-1A proteins work like that. Regarding B2, this small 12 kD protein binds to dsRNA *in vitro* with an affinity in the nanomolar range

and prevents their cleavage by Dcr-2 [Chao et al., 2005, Li et al., 2002]. B2 can also bind to the siRNA duplexes, therefore inhibiting their loading onto the RISC complex. *In vivo*, it seems that this protein interacts predominantly with the long dsRNA [Fagegaltier et al., 2009]. B2 interacts with the viral RNA-dependent RNA polymerase, and is therefore closely associated with the replication complex in infected cells. The presence at the place where the dsRNAs are generated allows the immediate binding of the VSR and efficient supression of antiviral silencing [Aliyari et al., 2008]. DCV protein 1A functions in a similar manner. This protein of 97 amino acids is located at the N-terminal part of ORF1 and contains a canonical dsRNA binding domain (dsRBD). DCV-1A binds to long dsRNA regardless of their sequence, and prevent their recognition and cleavage into siRNAs by Dcr-2 [van Rij et al., 2006].

CrPV-1A is the third VSR characterized in insect viruses and acts differently from FHV-B2 and DCV-1A. CrPV protein-1A is located at the N-terminal part of ORF1 of Cricket paralysis virus (CrPV). Although CrPV and the DCV belong to the same family of viruses, and their sequences are very similar, they differ for the N-terminus of ORF1. Unlike DCV-1A,CrPV-1A does not contain a dsRBD motif. The suppressor of CrPV does not inhibit the production of siRNAs, but blocks RNA interference downstream by binding to AGO2 and disrupting its function within the RISC [Nayak et al., 2010].

The importance of RNA interference in controlling viral infections is illustrated by the fact that VSRs represent an essential determinant of pathogenicity of viruses. Several studies have highlited the importance of VSRs in virus replication and pathogenesis. FHV-B2 was shown to be required for FHV replication and production of viral particles. This was exemplified by the fact that FHV RNA1 was undetectable in UAS-RNA1$\triangle$B2 *Drosophila* lines whereas in UAS-FHV1 flies the viral RNA1 was fully detectable and even able to produce viral particles [Galiana-Arnoux et al., 2006]. Hemolymph transfer from UAS-RNA1 into

non-infected flies killed them within few days, whereas hemolymph transferred from UAS-RNA1$\triangle$B2 did not kill the newly infected flies, suggesting an important role for B2 in virus production and pathogenesis. Infection of flies with recombinant SINV carrying the CrPV-1A VSR was associated with increase in mortality and virus production, in contrast to SINV carrying th DCV-1A VSR, which had only modest impact on SINV pathogenecity [Nayak et al., 2010]. Finally, studies in the mosquito *Aedes aegypty* showed that infection with recombinant SINV carrying FHV-B2 triggers increased mortality and accumulation of viral RNA. Infection was also associated with reduction in the production of vsiRNA, highlithing the importance of the VSR in the pathogenecity of the virus [Myles et al., 2008].

2.2 Antiviral inducible response

A hallmark of the mammalian antiviral immune response is the production of interferons and the subsequent interferon-dependant induction of antiviral molecules. This induction relyes on the recognition of the viruses by innate immune receptors, such as TLRs and RIG-like Receptors (RLRs). There is also now evidence for an inducible innate antiviral response in *Drosophila*. In addition to RNA interference, the inducible response triggered by viral infections also contributes to the control of the survival and viral load in flies.

2.2.1 Toll and IMD pathways

Proteomic analysis of the hemolymph of DCV-infected flies and FHV-infected *Drosophila* cultured cells revealed that antimicrobial peptides regulated by Toll and IMD pathways are not induced upon infection with this virus [Sabatier et al., 2003, Go et al., 2006].

However, genetic experiments suggest the involvement of Toll and IMD signaling pathways in antiviral immunity. The NF-κB -like transcription factor Dif

appears to be necessary for resistance to DXV infection [Zambon et al., 2005]. Curiously, several other mutants of the Toll pathway are not susceptible to this virus, suggesting that alternative signaling pathway may regulate the activity of Dif in the context of infection by this virus. In addition, constitutive expression of antimicrobial peptides is not sufficient to protect the flies against DXV infection, suggesting that other effector mechanisms than those controlling bacterial and fungal infections are involved [Zambon et al., 2005]. A role for the Toll pathway in the control of Dengue virus infection in *Aedes* mosquitoes has been described [Xi et al., 2008, Ramirez and Dimopoulos, 2010].

Another component of the Toll pathway, the highly polymorphic *ref(2)P* gene has also been connected to antiviral resistance. SIGMAV was shown to induce the expression of the antimicrobial peptide-coding genes *diptericin* and *drosocin*, but not the antifungal *drosomycin*, pointing to regulation by the IMD, rather than Toll pathway [Tsai et al., 2008]. However, the expression of antimicrobial peptides does not confer a protection to SIGMAV in *Drosophila*. Conserning the IMD pathway, two recent studies proposed that it is involved in the control of SINV and CrPV infections. The measurement of SINV RNA levels in flies expressing a SINV replicon in an *imd* deficient or wild type genetic background pointed to a potential role for the IMD pathway in the control of SINV replication [Avadhanula et al., 2009]. Loss of function mutations in several genes of the IMD pathway showed higher susceptibility to infection and increased viral load after challenge with CrPV [Costa et al., 2009]. If infection with SINV leads to modest induction of the expression of certain antimicrobial peptides, it is not the case for the CrPV, suggesting again that other types of antiviral effector molecules are induced in the context of these viral infections. Clearly, the involvement of the Toll and IMD pathways in antiviral immunity deserves further investigations.

2.2.2 The JAK/STAT pathway

Transcriptome analysis of DCV-infected flies identified some 150 genes induced in response to infection. Only one third of these genes are induced after bacterial and fungal challenge, suggesting that pathways different from Toll and IMD are activated after DCV infection [Sabatier et al., 2003]. The analysis of the regulation of DCV-induced genes highlighted the importance of motifs recognized by the transcription factor STAT92E (the only STAT factor present in the fly). Genetic analysis confirmed that the JAK/STAT signaling pathway is involved in resistance to the DCV. In particular, *Drosophila* mutant for the *hopscotch* gene, which encodes the only *Drosophila* JAK kinase, succumb to infection faster than wild type flies, with higher viral titers [Dostert et al., 2005]. The identity of antiviral effectors induced by this signaling pathway remains to be determined in *Drosophila*. However, in the *Aedes* mosquito two virus-induced genes regulated by the JAK/STAT were identified. They were shown to encode Dengue virus restriction factors (DVRFs), which mode of action remains unknown [Souza-Neto et al., 2009]. Similarly to mammals, the JAK/STAT pathway in *Drosophila* is induced by cytokines. The receptor Domeless is an ortholog of the family of receptors for the cytokine IL-6 (IL-6R) and shares similarities with the gp130 subunit of IL-6R. Three cytokines, Unpaired (Upd) -1, -2 and -3 activate the receptor Domeless and consequently the JAK/STAT pathway in flies. The expression of two of these cytokines, Upd-2 and Upd-3, is induced after DCV infection. All these data suggest that detection of viral infection triggers the expression of cytokines Upd, which then induce the JAK-STAT pathway and an antiviral state in uninfected cells. The JAK/STAT pathway is activated in response to stress, and it is possible that this pathway is activated in response to tissue damage caused by viral infections [Agaisse and Perrimon, 2004].

2.3 Other mechanisms regulating antiviral immunity in *Drosophila*

2.3.1 The induction of Vago: connecting RNAi and inducible response

One of the DCV-induced genes, *Vago*, helps to control viral infection. Indeed, the viral load increases by a factor of 5 to 10 in the fat body (the tissue in which *Vago* is specifically expressed) of *Drosophila* mutant flies harbouring a deletion of the gene *Vago* compared to control wild type flies [Deddouche et al., 2008]. The detection of dsRNA formed during viral replication triggers the induction of *Vago*. Indeed, the induction of this gene is inhibited in transgenic *Drosophila* expressing FHV-B2, which binds with high affinity to dsRNA. Induction of *Vago* is also reduced in the mutant *Dcr-2*, but not in the mutant *AGO2* or *r2d2*. This result shows that Dcr-2 acts both in the induction of the RNAi mechanism, and as a receptor involved in the inducible response. Interestingly, receptors detecting viral RNA in the cytosol of infected cells and induce interferon (RIG-I, MDA5 and LGP2) contain a DExD/H box helicase domain phylogenetically close to that present at the N-terminus of Dicer, suggesting a common evolutionary origin for these molecules [Deddouche et al., 2008]. The mode of action of Vago, a 16kDa protein containing eight cysteines remains to be determined.

2.3.2 Autophagy

Another effector mechanism induced by viral infection in *Drosophila* is autophagy, as demonstrated by studies on VSV. Autophagy is a process, in which cellular components are degraded in response to a range of stimuli, including nutrient availability. VSV was shown to induce autophagy both in *Drosophila* cell lines and *in vivo*. The RNAi-mediated knockdown of several autophagy-related

genes increased the viral titer in cultured cells and flies, leading to increased lethality [Shelly et al., 2009]. The induction of autophagy involves the recognition of the VSV-G glycoprotein by a receptor that has not been identified yet. Induction of antiviral autophagy upon sensing VSV infection involves the AKT/PI3K pathway.

2.3.3 Antiviral impact of *Wolbachia pipientis*

Since their discovery in 1924 by Hertig and Wolbach in the ovary of mosquito *Culex pipiens*, *Wolbachia* species have been detected in every insect order, as well as crustaceans, mites and filarial nematodes [Serbus et al., 2008]. *Wolbachia pipientis* is an obligate intracellular, Gram-negative bacterium, transmitted maternally. *Wolbachia* manipulates its host in different ways. For example, it causes cytoplasmic incompatibility, parthenogenesis, feminization and male killing [Stouthamer et al., 1999]. Interestingly, flies infected with *Wolbachia* are protected from infection with the RNA viruses DCV, CrPV, Nora and FHV [Hedges et al., 2008, Teixeira et al., 2008], but not the DNA virus IIV6 [Teixeira et al., 2008]. Importantly, DCV and Nora viral titers are extremely reduced in *Wolbachia*-infected flies, suggesting that *Wolbachia* affects the resistance of the host. Since DCV and Nora virus are natural pathogens of *Drosophila* that co-evolved with their host, this antiviral effect may confer selective advantage for the *Wolbachia*-infected flies. This may explain the wide distribution of this bacterium in *Drosophila* laboratory stocks and natural populations. In the case of infection with FHV, flies infected with *Wolbachia* are protected, without obvious reduction in the virus titers. This effect of *Wolbachia* may mostly be associated with the control of endurance mechanisms (see next chapter) and tissue damages caused by the virus [Teixeira et al., 2008]. For example, FHV was shown to induce apoptosis in cultured *Drosophila* cells [Settles and Friesen, 2008], whereas *Wolbachia* inhibits apoptosis in the germline of the parasitic wasp *Asobara tabida*,

to assure normal oogenesis [Pannebakker et al., 2007]. *Wolbachia* may thus limit the virus-induced apoptosis and contribute to the survival of the fly. Interestingly, recent studies have shown that *Wolbachia* can be successfully introduced in the mosquito vector *Aedes aegypty* and limit the ability of a range of pathogens, to infect this mosquito species. *A. aegypty* infection with *Wolbachia* is associated with upregulation of some immune effector genes encoding cecropin, defensin, thioester containing protein (TEP) and C-type lectin, wich may account for the protective effect of the bacterium [Moreira et al., 2009]. *Wolbachia*-mediated protection of *A. aegypty* in the case of infection with Dengue virus-2 (DENV-2) may result from potential competition for limiting cellular resources required for pathogen replication. This is supported by the fact that DENV-2 infection was only observed in *Wolbachia*-infected mosquitoes in cells that lacked the *Wolbachia* infection.

However, the exact mechanism of the antiviral effect of *Wolbachia* remains mysterious.

Chapter 3

Physiology and infection

Research on *Drosophila* immunity has successfully deciphered the molecular mechanisms controlling the resistance to microbial challenge. Surviving infections relies not only on resistance mechanisms, but also on homeostatic mechanisms involved in the integration of the immune response in the general physiology of the host.

3.1 Resistance and endurance: two ways of surviving infection

3.1.1 Definition

Evolutionary studies on plant-herbivore interactions originally formulated the terms of resistance and tolerance to a threat. Resistance traits such as thorns, spikes and secreted chemicals are protective for the plants. Unlike resistance, tolerance does not prevent herbivory, but allows the plant to compensate the damage that herbivores have caused. Both resistance and tolerance have the same function- to defend the plant against the herbivore attack [Mauricio, 2000]. These definitions became extended to the studies of host-microbe interactions,

suggesting that the outcome of infection is determined by the ability of the host to limit the pathogen burden (resistance) or to withstand pathology (tolerance).

It should be mentioned that the meaning of the term "tolerance" is ambiguous. In immunology, tolerance is defined as mechanism of antigen non-responsivness [Schwartz, 2005]. For example in vertebrates, the mechanisms that control the responsiveness of the immune system to "self" antigens often employ the term of "self-tolerance". For this reason it might be appropriate to distanguish the different meanings of "tolerance" in evolutionary plant ecology and immunology. In the following parts I will use the term of "endurance", as definition of the ability of the host to withstand pathology.

Evolutionary studies of *Drosophila* model of host-pathogen interactions exemplified the importance of endurance in the case of infection with *Pseudomonas aeruginosa*. No correlation between the rate of survival and the bacterial load was observed in susceptible strains, suggesting that endurance plays an important role for the outcome of infection [Corby-Harris et al., 2007]. A diagram of the possible interactions between the resistance and endurance during infection is drawn on Figure 3.1.

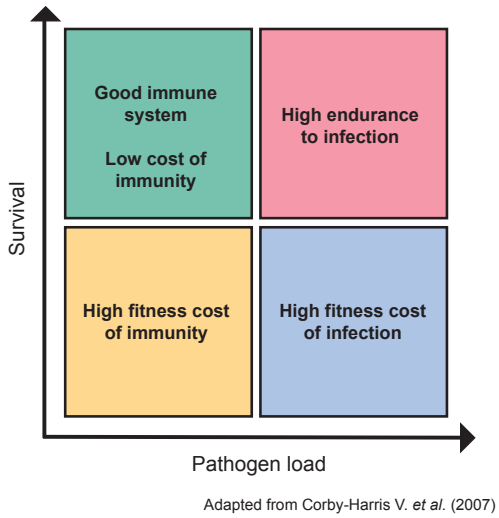

Figure 3.1: Relationship between survival and pathogen load: resistance and endurance of infection .

The most general feature of pathogenic microorganism is to cause disease leading to the dysfunction of organs and tissues. The pathology associated with such infections is due to the pathogen itself, or in some cases results from the detrimental activation of the host's immune response. A well-known example from the mammalian system is the dual effect of the Tumor Necrosis Factor-alpha (TNF-α). TNF-α is mainly produced by activated macrophages and its moderate secretion has a protective effect against infection. However, in the case of lipopolysaccharide (LPS)-induced septic shock this inflammatory cytokine becomes extremely harmful and detrimental, causing failure of organs and tissues and even the death of the host [Vassalli, 1992].

The studies of the pathophysiological mechanisms associated with infection in insects can provide answers to the fundamental question of the cause of the death following infection, and whether it involves toxic side effects of the immune response.

3.1.2 K_{ATP}- sensitive potassium channels and MCMV infection in mice: an example of endurance

Genetic analysis in mice demonstrated that the ENU-induced strain of mutant mice *mayday* show an increased frequency of sudden death upon infection with the mouse cytomegalovirus (MCMV) with viral titers comparable to the controls [Croker et al., 2007]. That mutation appeared to be allelic to the *Kcnj8* locus, encoding the pore-forming component of an inwardly rectifying ATP-sensitive potassium channel (K_{ATP}) subunit Kir6.1, expressed in the coronary artery smooth muscle cells. In addition to the Kir6.1 subunit forming the pore, the K_{ATP} channel contains a regulatory subunit SUR2 (sulfonylurea receptor 2) (Figure 3.2). K_{ATP} channels are evolutionary conserved and have orthologues in flies. The mammalian gene coding the pore has two orthologues in *Drosophila*

(*Ir* and *Irk2*), whereas the gene encoding the regulatory subunit SUR2 of the K_{ATP} channel has a single orthologue in flies, called *Drosophila* SUR (*dSUR*). *dSUR* is mainly expressed in the *Drosophila* heart, and was shown to play a protective role against hypoxic stress and heart failure induced by electrical pacing [Akasaka et al., 2006]. The fact that hypoxia is a commonly used readout for susceptibility to SIGMAV and DXV increased the interest in studying the role played by the potassium channels during viral infections in flies. The knock down of dSUR in the *Drosophila* heart, but not in the other tissues, resulted in increased susceptibility to FHV, but not DCV nor bacterial and fungal infections [Croker et al., 2007].

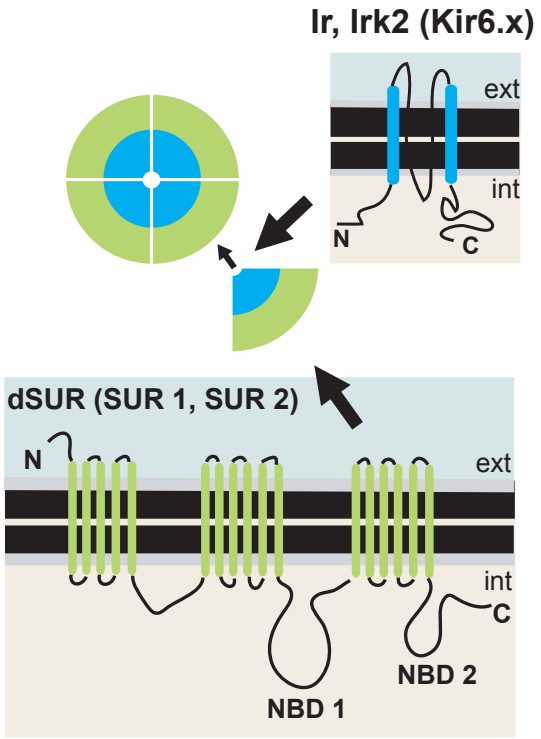

Figure 3.2: Schematic representation of the cardiac K_{ATP} channel . Kir and SUR are the constitutive subunits of the cardiac K_{ATP} channel. Four subunits of the inwardly rectifying K^+ channel, encoded by the genes *Ir* or *Irk2*, associate with the ATP-binding cassette (ABC) regulatory protein encoded by *dSUR*, to form a functional K_{ATP} channel octamer. SUR possesses two cytoplasmic nucleotide binding domains (NBD1 and NBD2). The names of the mammalian orthologs are given in parentheses.

3.2 Metabolism and energy homeostasis in *Drosophila*

All processes of life and all physiological events, including the immune response require continuous supply of energy. However, animals face the possibility of limitation in food resources ultimately leading to starvation-induced death. In the past years, the fruit fly *Drosophila melanogaster* witnessed its utility as model for research on energy homeostasis, including food perception, feeding control, energy flux and lipid metabolism [Kuhnlein, 2010]. In the following part, I will overview the energy homeostasis in *Drosophila* and its regulation upon starvation and infectious conditions.

3.2.1 *Drosophila* tissues and organs governing energy homeostasis

In the adult *Drosophila*, several tissues and organs contribute to the energy homeostasis of the fly, by regulating food perception and uptake, nutrient processing, fuel storage and remobilization, energy consumption and waste excretion [Buch and Pankratz, 2009, Kuhnlein, 2010]. The *Drosophila* mouthparts and legs contain chemosensory *sensilla* and gustatory receptors that trigger feeding behavior, coordinated by the suboesophagial ganglion (SOG) of the central nervous system [Kuhnlein, 2010, Melcher and Pankratz, 2005, Thorne and Amrein, 2008]. The ingested meal entering the alimentary tract *via* the foregut (composed of the pharynx, oesophagus and the crop) is temporary retained in the crop and subsequently transported to the major site of digestion and nutrient absorption: the midgut (see section 3.3). Absorbed nutrients diffuse in the hemolymph and are subsequently stored in the major metabolic hub, the fat

body. Depending on the metabolic needs of the animal, the nutrients are released from the fat body in order to reach different cells of the organism (Figure 3.3).

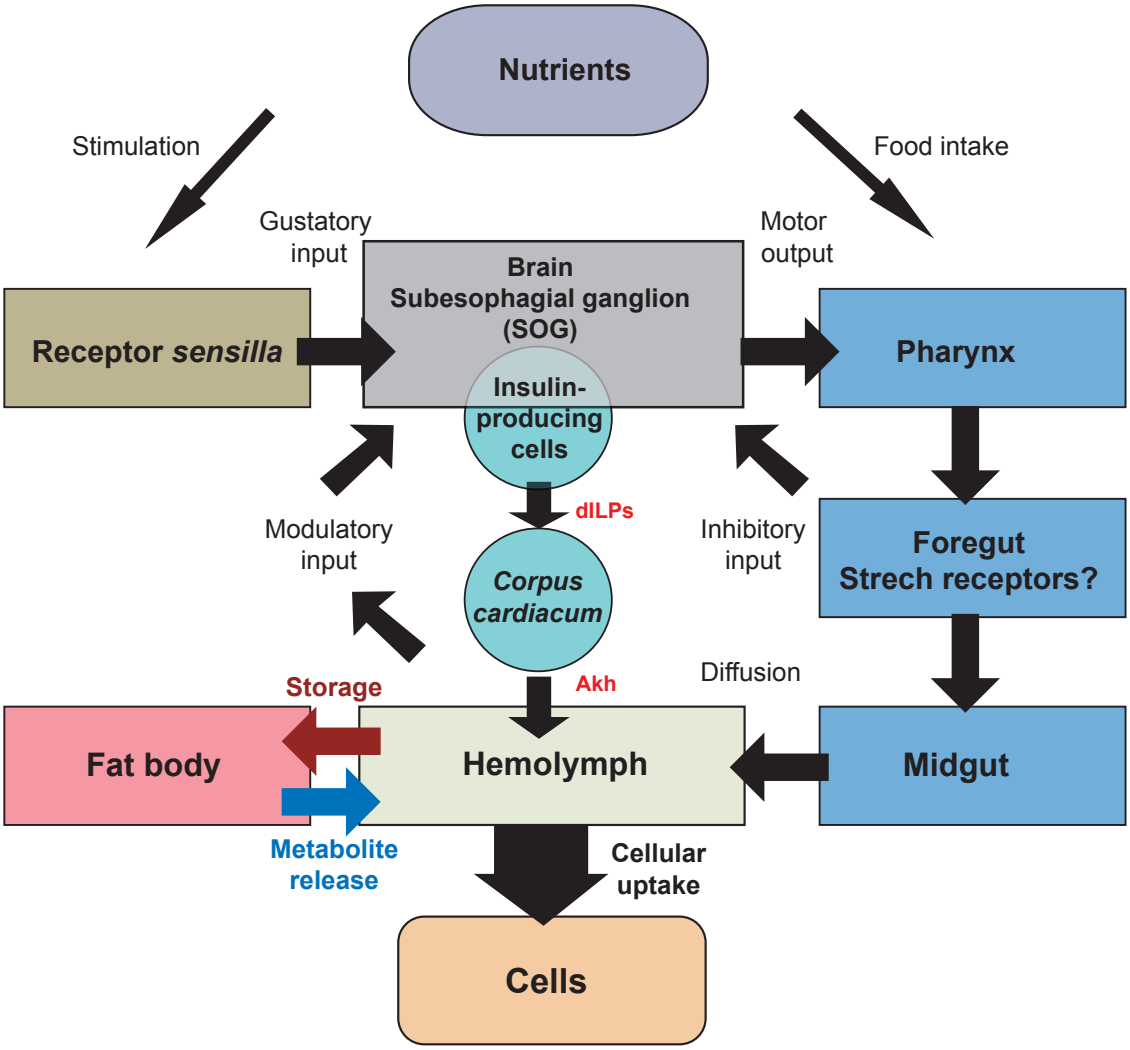

Figure 3.3: Tissues and organs involved in the metabolic homeostasis in *Drosophila* .

Several signals regulate communication between the different organs involved in energy metabolism. In addition to the stomatogastric nervous system (SNS), which controls the mechanism of feeding [Heinz, 1985], a neuro-endocrine axis also orchestrates the energy homeostasis. In the adult fly, the Insulin producing cells (IPCs), which are analogous to the mammalian pacreatic β-cells, are

located in the *pars intercerebralis* of the brain and produce insulin-like peptides. Genetic ablation of IPCs in *Drosophila* larvae leads to increased carbohydrate levels in the hemolymph and global physiological alterations in processes such as animal growth [Rulifson et al., 2002]. During conditions of food deprivation in *Drosophila* larvae, clusters of cells, called the oenocytes, accumulate lipid stores and process them into free fatty acids [Gutierrez et al., 2007]. The *pars intercerebralis* region of the fly's brain is in connection with the *corpus cardiacum* (CC) cells, located at the level of the foregut, which are analogous to the mammalian pancreatic α-cells. CC cells secrete the adipokinetic hormone (AKH), which functions as a prolipolytic neuropeptide and promotes the mobilization of energy stores. In contrast to IPCs, flies with ablated CC cells develop and reproduce normally, suggesting that AKH signaling is not essential under normal growth conditions [Kim and Rulifson, 2004]. Interstingly, the secretion of AKH is regulated by dSUR in CC cells [Kim and Rulifson, 2004]. In mammals, SUR1, an orthologue of dSUR, also participates in the regulation of glucagon secretion [Rorsman et al., 2008]. Indeen, Tolbutamide, a sulfonylurea drug that acts as antagonist of K_{ATP} channels, is used as an anti-diabetic treatment.

3.2.2 Regulation of energy metabolism

Many animals face in their environment food shortage, periodical malnutrition or starvation, leading to reduction in fitness. The energy homeostasis of the organism needs to be tightly regulated in order to guarantee survival in such situations. *Drosophila* and vertebrates rely on mostly the same metabolic functions for their living and flies have provided a good model for defining the genetic regulation of metabolism [Baker and Thummel, 2007]. For example, the insulin/insulin growth factor (IGF) and the target of rapamycin (TOR) pathways were shown to regulate the metabolism of the fly.

3.2.3 Energy management: survival for immunity

Discussions in the field of evolutionary ecology have proposed that physiological programming decisions evolve because of internal competition for ressources. For example, the activation of the immune system is thought to be costly, and cannot be sustained with other demanding activities [Kraaijeveld and Godfray, 1997]. However, such changes in energy utilisation are difficult to assess, because of compensatory mechanisms of the other systems. Studies in the bumblebee *Bombus terrestris* have provided example of ressource allocation after immune challenge [Moret and Schmid-Hempel, 2001]. When they were subject of the experiments, bumblebees were starved, and interstingly food-deprived animals die, without be able to compensate energy by eating more. Animals, which were forced to rise an immune response by challenge with LPS died faster than controls, suggesting that the immune system uses the enrgy that otherwise will be used for the survival of the bee during starvation [Moret and Schmid-Hempel, 2001]. This interesting example, however, does not answer the question how energy use changes during in infected, but otherwise fed animals.

Interestingly, infection of *Drosophila* with *Mycobacterium marinum* was shown to cause a pathology described as wasting [Dionne et al., 2006]. *M. marinum* which is a bacterium species closely related to *Mycobacterium tuberculosis*, was shown to cause lethality of flies and was proposed to serve as model to study tuberculosis-like disease in *Drosophila* [Dionne et al., 2003]. Flies infected with *M. marinum* showed hyperglycemia and decrease in their glycogen and fat stores, dependant on the insulin signaling (IS). It appears that *M.marinum*-infected flies do not properly activate the insulin signaling pathway. Flies carrying a mutation in the gene coding the transcription factor *Foxo* in which the IS is active, as well as flies treated with insulin showed increased survival rates when compared to controls [Dionne et al., 2006]. Infection with *M. marinum* seems to affect the

endurance mechanisms of the fly since the wasting-accelerated death is not correlated to an increase in the bacterial load. However, the exact mechanism by which IS affects immunity is not clear.

3.3 Infection-induced intestinal pathology: the example of *Drosophila* gut

In Asian medicine, the abdomen is considered as the location of the soul, and the gut is believed to be the "honoured middle" and the "center of the spiritual and physical strength" [Yu et al., 2006]. In the Western world, the intestine is increasingly recognized to play an important role in human health and infections, as well as in inflammatory and neoplastic disease [Markowitz and Bertagnolli, 2009]. In the recent years, the fruit fly *Drosophila melanogaster* became an interesting model for studying the "gut health". Research on immunity and pathogenesis of the arthropod gut is also particularly important because several arthropod-transmitted pathogens and parasites causing illness in humans evolved to use the host's gut as route of transmission [Schneider, 2000]. In the following subsections I will describe our current knowledge conserning the physiological roles of *Drosophila* gut, and its implication in microbe-induced pathology.

3.3.1 Anatomy and physiology of *Drosophila* gut

The *Drosophila* digestive system can be divided into three major parts: *(i)* the most anterior part: foregut, followed by *(ii)* the midgut and *(iii)* the posterior part: the hindgut. The midgut itself is segmented in three regions: the anterior, middle (or low pH) region, and posterior midgut. The intestinal epithelium is a cellular monolayer and derives from the embryonic endoderm (midgut) and ectoderm (foregut and hindgut) [Nakagoshi, 2005].The organization of the fly's diges-

tive tract is schematically presented in Figure 3.4A. The midgut is composed of two differentiated cell types: absorptive enterocytes (EC) and secretory enteroendocrine cells (EE) [Siviter et al., 2000, Yoon and Stay, 1995]. It also contains undifferentiated intestinal progenitor stem cells (ISC) [Micchelli and Perrimon, 2006, Ohlstein and Spradling, 2006], (Figure 3.4B). Functionally, EC are involved in nutrient absorption, but they can also produce antimicrobial peptides (AMPs) and reactive oxygen species (ROS) locally, upon bacterial infection. EE cells are secretory cells characterized by the peptides they produce such as allatostatins [Yoon and Stay, 1995], tachykinins [Siviter et al., 2000] or the Diuretic hormone 31 (DH31) [LaJeunesse et al., 2010]. The basal side of the epithelial monolayer rests on the basal lamina, a thin layer of extracellular matrix [Sengupta and MacDonald, 2007] and is surrounded by two layers of circular and longitudinal visceral muscles that drive peristalsis [Jiang and Edgar, 2009]. On their apical side, *Drosophila* EC and ISC are featured with cytoplasmic extensions, called the *microvilli*, which face the intestinal lumen and constitute the intestinal brush border [Shanbhag and Tripathi, 2009]. The midgut and hindgut epithelia are protected from the direct contact with abrasive particles, digestive enzymes or infectious agents present in the gut lumen by a physical barrier, called the peritrophic matrix (PM). The PM, which is composed of two layers, is produced by the cardia (also called proventriculus) in the most anterior part of the midgut. It is mainly composed of chitin and glycoproteins [Hegedus et al., 2009]. The *Drosophila* midgut epithelium undergoes constant renewal. Active digestion is associated with cell loses, as soon as apoptosis-positive staining is observed in the gut of the fly. In parallel, ISC divisions occur, with turnover competed whithin a week [Crosnier et al., 2006, Micchelli and Perrimon, 2006, Ohlstein and Spradling, 2006].

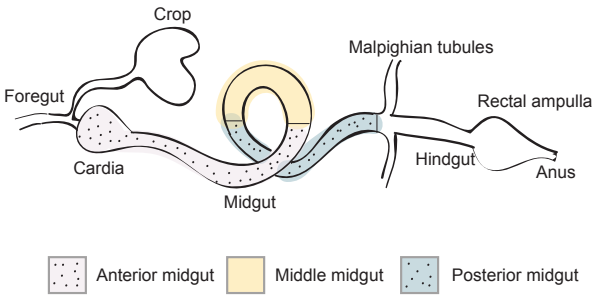

A Schematic representation of *Drosophila* digestve tract

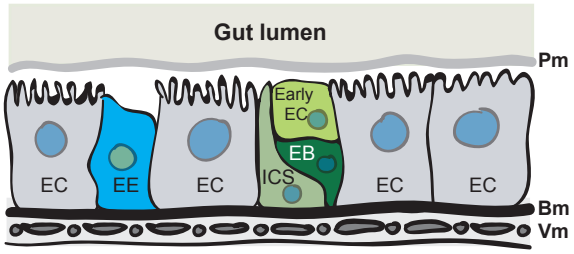

B Representation of gut epithelium

Figure 3.4: Organization of *Drosophila* gut . EC: enterocyte, EE: enteroendocrine cell, ICS: intestinal stem cell, EB: enteroblast, Bm: basal membrane, Pm: peritrophic matrix, Vm: visceral muscle.

The *Drosophila* gut plays an essential role in providing the organism with energy supplies by processing the food and absorbing the nutrients. The ingested food passes trough the foregut (esophagus) and is retained temporally in a collapsible food-storage sac, called the crop. Subsequently, it moves to the anterior midgut where the digestion and absorption proces begins. The cardia acts as a stomodeal valve and controls this transition. Additional break down of the food occurs in the very low pH region of the middle midgut, where the so called Copper cells reside. Afterwords, during the transition through the posterior midgut, absorption takes place. In the hindgut and the rectum the water and electrolytes are exchanged and the waste is then excreted via the anus. Kidney-like structures, the Malpighian tubules, are connected at the junction of the posterior midgut and the hindgut. Their function is to absorb solutes, water

and waste from the surrounding hemolymph, and assure their release in the gut [Apidianakis and Rahme, 2011].

3.3.2 ISC: maintaining gut homeostasis after bacterial infection

Functionally, the gut is by far not restricted to food processing and the subsequent uptake of nutrients and fluid. This organ is situated at the interface between the external and internal milieu of the organism and is in constant contact with microorganisms. It is of great interest to study how the intestinal integrity is maintained in presence of microorganisms and what the mechanisms controlling the intestinal homeostasis are. The fruit fly *Drosophila* is a good model for the study of microbe-gut interactions and experimental system of intestinal bacterial infections were efficiently developed. For example, the invasive pathogen *Serratia marcescens*, when fed to the flies, is able to kill them within a week [Nehme et al., 2007]. In order to identify the genes and pathways of the host response to orally fed *S. marcescens*, a genome-wide *in vivo* genetic screen was performed [Cronin et al., 2009]. In another study, the transcriptional gut response of flies fed with the non-lethal pathogen *Erwinia carotovora carotovora* was studied using genome-wide microarrays [Buchon et al., 2009]. In both experimental conditions, the gut reaction to lethal and non-lethal bacteria showed not only activation of the immune response, but also modification of different aspects of gut cell physiology. Indeed, several genes controlling cellular growth and development, wound repair and stress response were upregulated following bacterial ingestion, suggesting that the damaged gut is regenerated.

In non-infectious conditions, the *Drosophila* ECs are replaced within a week [Micchelli and Perrimon, 2006] and the ISC division is controlled by the Wnt signaling pathway [Lin et al., 2008]. Importantly, feeding *Drosophila* on tissue-

damaging agents, or gut-specific expression of apoptotic genes triggers faster ISC division [Buchon et al., 2009]. The ISC proliferation is also modulated by the presence of bacteria in the fly's digestive tract [Chatterjee and Ip, 2009, Jiang et al., 2009, Buchon et al., 2009, Cronin et al., 2009]. This observation, as well as the information obtained from the large-scale *in vivo* screens pointed to the following model accounting for the rapid ISC division in an infectious context. Upon infection with *E.carotovora*, *S.marcescens* and *P. entomophila* the cytokines of the unpaired (Upd) family Upd-1, Upd-2 and Upd-3 are secreted and activate the JAK/STAT pathway. Because this pathway plays an important role in tissue-damage repair and regeneration [Agaisse and Perrimon, 2004], it might also be associated with the maintenance of intestinal homeostasis by regulating the ISC divisions. Upd induction and JAK/STAT pathway activation are required for the ISC division after bacterial challenge as evidenced by the double positive staining in the gut with the dividing cell marker phospho-histone H3 and the marker of ISCs and EBs escargot (esg) [Buchon et al., 2009, Cronin et al., 2009, Jiang et al., 2009]. In addition to the JAK/STAT pathway, the JNK and Notch signaling pathways participate to the induction of stem cell proliferation by bacteria in *Drosophila* intestine. The absence of Notch in the progenitor cells confers an increased susceptibility to infection with *P. entomophila* [Jiang et al., 2009]. Since Notch is required for ISC differentiation, but not ISC mitosis, the progenitor differentiation appears to be important for the resistance against pathogens [Jiang et al., 2009]. The JNK pathway was shown to participate in gut regeneration in old flies [Jiang et al., 2009] and its implication in maintaining of gut homeostasis following infection with *E.carotovora* was also proven. Reduced JNK signaling in ISCs results in premature loss of ISC and the subsequent absence of epithelial renewal upon bacterial challenge. Interestingly, the ISC-specific knockdown of JNK pathway components such as *basket* and *hemipterous*, as well as

the overexpression of the JNK pathway negative regulator *puckered* did not alter the number of ISCs in unchallenged flies [Buchon et al., 2009].

3.3.3 Mechanism of ISC-mediated intestinal homeostasis after microbial infection

The identification of cytokine-triggered gut regeneration in *Drosophila* provides a novel concept of regulation of host intestinal homeostasis after bacterial infection. However, how the damaged tissue turns into physiological signals leading to the stem cells proliferation remains unknown. Once ingested, the bacterial pathogen causes boths activation of gut immune signaling and apoptosis of intestinal cells (Figure 3.5). The IMD pathway activation leads to the transcription of antimicrobial peptides in *Drosophila* gut [Lemaitre and Hoffmann, 2007], but it is unlikely that IMD triggers the JAK/STAT signaling, neither the division of ISC [Jiang et al., 2009]. On the other hand, the challenge of the flies with orally fed bacteria induces the rapid production of Reactive Oxygen Species (ROS) in the gut. ROS are produced by the dual oxydase (DUOX) membrane protein and were shown to be major microbicidal immune effectors [Ha et al., 2005]. The involvement of ROS in ISCs activation seems possible, since flies which cannot generate microbe-induced ROS, as well as flies exhibiting high antioxidant potential showed reduced levels of bacteria-induced ISCs proliferation [Buchon et al., 2009].

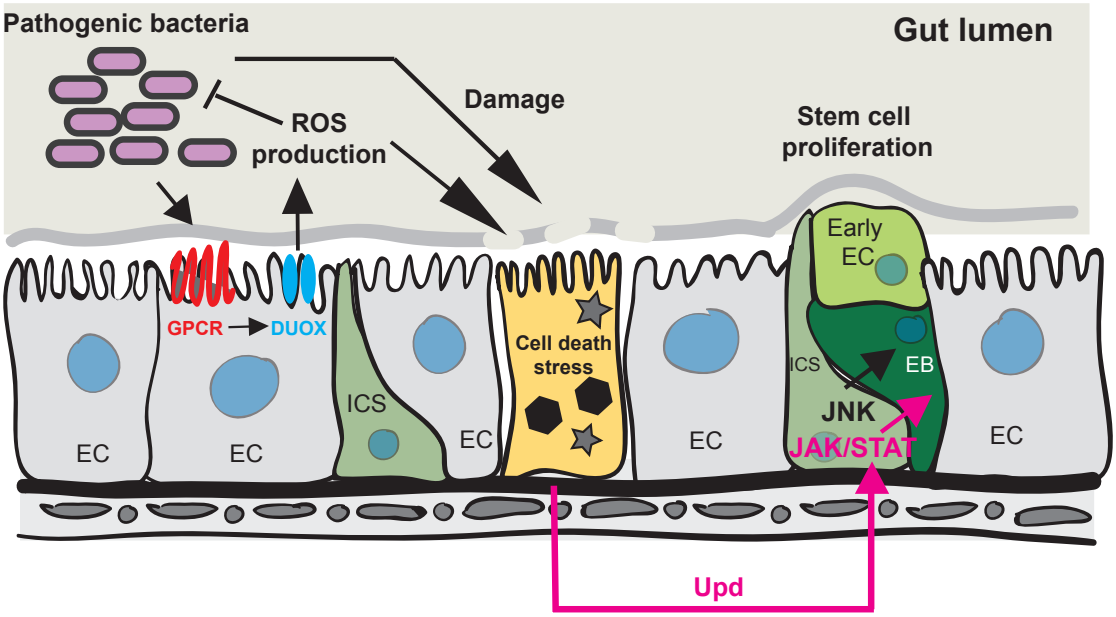

Adapted from Charroux and Royet, 2010

Figure 3.5: Pathways controlling *Drosophila* gut homeostasis after bacterial challenge . G-protein coupled receptor (GPCR)-dependent signaling controls the basal levels of ROS production and gut microbiota. Ingestion of infectious bacteria triggers strong ROS burst, damaging the midgut epithelim.Damged ECs trigger the production of Upd-3, which activates the JAK/STAT pathway in neighbouring ICS cells.The JAK/STAT and JNK pathways synergize to promote ISC proliferation and epithelium renewal.

Part II

Material and methods

Chapter 4

Material and methods

4.1 Fly strains and infections

4.1.1 *Drosophila* strains

w^{A5001}, *yw*, Oregon^{R} and DD1;*cnbw* flies were used as wild type controls. The *hopscotch* alleles M38 and msv1, as well as the *Dcr-2*^{R416X}, *Dif*^{1}, *Imd*^{Shadok} and *KCNQ* mutants were previously described [Lee et al., 2004, Rutschmann et al., 2000, Agaisse et al., 2003, Gottar et al., 2002, Ocorr et al., 2007]. UAS-Ir (v28430, v28431) and UAS-Irk2 (v4341) RNAi lines were purchased from the Vienna *Drosophila* RNAi Center (VDRC). Fly stocks were raised on standard cornmeal–agar medium at 25°C. Adult flies 4–7 days of age were used in infection experiments. For heat-shock induction of transgene expression, flies were placed at 37°C for 20 min, following 30 min at 18°C and finally 20 min at 37°C. After the treatment flies were allowed to recover for 6 h at 25 °C before immune challenge. All flies were tested for *Wolbachia* infection and treated whenever necessary.

4.1.2 Generation of transgenic lines

For the construction of all reporter plasmids, PCR fragments of different size, amplified from the 5'UTR region of *Jon65Ai* and *LysE* genes, were inserted into pCasper expression vector containing the *LacZ* gene, the *Drosomycin* poly A sequence and ampicilline resistance cassette. The PCR products were amplified with the primers shown on Table 4.1, digested with NotI and NheI restriction enzymes and placed between the crresponding sites in pCasper transformation vector. The resulting constructs were then injected into *Drosophila* embryos (w^- strain) to obtain transgenic lines. At least two independent lines were analyzed for each construct.

Primer	Forward (FW)/ Reverse (RV)	Used for	Sequence
OJL978	RV	Coning of different versions of *Jon65Ai* promoter in pCasper	**5'-TTTTGCTAGCCATGTTCCTTAAGTTCAGCACACTT-3'**
OJL981	RV	Coning of **-1400** bp of *LysE* in pCasper	**5'-TTTTGCTAGCCATTTTGATTTGAATACCACAGTAAAC-3'**
OJL982	FW	Coning of **-1800** bp of *Jon65Ai* in pCasper	**5'-TTTGCGGCCGCTTCACTTGGCTGCTGATGGAG-3'**
OJL983	FW	Coning of **-1400** bp of *LysE* in pCasper	**5'-TTTGCGGCCGCAGCTTTTGGAGTGGGCAATTAC-3'**
OJL1180	FW	Coning of **-236** bp of *Jon65Ai* in pCasper	**5'-AAAGCGGCCGCAATAAATTCAAATTTGACAAGCCTCC-3'**
OJL1181	FW	Coning of **-483** bp of *Jon65Ai* in pCasper	**5'-AAAGCGGCCGCGAAAAGGAAATGTGACACGGAC-3'**
OJL1182	FW	Coning of **-733** bp of *Jon65Ai* in pCasper	**5'-AAAGCGGCCGCGAGCTGGTTCAACCAGTCACA-3**

Table 4.1: List of the primers used for the cloning of different versions of *Jon65Ai* and *LysE* promoter regions .

4.1.3 Infections

Virus infection

Viral stocks were prepared in 10 mM Tris-HCl, pH 7.5. Flies were infected by intrathoracic injection (Nanoject II apparatus; Drummond Scientific) with 4.6 nl of a viral suspension corresponding to 500 pfu/fly for DCV, FHV and CrPV. Injection of the same volume of 10 mM Tris-HCl, pH 7.5, was used as a control. Infected flies were then incubated at 22°C. For survival experiments, two tubes of 10 flies were injected per virus and flies were kept on standard cornmeal-agar. Survival rates were recorded every 24h post-injection. Groups of 20 and 5 flies were frozen for Northern blot and qRT-PCR analysis, respecively.

Bacterial infection

For bacterial infection flies were pricked with thin tungsten needle previously dipped in the concentrated overnight culture in Luria Bertani (LB) medium at 37°C of *Enterococcus faecalis* (Gram positive) and *Enterobacter cloacae* (Gram negative). Injection with "clean" needle was used as control.

4.2 DNA extraction

DNA from whole flies was extracted by homogenizing single fly in 50 μL of "Squishing" buffer (10 mM of Tris-HCl,pH 8.2, 1mM of EDTA, 25mM of NaCl and 200 μg/mL of Proteinas K. The homogenate was incubated 30 min at 37°C and the Proteinase K inactivated at 95°C for 10 min.

4.3 RNA analysis

4.3.1 RNA extraction

For qRT-PCR analysis, frozen flies were homogenized in 350 μL of Trireagent-RT, containing the phase separation reagent bromoanisole (BAN) (50 μL of BAN per mL of Trireagent-RT)(Molecular Research Central, Inc.). Tubes were vortexed and incubated at room temperature for 5 min. Tubes were next centrifuged for 15 min at 12500 rpm, at 4°C. The aqueous phase was carefully transferred into a fresh tube and 300 μL of Isopropanol were added. Samples were mixed and incubated for 10 min at room temperature before being centrifuged for 10 min at 12500 rpm at 4°C. Supernatants were removed and the pellet washed with 70% of EtOH. After 5 min of centrifugation at 7500 rpm at 4°C, supernatants were removed and pellet was dried 10 min at 65°C. RNAs were resuspended in 30 μL of RNase-free water and quantified with the Nanodrop spectrophotometer.

For Northern blot analysis,frozen flies were homogenized in 500 μL of Trireagent (Molecular Research Central, Inc.). Tubes were vortexed and incubated at room temperature for 5 min. 100 μL of chloroform was added and each tube was vortexed for 30 sec. Tubes were next centrifuged for 15 min at 12500 rpm, at 4°C. The aqueous phase was carefully transferred into a fresh tube and 500 μL of Isopropanol was added. The next steps are identical to the RNA extraction for qRT-PCR analysis.

4.3.2 cDNA synthesis

For qRT-PCR analysis a cDNA were synthesized from RNA template by using the iScriptTM cDNA kit (Biorad). 1 μg of RNA template was mixed with 4 μL of 5x Reaction mix and 1 μL of reverse transcriptase and nuclease-free water in a total reaction volume of 20 μL. For the reaction the thermocycler T3000 (Biometra)

was used for the following cycle: **step 1**: 5 min at 65°C, **step 2**: 5 min at 4°C, **step 3**: 25 min at 42°C, **step 4**: 15 min at 70°C, **step 5**: pause at 16°C. The synthesized cDNA was diluted 20 times for qRT-PCR analysis.

4.3.3 Quantitative RT-PCR (qRT-PCR)

The iQTM Custom SYBR Green Supermix kit (Biorad) was used for desired amplicon synthesis. 2.4 μL of Supermix, 0.3 μL of forward and 0.3 μL of reverse primers and 5 μL of water were added to 20 times diluted cDNA in a total volume of 10 μL. For the reaction the CFX384^{TM} Real-Time System (Biorad) was used with the following program: **step 1**: 3 min at 95°C, **step 2**: 10 sec at 95°C, **step 3**: 30 sec at 55°C. Go to step 2 and repeat 39 times. The primers used for qRT-PCR analysis are shown on Table 4.2. The relative gene expression was normalized to the expression of the "housekeeping" ribosomal protein-coding gene *rp49*.

Amplicon	Forward (FW)/ Reverse (RV)	Sequence
RP49	FW	**5'-GACGCTTCAAGGGACAGTATCT-3'**
RP49	RV	**5'-AAACGCGGTTCTGCATGAG-3'**
DCV	FW	**5'-TCATCGGTATGCACATTGCT-3'**
DCV	RV	**5'-CGCATAACCATGCTCTTCTG-3'**
FHV1	FW	**5'-TTTAGAGCACATGCGTCCAG-3'**
FHV1	RV	**5'-CGCTCACTTTCTTCGGGTTA-3'**
FHV2	FW	**5'-CAACGTCGAACTTGATGCAG-3'**
FHV2	RV	**5'-GCTTTACAGGGCATTTCCAA-3'**

Table 4.2: List of the primers used for qRT-PCR analysis .

4.3.4 Northern blot (NB)

Electrophoresis and transfer

RNAs were separated by electrophoresis on 1% agarose gel containing 6% formaldehyde in MOPS 1x buffer. 30 μg of total RNA were mixed in a loading buffer (50% formamide, MOPS 1x, 1.8 M formaldehyde, 0.15% bromophenol blue, 7% glycerol) and heat-denatured 10 min at 65°C. RNAs were transferred by capillarity overnight onto a nitrocellulose membrane, in 10x SSC solution (1.5 M NaCl, 0.15 M sodium citrate). RNAs were crosslinked to the nitrocellulose membrane by UV treatment.

Probe synthesis and labelling

25 ng of cDNA fragment of the gene of interest were labelled with the α-^{32}P dCTP by random priming using Rediprime II Random Prime Labelling Kit (Amersham Biosciences), according to manifacturer's instructions. The unincorporated nucleotides were removed by passing the sample through mini-column (Bio-gel P10, Biorad). The list of primers used for the synthesis of the different probes is shown of Table 4.3.

Hybridization

The membrane containing the RNAs was prehybridized in the following solution: 50% formamide, 5x Denhardt, 6x SSC, 0.1% SDS ; 100 μg/mL of salmon sperm DNA for 2 hours. Hybridization with the probe was done overnight at 42°C in the same solution. The membrane was washed twice in 2 $\times$ SSC, 0.1% SDS at 42°C, followed by two additional washes in 0.2 x SSC, 0.1% SDS at 42°C and 65°C, respectively. The membrane was exposed overnight in contact with an autoradiographic film at -80°C. The signal was quantified with the Bioimager analyzing system.

Forward(FW)/ Reverse (RV)	Probe	Sequence
FW	*Jon65Ai*	5'-GGAGGCACCTGGTGCGGCGG-3'
RV	*Jon65Ai*	5'-GAGATGCCAGTGTTGTCGCGG-3'
RV	*Ser4*	5'-CCACGACAGCTTTGCCGGCTGG-3'
FW	*Ser4*	5'-GGTCGCGGATCCAGTCCAGG-3'
RV	*Jon25Biii*	5'-GGAGCTCCCCAGCTACAACG-3'
FW	*Jon25Biii*	5'-CGCTGGAATCCAGCAGGAGC-3'
FW	*Jon99Ci*	5'-GTGAGCTTGAACAGCAACGG-3'
RV	*Jon99Ci*	5'-CCTCCTTTATCCATTCCAGG-3'
FW	*Vir-1*	5'-GATCCCAATTTTCCCATCAA-3'
RV	*Vir-1*	5'-GATTACAGCTGGGTGCACAA-3'
FW	*Rp49*	5'-GACGCTTCAAGGGACAGTATCTG-3'
RV	*Rp49*	5'- AAACGCGGTTCTGCATGAG-3'

Table 4.3: List of primers used for the synthesis of indicated probes .

4.3.5 Whole mount *in situ* hybridization

Cloning

Groups of 20 flies (w^- strain) were infected with DCV and CrPV and total RNA was extracted 4 days post-infection. cDNA was prepared and fragments corresponding to the 5' variable region of DCV and CrPV genomes (Table 4.4) was amplified by PCR, using the Phusion polymerase with proofreading activity. Reactions took place in final volume of 50 μL, including 1 μL of 10 times diluted cDNA, 10μL of 5x Reaction Buffer, 5 μL of 2mM dNTPs, 32 μL of water and 1 μL of forward and reverse primers at the concentration of 100 μM.

Forward(FW)/ Reverse (RV)	Probe	Sequence
FW	***DCV***	**5'-ATACGTTGTTTTCATTGTTGATGG-3'**
RV	***DCV***	**5'-AACATCTGACGTGCAGCTTCC-3'**
FW	***CrPV***	**5'-GCTCTATGTTACAATTGGGAGGAG-3'**
RV	***CrPV***	**5'-TCAAAAGTTGCGTTCTCTTTCTC-3'**

Table 4.4: List of primers used for the cloning of 5' end sequences of DCV and CrPV into PSK+ transformation vector .

The PCR products were purified through column (Machery/Nagel PCR clean up) and cloned into PSK+ transformation vector (Invitrogen), that contains phage T3 and T7 promoter sequences. Resulting clones were linearized using EcoRV and EcoRI restriction enzymes in order to determine orientation in the vector (T3 or T7 sens).

Plasmids were next linearized with Hind III and EcoR I and 4 μg of plasmid was used and the digestion mix was incubated at 37°C for 1h. Linearized plasmids were purified with phenol/chloroform and DNA was precipitated in EtOH 100%, 0.3M sodium acetate, overnight at -20°C. The precipitation mixture was centrifuged for 30 min at 12500 rpm, and the pellet washed with EtOH 70% and dried. The pellet, corresponding to the linearized plasmid was resuspended in water at final concentration of 1 μg/μL.

In vitro transcription and DIG-labelling

For *in vitro* transcrption, a DIG-RNA labelling Kit was used (Roche). Plasmids linearized with Hind III were used as template for transcription from the T3 promoter, creating the sense probe, whereas EcoR I-digested plasmids were used for T7 transcrption, creating the antisense probe. The reaction took place in a total volume of DNA (1 μg/μL) 2 μL, 10x reaction buffer 2 μL, T7 or T3 enzyme 2 μL, RNAse OUT 1 μL, labelled nucleotide mix (dGTP, dCTP, dATP, dUTP) 2μL and

water 11 μL. The reaction mix was incubated for 2 h at 37°C. RNA was precipitated at -80°C for 30 min using EDTA (0.2M) 2 μL, LiCl (4M, RNAse free, Sigma) 2.5 μL, EtOH 100% 75 μL. Following centrifugation at 12500 rpm (4°C) for 30 min, the pellet was washed with EtOH 70% and centrifuged for further 10 min. The pellet was dried and resuspended in 10 μL water, before addition of 90 μL hybridisation (HS) buffer (deionised formamide 50% final volume, 20x SSC 5% final volume, salmon sperm 100 μg/ml, heparin 50 μg/ml, Triton X-100 0.1% final volume, fill up to final volume with water).

Preparation of the anti-DIG antibody

In order to minimize the background, anti-DIG-alcaline phosphatase antibodies were pre-absorbed using *Drosophila* embryos. Embryos were collected and dehydrated in EtOH overnight at -20°C. 100μL of these embryos were then washed in 1ml of a 1:1 mixture of EtOH and PBT (PBS 1x, 0.1% Tween-20) whilst shaking in order to rehydrate them. Then embryos were washed twice with 1ml PBT whilst shaking for 10 min. The anti-DIG antibody, cojugated to alcaline phosphatase was diluted 1:100 in PBT. 1 ml of this dilution was incubated with the rehydrated embryos overnight at 4°C. After removal of the embryos, the pre-absorbed antibody solution was aliquoted and then stored at 4°C.

In order to test the DIG-labelled probes, 2 μL of different probe concentrations were fixed by UV-croslinking on a nitrocellulose membrane. The membranes were then saturated with BSA (3% BSA in PBT) for 30 min at room temperature. Membranes were washed twice with PBT, followed by a 30 min wash in PBT whilst shaking. The antibody was then diluted in PBT, 0.5% BSA (1:2000) and incubated with the membrane for 30 min at room temperature. Afterwards, the membrane was washed twice with PBT followed by two washes with AP buffer (100mM TrisHCl pH 9.5, 100 mM NaCl, 50 mM MgCl2, 0.1% Tween-20, fill up with water to final volume). Coloration was achieved by adding NBT and BCIP

in AP buffer (Roche) according to the manufacturers instructions. The coloration reaction was then stopped by adding PBT.

Fixation, post-fixation and permeabilization of the tissues

Tissues from infected flies were dissected and kept in PBT (PBS, 0.1% Tween-20)-containing eppendorf tubes. To avoid RNA degradation tissues were kept on ice for maximum 30 min, and then PBT buffer was exchanged with fixation solution (280 μL PBT, 120 μL 10% formaldehyde and finally 500 μL heptan). Tubes containing the samples were shaked gently by turning the tube upside down (30-45 sec). The first fixation solution was replaced by second fixation solution (520 μL PBT, 240 μL 10% formaldehyde and 40 μL DMSO) and samples incubated for 20 min at room temperature. The fixed tissues are washed twice for 5 min with 1 mL MeOH. Samples can be stored in MeOH at -20°C for several weeks. Samples were post-fixed by exchange of the MeOH with 980 μL MeOH and 20 μL Hydrogen peroxyde and incubated for 30 min. They were washed three times with 1 ml PBT for 5 min. Tissues were then incubated for 30 min with 1 mL of PP buffer (PBS, 4% formaldehyde, 0.1% Triton-X100) and washed twice with 1 ml of PTX buffer (PBS, 0.3% Triton-X100). Finally, samples were incubated for 10 min in 500 μL of PTX and 500 μL of HS, followed by a 5 min wash with 1 ml HS.

Pre-hybridization and hybridization

Samples were pre-hybridized in 500 μL of HS buffer for 3 hours at 65°C. 400 μL of HS buffer was removed and 5 μL of the denatured DIG-labelled probe (following manifacturer's instructions) was added to the 100 μL of HS. Hybridization was done overnight at 65°C. After hybridization the samples were washed twice in pre-heated HS buffer at 55°C for 20 min. Then samples were washed three times for 20 min in 1 mL of HS/PBT (3 volume/ 1 volume) followed by HS/PBT (1 volume/ 1 volume) and finally HS/PBT (1 volume/ 3 volume) at 55°C. Samples

were then placed back at room temperature and washed four times for 10 min with 1 mL PBT. Then, samples were incubated with pre-absorbed anti-DIG antibody diluted 1:2000 in PBT for 1h at room temperature, followed by three 10 min washes in 1 mL of PBT.

Staining

Samples were washed twice for 5 min in AP buffer and transferred in 24 well plate. The coloration substrate for the alcaline phosphatase was prepared during the second wash by mixing 1 ml of AP buffer with 4.5 μL NBT (50mg/ml) and 3.5 μL BCIP (50 mg/mL). The substrate mixture was then applied to the samples and stored in dark until the coloration became apparent. The reaction was then stopped by adding PBT. Tissue samples were mounted in Glycerol 100% and analyzed under phase contrast microscope.

4.4 β-Galactosidase reporter assay

β-galactosidase activity was measured by fluorescent assay in 96-well plate. Individual flies were placed in each well and homogenized in 100 μL of Chalfie buffer, pH8 (Tris pH 8,4 10 mM, 100 mM NaCl, 1 mM $MgCl_2$; DTT 10 mM). Adding 4-methylumbelliferone β-d-galactopyranoside (MUG) allows the detection of β-galactosidase activity in the plate reader Fluoroscan.

4.5 Protein analysis

4.5.1 Antibody generation

Antiserum directed against the protease Jon65Ai was obtained after injection of the peptide NH2-IGNSVCENYYGSFSGDLICIPTPENK-OH in two rabbits

(BSYN5165 an BSYN5166) by the company BIOSYNTHESIS. Pre-immune, 6, 8 and 10 weeks bleeds were taken from the rabbits, aliquoted and stored at -80°C. For Western blot experiments, the antiserum Jon65Ai BSYN5165, 8 weeks bleed was used at the optimal dilution of 1:200.

4.5.2 Protein extraction and quantification

For Western blot analysis samples were homogenized in lysis buffer (20 mM Tris pH 7.5, 150 mM NaCl, 1% Trition-X100 and 1 dose of protease inhibitor cocktail complete mini (Roche)). 5 whole flies, guts and fat bodies from 10 flies were homogenized in 150 μL of lysis buffer. Brains and cardias from 50 flies were homogenized in 75 μL of lysis buffer. Proteins were quantified by Bradford Protein assay (Biorad). BSA was used to generate a standard curve ranging from 0 μg/mL to 21 μg/ml. Samples were mixed with 10 μL of 5x Laemmli loading buffer (400 mM Tris Base, 8% LiDS, 30% Glycerol, 408 mM MAC, 0.1% bromophenol blue, final pH 6.8), incubated at 95°C for 5 min and applied to 12% SDS-PAGE gel.

4.5.3 Western blot

Migration of samples was done in 1x TCG buffer (Tris/ glycine/ SDS Buffer, Biorad) for 90 min at 90 V. Proteins were transferred under standard conditions to nitrocellulose membrane for 90 min at 100 V under agitation using a commercially available blotting buffer (Biorad). The membrane was saturated in TBST 2x 3% milk (Biorad) for 1 h at RT (10x TBST pH 7.6 containing TrisHCl pH 7.2 100 mM, NaCl 90 g/L and 0.5% Tween-20). After two washes with TBST 2x and the primary antibody was incubated overnight at 4°C in TBST 2x 0.3% milk . The membrane was washed twice for 10 min with TBST 2x and the secondary antibody was added in TBST 2x for 1 h at room temperature. After incubation, the

membrane was washed three times with TBST 2x and proteins on the blot were visualized with ECL Chemiluminescent Detection reagents (Amersham) according to the manufacurer's instructions. Polyclonal rabbit antiserum directed against DCV was used in a dilution of 1:5000. The anti-actin monoclonal antibody (Millipore) was used at the dilution of 1:2500. Secondary antibodies aganist mouse or rabbit (Fisher Scientific) conjugated to horseradish peroxidase were used at the dilutions of 1:5000 and 1:10000 respectively.

4.6 Microarray analysis

For microarray analysis, 45 males OregonR flies were injected with Tris, DCV, FHV and SINV. RNA extraction, biotinylation and hybridization to Affymetrix *Drosophila* GeneChip microarrays (Affymetrix) were done as described [Irving et al., 2001]. The Affymetrix Microarray Suite 5.0 (Affymetrix) or Excel (Microsoft) were used for data analysis. Raw data were sorted with the "absent-marginal-present flags" generated by the Microarray Suite functions. For the gene repression analysis, only data points for marked as "present" were retained for the Tris controls with P value ≤ 0.05.

4.7 Dissections and staining of *Drosophila* tissues

4.7.1 Oil Red O staining

Fat bodies from virus-infected or control flies 3 days post-injection, were dissected in PBS 1x and fixed in 4% paraformaldehyde for 20 min. Samples were then incubated for 30 min in the Oil Red O stain (6 mL of 0,1 % Oil Red O (SIGMA) in isopropanol and 4 mL of MilliQ water, filtered through 0.45 μm syringe filter) and quickly washed with MilliQ water [Gutierrez et al., 2007]. Samples were then mounted in 100 % Glycerol and observed under phase contrast microscope.

4.7.2 Calcofluor staining

Calcofluor (Fluorescent Brightener 28, F3543, SIGMA) solution was prepared at 1% in MilliQ H_2O. 1.5 mL of Sucrose 1% solution was mixed with 500 μL of Calcofluor 1% solution and added to filterpaper pad (Millipore) placed in a vial. Virus-infected or control flies were placed 96h folloing injection on this solution no longer than 6 hours to avoid destruction of the peritrophic matrix. Digestive tracts were dissected in PBS 1x and fixed for 20 min in 4% paraformaldehyde for 30 min. Samples were washed 3 times for 10 min with PBS 1x, mounted in 100 % Glycerol and observed under fluorescent microscope.

4.7.3 Immunostaining

For immunostaining experiments, tissues were dissected in PBS 1x and fixed for 30 min in 4% paraformaldehyde under agitation. Tissues were next permeabilized in three successive washes in PBS- 0.01% Triton-X100. Samples were placed in the blocking solution PBT-A (PBS-0.01% Triton-X100, 0.5% BSA) for 1 hour. Tissues were incubated with primary antibodies overnight at 4°C. The removal of execcive primary antibody was done by two successive washes, 15 minutes each in PBT-B buffer (PBS-0.01% Triton-X100, 0.05% BSA). Samples were incubated with fluorescent molecules-conjugated secondary antibodies in PBT-B for 4 hours at room temperature. Before mounting of the tissues in Vectashield DAPI-containig medium, samples were washed three times in PBT-B. The primary antibodies were used at the following dilutions: mouse anti-Cyp4g1 (gift of S. Kennel) 1:500, rabbit anti-Akh (gift from S. Kim) 1:300, rabbit anti-VP2 of DCV 1:500, mouse anti-GFP 1:500, rabbit anti-FHV capsid protein 1:1000, mouse anti-ATP synthase subunit α (Mitoscience, MS507) 1:500. The actin-staining Texas Red-X phalloidin (Invitrogen, T7471) was used at 0,066 μM. The secondary antibodies were used at the following dilutions: Alexa 488 goat anti-mouse IgG (A11001,

Invitrogen) 1:500, goat anti-mouse IgG, Cy3-linked (PA43002, GE Healthcare) 1:500, Cy3 goat anti-rabbit IgG (81-6115, Zymed) 1:500, Alexa 488 goat anti-rabbit IgG (A11003, Invitrogen) 1:500.

4.8 Measurment of physiological parameters

4.8.1 Colorimetric food ingestion and defecation rate assays

Three groups of 10 flies were Tris or virus injected and placed on 0,1% Bromophenol blue and 0,5% xylen cyanol containing "tracking" medium. For food ingestion experiment, flies were collected 96h post-injection, homogenized in 1xTris-EDTA buffer containing 0,1% Triton-X100 and centrifuged at 14000 rpm for 3 min. The OD of the supernatants was measured, as previously described [Ayres and Schneider, 2009]. For defecation assay, Tris or virus-injected flies were kept on the "tracking" medium for 3 days, and then transferred in empty vials for 5h. The blue excretion spots, corresponding to fly defecation rate were counted.

4.8.2 CApillary FEeder (CAFE) assay

Virus-infected or control flies were transferred 72h post-infection to 24 well plate. Single fly was placed in individual well, filled with 500 μL of 1% agarose to provide moisture. One capillary, filled with 10 μL of 5% Sucrose and 2% Yeast extract (Yeast extract ultrafiltrate 50x, Y-4375, SIGMA) solutions was provided per well [Ja et al., 2007]. Flies were capillary fed for 24h and the volume of ingested food was measured for individual flies. The experimental set up is shown on Figure 4.1.

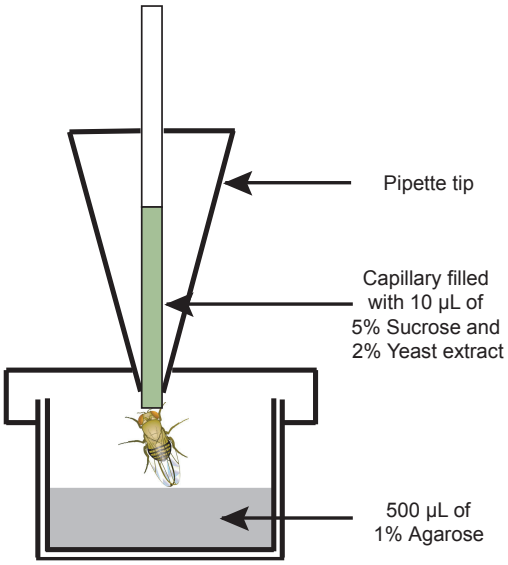

Figure 4.1: CApillary FEeder assay: experimental set up .

4.8.3 Measurment of body weight, total glucose and tryglycerides levels

A group of 10 (5 male and 5 female) Tris or virus-injected flies was weighted for body weight determination. Triglycerides (TG) and glucose (Glc) in Tris or virus-infected flies were measured with Infinity Triglycerides and Glucose Hexokinase kits (Thermo scientific). Before extraction, the body weight of the three groups of 5 female flies was determined and used for normalization. For TG measurement, flies were homogenized in 1ml of PBS, containing 0,05% Tween-20. Samples were incubated for 5 min at 70°C. 500 μL of the supernatant was transferred into a new tube and centrifuged for 3 min at 14000 rpm. 50 μL of the supernatant was distributed per well of 96 micro titer well plates, to which were added 200 μL of Infinity TG kit. The plate was incubated for 5 min at 37°C and the O.D$_{540}$ measured. For Glc titers determination, flies were homogenized in 200 μL of 1x Tris-EDTA buffer, supplemented with 0,1% Triton X-100, centrifuged for 3 min at 14000 rpm and 100 μL of the supernatant was transferred into the wells of 96 well micro titer plates. 100 μL of Infinity Glucose Hexokinase kit, supplemented

with of porcine kidney trehalase (Sigma, T8778) were added to each well and the $O.D_{340}$ measured. For both TG and Glc measurements, standard curves were generated according to the manufacturer instructions.

4.8.4 Statistical analysis

An unpaired two-tailed Student's *t*-test was used to determine statistical significance. *P*-values of less than 0.05 were considered significant. Data were analyzed using GraphPad Prism 4 for Macintosh (GraphPad software.Inc).

Part III

Results

Aims of the study

The general aim of my PhD work was to study the physiopathological mechanisms that underlie the resistance to virus infection in the fruit fly *Drosophila* after infection with two small, positive single stranded RNA viruses: the *Drosophila* C virus (DCV) and the Flock House virus (FHV). In addition to the innate immune response that controls the resistance to virus infection, homeostatic mechanisms also contribute to the control of the cellular and tissue damage caused by the pathogen. Collaborative studies between the laboratories of Prof. Jean-Luc Imler here in Strasbourg and Prof. Bruce Beutler at the Scripps Research Institute in La Jolla, California, USA, identified a mutation affecting an inwardly rectifying ATP-sensitive potassium channel K_{ATP} that causes rapid mortality of mice and flies after viral infection. In flies, the impairment of the cardiac expression of the regulatory subunit of the channel encoded by the gene *dSUR* accelerated the death of the flies after infection with the RNA virus FHV. During my thesis, I participated to the description of the role played by K_{ATP} channels in the resistance to FHV infection. We identified a novel tissue-specific and K_{ATP}-dependent regulation of antiviral immunity. This part of my work is discussed in Chapter 5.

Prior to my arrival in the lab, a comparative study of the transcriptome of infected flies showed that several hundred of genes are repressed in DCV-infected flies, compared to FHV and another RNA virus: Sindbis virus (SINV). The initial aim of my PhD work was to focus on a subset of the DCV-repressed genes, encoding midgut specific serine proteases and to study their role in antiviral defenses. Very rapidly my work on this project showed that the strong gene repression might reflect disturbances in the digestive physiology of the fly after infection with the virus. I characterized the pathology associated with DCV infection and the results of this part of my work are shown in Chapter 6.

Chapter 5

K_{ATP}-sensitive potassium channels and resistance to cardiotropic viral infections

The fruit fly *Drosophila melanogaster* represents a good experimental system to decipher the complex issues of homeostasis in virus-infected animals. This model could also provide an integrative view at the level of the whole organism of the complex interactions between viruses and their hosts.

5.1 K_{ATP}-sensitive potassium channels regulate antiviral innate immunity

We previously showed that SUR channels regulate survival to virus infection in mice and flies. In mice K_{ATP} channels regulates vasoconstriction, essential for homeostasis mechanism to temper effects of the inflammatory cytokines induced by infection. We were curious to understand the role of dSUR in FHV-infected flies since flies and mammals have very different physiologies. We took advantage of the availability of genetic and pharmacological tools to get further insights into

the role, played by the cardiac K_{ATP} channel in FHV-infected *Drosophila*. We showed that the impairment of the K_{ATP} channel controls the resistance to FHV in the *Drosophila* heart by acting on the antiviral RNAi pathway. The data we obtained in the invertebrate model were strongly supported by the results in the mammalian model, in which the *mayday* mutant mice showed higher viral loads in the heart, after infection with the cardiotropic Coxsakievirus B3.

The following article describes our findings and reveal a novel role for K_{ATP} channels in the control of viral infections in the heart.

ATP-sensitive potassium channel (K_{ATP})–dependent regulation of cardiotropic viral infections

Ioannis Eleftherianos[a,1], Sungyong Won[b], Stanislava Chtarbanova[a], Barbara Squiban[a], Karen Ocorr[c], Rolf Bodmer[c], Bruce Beutler[b], Jules A. Hoffmann[a,2], and Jean-Luc Imler[a,d]

[a]Centre National de la Recherche Scientifique, Unité Propre de Recherche 9022, Institut de Biologie Moléculaire et Cellulaire, Université de Strasbourg, 67 084 Strasbourg Cedex, France; [b]Department of Genetics, The Scripps Research Institute, La Jolla, CA 92037; [c]Development and Aging Program, Sanford–Burnham Medical Research Institute, La Jolla, CA 92037; and [d]Faculté des Sciences de la Vie, Université de Strasbourg, 67 081 Strasbourg Cedex, France

Contributed by Jules A. Hoffmann, June 5, 2011 (sent for review April 18, 2011)

The effects of the cellular environment on innate immunity remain poorly characterized. Here, we show that in *Drosophila* ATP-sensitive potassium channels (K_{ATP}) mediate resistance to a cardiotropic RNA virus, Flock House virus (FHV). FHV viral load in the heart rapidly increases in K_{ATP} mutant flies, leading to increased viremia and accelerated death. The effect of K_{ATP} channels is dependent on the RNA interference genes *Dcr-2*, *AGO2*, and *r2d2*, indicating that an activity associated with this potassium channel participates in this antiviral pathway in *Drosophila*. Flies treated with the K_{ATP} agonist drug pinacidil are protected against FHV infection, thus demonstrating the importance of this regulation of innate immunity by the cellular environment in the heart. In mice, the Coxsackievirus B3 replicates to higher titers in the hearts of *mayday* mutant animals, which are deficient in the Kir6.1 subunit of K_{ATP} channels, than in controls. Together, our data suggest that K_{ATP} channel deregulation can have a critical impact on innate antiviral immunity in the heart.

ion channel | myocarditis | potassium efflux | aging | tolbutamide

Viral infections represent a major threat for living organisms, from prokaryotes to complex eukaryotes, including humans. Therefore, the characterization of the cellular and molecular mechanisms determining the outcome of viral infections is a focus of intense investigation.

A primary determinant of survival to virus infection in animals is the innate immune response, which allows the host to interfere with viral replication and to control the viral load (1). Considerable efforts on different experimental models have led to the realization that dsRNAs, which are produced in the course of viral replication, are a major trigger of innate antiviral responses. In vertebrates, foreign dsRNA molecules are recognized by proteins of the Toll-like receptor (TLR) and RIG-I–like receptor (RLR) families, leading to the production of type I and III interferons, which in turn mediate induction of antiviral molecules (2). In both plants and invertebrates, dsRNAs are recognized by RNase III enzymes of the Dicer (Dcr) family, and trigger antiviral RNAi (3). Interestingly, the cytosolic RLRs and the Dicer enzymes share an evolutionary conserved DExD/H box helicase domain, revealing some similarities in the sensing of viral nucleic acids by plants, invertebrates, and vertebrates (4). In the fruit fly *Drosophila melanogaster*, Dcr-2 accounts for the production of siRNAs of viral origin, which are loaded on the Argonaute (AGO) protein family member AGO2, with the help of the dsRNA binding protein R2D2. These siRNAs guide the slicer enzyme AGO2 toward cRNA sequences, thus achieving antiviral silencing. In agreement with the essential roles of Dcr-2 and AGO2 in the siRNA pathway, flies mutant for these genes are highly susceptible to viral infections (5–7). Though our information on the biochemistry of RNA interference is rapidly expanding, a central and as yet poorly explored area is the control of RNA interference by the cellular environment.

In addition to the immune response, which controls the viral load, it is becoming apparent that homeostatic mechanisms enable the host to control the cellular or tissue damage caused by a given dose of virus (8, 9). In the course of a collaborative effort aimed at understanding the genetic basis of antiviral defenses, one of our groups recently identified an *N*-ethyl-*N*-nitrosourea (ENU)-induced strain of mutant mice, *mayday*, which show an increased frequency of sudden death upon infection with the mouse cytomegalovirus (MCMV). These mice produce normal levels of cytokines upon infection, and die with viral titers in the spleen similar to wild-type controls, indicating that their death does not result from a failure to control the viral burden (9). The *mayday* mutation is an allele of the gene *Kcnj8*, which encodes the inwardly rectifying ATP-sensitive potassium (K_{ATP}) channel Kir6.1. K_{ATP} channels are octameric complexes composed of four pore-forming Kir subunits and four sulfonylurea receptor (SUR) subunits that regulate the opening of the channel (10) (Fig. 1*A*). In mice, these channels allow smooth muscle cells in coronary arteries to adapt to the vasoconstriction triggered by the inflammatory cytokines produced by the innate immune system in response to infection (9, 11). K_{ATP} channels are evolutionarily ancient, and we previously reported that silencing of the SUR ortholog (dSUR) in the *Drosophila* heart reduces the survival following infection by the RNA virus Flock House virus (FHV) (9). This observation suggests that K_{ATP} channels play an evolutionarily conserved role in host–virus interactions, and raises the question of the exact mechanism by which they regulate survival to viral infection in organisms with physiologies as different as flies and mammals.

Here we have characterized the role of K_{ATP} channels in FHV-infected *Drosophila*. Using both genetics and pharmacology, we show that K_{ATP} channels are involved in an antiviral resistance mechanism, as impairment of their expression or function leads to a strong increase of the viral titer and accelerated death of the FHV-infected flies. We further show that FHV is a cardiotropic virus and that K_{ATP} channels control the FHV viral load in the heart. Potassium efflux does not affect an intrinsic property of the viral replication cycle, but rather modulates antiviral RNA interference in the heart. These results indicate that tissue-specific regulation of resistance mechanisms by the cellular environment can have dramatic consequences on the outcome of an infection. We illustrate this point by showing that the K_{ATP} agonist drug pinacidil exerts a spectacular protective effect against FHV infection in *Drosophila*.

Author contributions: I.E., S.W., K.O., R.B., B.B., J.A.H., and J.-L.I. designed research; I.E., S.W., S.C., B.S., and K.O. performed research; I.E., S.W., S.C., B.S., K.O., R.B., B.B., J.A.H., and J.-L.I. analyzed data; and I.E., S.W., S.C., B.B., J.A.H., and J.-L.I. wrote the paper.

The authors declare no conflict of interest.

[1]Present address: Department of Biological Sciences, George Washington University, Washington, DC 20052.

[2]To whom correspondence should be addressed. E-mail: j.hoffmann@ibmc-cnrs.unistra.fr.

This article contains supporting information online at www.pnas.org/lookup/suppl/doi:10.1073/pnas.1108926108/-/DCSupplemental.

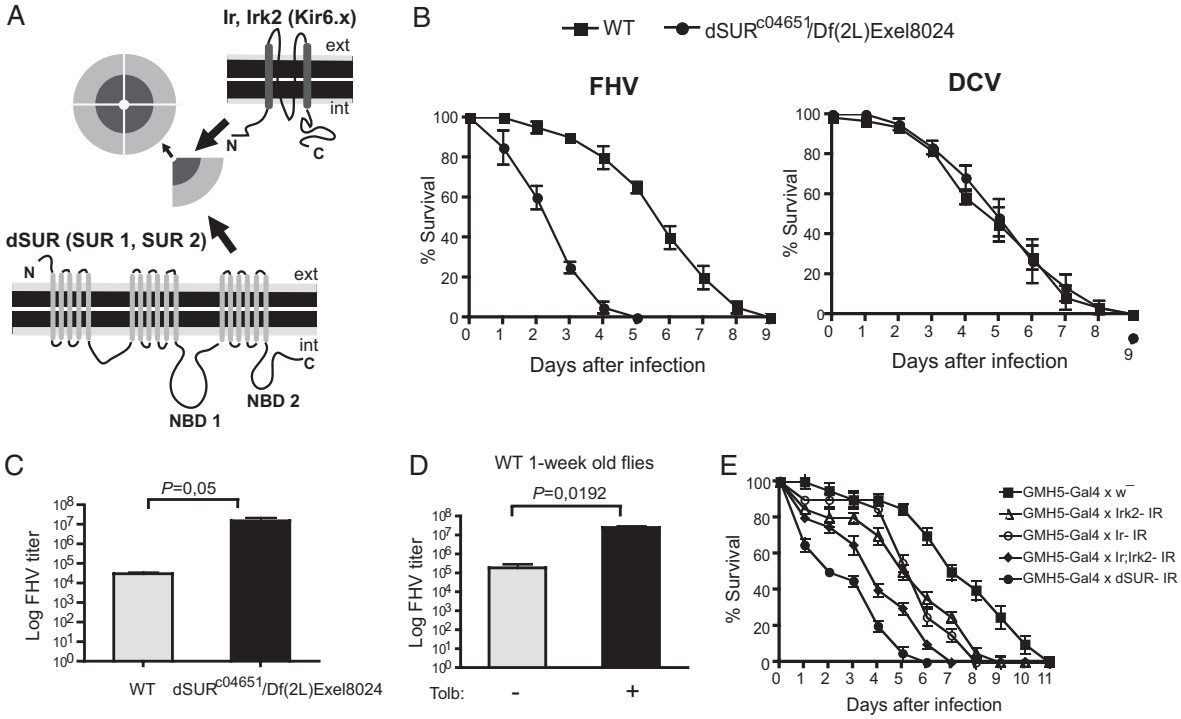

Fig. 1. dSUR, Ir, and Irk2 are important for resistance to FHV infection in *Drosophila*. (*A*) Structural organization of the cardiac K_{ATP} channel. Kir and SUR are the constitutive subunits of the cardiac K_{ATP} channel. Four subunits of the inwardly rectifying K^+ channel, encoded by the genes *Ir* or *Irk2*, associate with the ABC regulatory protein encoded by *dSUR*, to form a functional K_{ATP} channel octamer. SUR possesses two cytoplasmic nucleotide binding domains (NBD1 and NBD2). The names of the mammalian orthologs are given in parentheses. (*B*) Survival curves of *dSUR* mutant and control flies after infection with 2×10^6 pfu/mL FHV or 2×10^6 DCV particles of a dose lethal to 50% of flies tested, per milliliter. (*C*) FHV titers in *dSUR* mutant and control flies at day 3 following virus infection. (*D*) FHV titers in wild-type (WT) 1-wk-old flies fed on the K_{ATP} antagonist tolbutamide and control flies fed on sucrose solution only, at day 3 following virus infection. (*E*) Survival curves of flies obtained from crosses between UAS-*dSUR* RNAi, UAS-*Ir* RNAi, UAS-*Irk2* RNAi, and UAS-*Ir*;*Irk2* RNAi lines (IR, inverted repeat) with the heart-specific GMH5-Gal4 driver and control flies [GMH5-Gal4 line crossed with white (w^-) flies] after infection with FHV. Data represent the mean ± SDs of three (*C* and *D*) or two (*B* and *E*) independent experiments each involving two groups of 10 flies.

Results

***Drosophila* K_{ATP} Channels Are Involved in the Resistance to FHV Infection.** We previously reported that knockdown of the expression of the gene *dSUR*, which encodes the regulatory subunit of K_{ATP} potassium channels (Fig. 1*A*), increases the lethality of *Drosophila* after infection with FHV (9). Flies mutant for *dSUR* [c04651/Df(2L)Exel8024] are viable, indicating that *dSUR* does not carry essential developmental functions. When infected with FHV, *dSUR* mutant flies succumb rapidly, 4–5 d before control flies. By contrast, these mutant flies do not show increased lethality compared with controls when challenged with *Drosophila* C virus (DCV), the entomopathogenic bacteria *Enterococcus faecalis*, *Enterobacter cloacae*, or the fungus *Beauveria bassiana* (Fig. 1*B*) (9). To see if the rapid death of FHV-infected *dSUR* mutant flies reflects a defect in homeostasis or resistance, we monitored the viral load in *dSUR* mutant and control flies. *dSUR* mutant flies show increased accumulation of viral RNAs, and contain up to two logs more infectious viral particles than control flies 3 d after infection, indicating that dSUR regulates the resistance to FHV infection (Fig. 1*C*). Consistent with the survival data, DCV-infected *dSUR* mutant flies contain similar viral titers as control flies.

As an independent test of the requirement for K_{ATP} channels during infection, we investigated the effect of the drug tolbutamide, which acts as an antagonist of K_{ATP} channels. We previously reported that flies fed on a tolbutamide solution died more rapidly than control flies after infection with FHV (9). The tolbutamide treatment leads to increased accumulation of viral RNAs and infectious particles in infected flies, with a two-log increase in viral load 3 d after infection (Fig. 1*D*).

SUR molecules function as the regulatory subunit of Kir6.x channels in mammals. The *D. melanogaster* genome contains three genes encoding channels related to mammalian *Kir* genes, known as *Ir*, *Irk2*, and *Irk3* (Fig. S1*A*). Among these, *Ir* and *Irk2* are closely related to one another, and belong to the same clade as mammalian *Kir2*, *Kir3*, *Kir5*, and *Kir6*, whereas *Irk3* is more distantly related to these molecules. Based on their expression in the hindgut and the Malpighian tubules, these genes have been proposed to function in the osmoregulation of the fly (12). We monitored expression of *Ir* and *Irk2* by RT-PCR, and found that these genes are indeed expressed in the excretory system of *Drosophila*, but that they are mainly expressed, like *dSUR*, in the heart (Fig. S1*B*). We knocked down expression of these genes in the heart using the heart-specific GMH5-Gal4 driver (13), and observed that both *Ir* and *Irk2* are required to slow infection by FHV (Fig. 1*E*). Knockdown of both *Ir* and *Irk2* caused a more severe phenotype than single knockdowns, but not as severe as the knockdown of dSUR. By contrast, silencing of *Irk3* expression did not affect resistance to FHV infection (Fig. S1*C*).

Overall, both genetic and pharmacological data point to an essential role for K_{ATP} channels in the resistance to FHV infection, raising the question of the mechanism involved.

FHV Is a Cardiotropic Virus. We monitored the presence of virus in the heart of infected wild-type flies by immunofluorescence, and observed that FHV efficiently infects heart muscle cells. By contrast, we did not detect the presence of DCV in the heart, even though the virus can readily be observed in surrounding fat body cells (Fig. 2*A*). Typical FHV-induced changes in the morphology of mitochondria (14) were observed in longitudinal fibers and cardiomyocytes (Fig. 2*B*). We noted a more rapid accumulation of FHV capsid proteins in the heart of *dSUR*-silenced flies compared with controls (Fig. S2*A*). Similar results were obtained when the amount of viral RNAs in the heart or the rest of the body was monitored by quantitative RT-PCR (Fig. 2*C*). Finally, tolbutamide treatment of wild-type flies led to an increase of FHV viral RNAs mostly in the heart (Fig. 2*D*) and to increased viremia at the early time points of infection (Fig. 2*E*). Together, these data indicate that FHV is a cardiotropic virus and that dSUR participates in a tissue-autonomous manner in the control of viral load in the heart, thus limiting viremia and spreading to other tissues.

K_{ATP} Channels Regulate Antiviral Innate Immunity in the Heart. To test whether potassium efflux regulates FHV infection at the level of viral replication, as opposed to other steps of the viral cycle, such as viral entry, viral uncoating, or capsid synthesis and assembly, we used a transgenic viral replicon. In this system, sequences corresponding to RNA1 from FHV and encoding the viral RNA-dependent RNA polymerase (RdRP) are placed under the control of the UAS_{Gal4} system in transgenic flies (Fig. S2*B*). We previously reported that RNA1 produced from this transgene, even at low levels (in the absence of a Gal4 driver), is rapidly amplified due to the expression of the viral RdRP (5). We monitored RNA1 expression by quantitative RT-PCR in UAS-FHV RNA1 transgenic flies treated with tolbutamide and untreated controls, and observed a strong increase in the levels of RNA1 in the treated flies. The majority of the increase of RNA1 in flies treated with the drug was attributed to the heart (Fig. S2*C*). Thus, K_{ATP} channels act at the level of the accumulation of viral RNAs in infected cells.

To test whether K_{ATP} channels have a direct effect on the viral polymerase or affect the host resistance to infection, we analyzed the effect of tolbutamide on FHV-infected flies carrying mutations in essential genes of the antiviral RNAi pathway. Whereas addition of tolbutamide resulted in an increase by two orders of magnitude in the FHV titer in wild-type flies, it had no effect in *Dcr-2*, *AGO2*, or *r2d2* mutant flies (Fig. 3*A*). Consistent with these data, tolbutamide treatment did not aggravate the survival of *Dcr-2*, *AGO2*, or *r2d2* mutant flies infected by FHV (Fig. S3*A*). We then tested for a genetic interaction between *AGO2* and *dSUR*. For this, we compared the resistance to FHV infection (survival and viral load) of flies heterozygous for *AGO2* and *dSUR*, as well as flies double heterozygous for both *AGO2* and *dSUR*. Flies heterozygous for both *AGO2* and *dSUR* die more rapidly (Fig. S3*B*) and contain higher viral loads than flies heterozygous for one of the mutants (Fig. S3*C*), pointing to a genetic interaction between *AGO2* and *dSUR*. Similar results were observed when *Dcr-2* was used instead of *AGO2* (Fig. S3 *D* and *E*). These data reveal that cardiac potassium channels do not affect an intrinsic property of the viral RdRP, but rather affect the antiviral RNAi pathway.

The K_{ATP} Agonist Drug Pinacidil Protects Flies Against FHV infection. Based on our findings, we reasoned that drugs activating potassium channels in the *Drosophila* heart may exert protective effects upon FHV infection. We investigated the effect of the K_{ATP} agonist drug pinacidil, and did not observe an effect in our standard assay conditions with young flies (1 wk old; Fig. S4*A*).

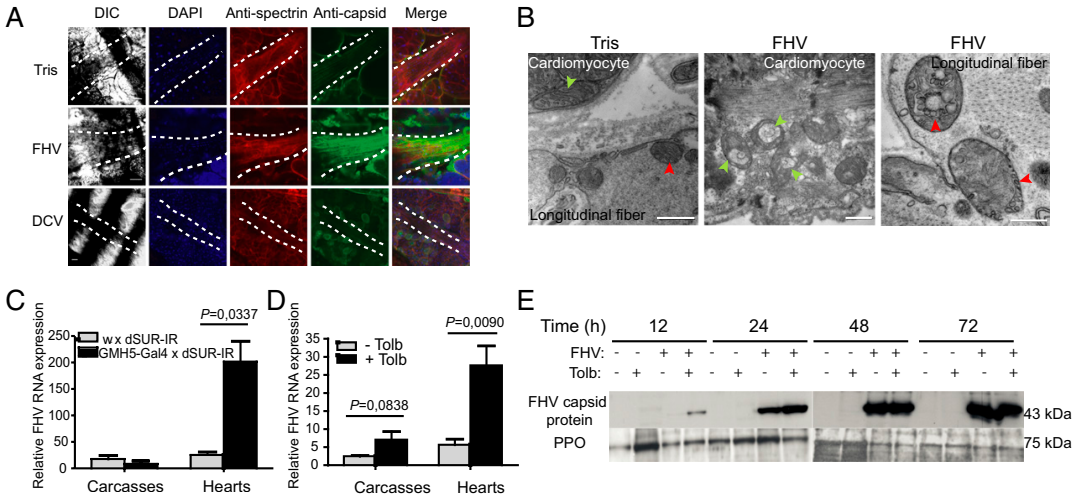

Fig. 2. FHV, but not DCV, infects the *Drosophila* heart. (*A*) Confocal microscopy of the colocalization of spectrin and FHV or DCV in the hearts of virus-infected WT 1-wk-old flies double-labeled with anti-spectrin (red; Alexa Fluor 546) and antibody to viral capsid protein (green; Alexa Fluor 488) at 3 d following virus challenge. Injections with Tris buffer were used as negative controls. Data are representative of three experiments with at least 10 flies for each treatment. (Scale bar: 35 μm.) (*B*) Electron micrographs showing FHV-induced spherular invaginations of the outer mitochondrial membrane (arrowheads) of infected, but not control (Tris) cardiomyocytes (green arrowheads) and longitudinal fibers (red arrowheads) that are associated ventrally with the *Drosophila* heart (33). (Scale bar: 500 nm.) (*C*) Quantitative RT-PCR of FHV RNA levels in the hearts and carcasses from *dSUR*-silenced flies and control flies at 3 d after virus infection. (*D*) Quantitative RT-PCR of FHV RNA levels in the hearts and carcasses from WT 1-wk-old flies fed on the K_{ATP} blocker tolbutamide and control flies fed on sucrose solution only, at day 3 following infection with FHV. For *C* and *D*, data represent the mean ± SD of three independent experiments involving at least 30 flies per replicate. (*E*) Immunoblot for expression of FHV capsid protein in the hemolymph of 1-wk-old WT flies treated with tolbutamide and control flies kept on sucrose solution only at different times after virus infection. Prophenoloxidase (PPO) protein levels in the hemolymph of flies served as a loading control. Data are representative of two independent experiments involving at least 30 flies for each treatment.

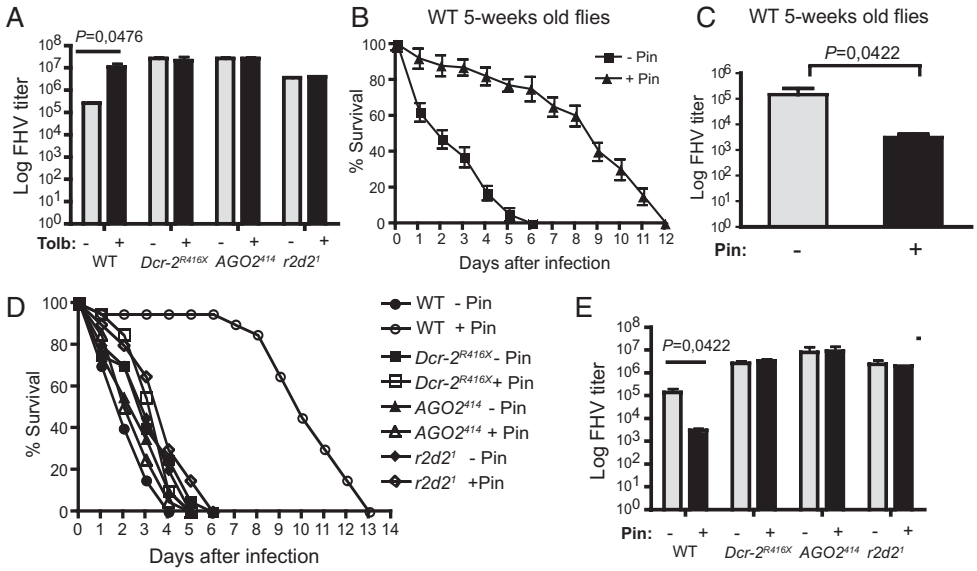

Fig. 3. Potassium channels regulate antiviral RNA interference in the *Drosophila* heart. (*A*) FHV titers in 1-wk-old *Dcr-2*, *Argonaute-2* (*AGO2*), *r2d2* mutant, and WT control flies at day 3 following feeding on tolbutamide or control sucrose solution alone and virus infection. (*B*) Survival curves of WT 5-wk-old flies fed on the K_{ATP} agonist pinacidil and control flies fed on sucrose solution alone after infection with FHV. (*C*) FHV titers in WT 5-wk-old flies fed on pinacidil and control flies fed on sucrose solution alone at 3 d following virus infection. (*D*) Survival curves of 5-wk-old *Dcr-2*, *AGO2*, *r2d2* mutant, and WT control flies following treatment with pinacidil and infection with FHV. (*E*) FHV titers in 5-wk-old *Dcr-2*, *AGO2*, *r2d2* mutant, and WT control flies at day 3 after feeding on pinacidil or sucrose solution and virus infection. Data represent the mean ± SD of three independent experiments each involving at least 30 flies (viral load) or two groups of 10 flies (survival) per treatment.

Previous work has shown that *dSUR* expression decreases with aging, and that this decrease in *dSUR* expression is associated with increased pacing-induced heart failure (15). We monitored resistance to FHV infection in aging flies, and observed a strong effect of aging on resistance to FHV infection (Fig. S4*B*). In particular, 5-wk-old wild-type flies were highly susceptible to FHV infection, with 50% of the flies dying within the first 24 h of the infection, reaching 100% mortality in 5–6 d. We treated 5-wk-old flies with pinacidil 3 h before infection with FHV, and observed a dramatic increase in their survival (Fig. 3*B*). Pinacidil treatment of *dSUR* knockdown old flies did not protect them against FHV infection, confirming that the drug was acting on K_{ATP} channels and not on other targets (Fig. S4*C*). Pinacidil-treated old, wild-type flies, but not *dSUR* knockdown old flies, exhibited a significantly reduced viral load compared with old control flies, indicating that the drug strongly increased the resistance to infection (Fig. 3*C* and Fig. S4*D*). Five-wk-old flies also died more rapidly than young flies when challenged with DCV or bacteria. In these cases, however, pinacidil treatment had only weak or no effect on the survival of the flies (Fig. S5 *A*–*C*).

Pinacidil treatment did not improve the resistance to FHV infection of *Dcr-2*, *AGO2*, and *r2d2* null mutant flies, indicating that a functional antiviral RNAi pathway is required for the effect of the drug (Fig. 3 *D* and *E*). These results confirm that potassium channels regulate innate immunity in the heart, and reveal that the K_{ATP} agonist drug pinacidil can be used to protect flies against a cardiotropic virus.

Mammalian K_{ATP} Channels Are Involved in the Control of Coxsackievirus B3 (CVB3) Infection in the Heart. Because K_{ATP} channels limit a cardiotropic infection in flies, we decided to test the importance of mammalian *Kcnj8* in the containment of a cardiotropic infection in mice. We assessed virus loads in the heart and serum of *mayday* mutants compared with WT C57BL/6J mice. Mice were infected with 500 pfu of CVB3 i.p., and virus loads were compared at 3 d postinfection (dpi). Though there was no significant difference in viremia between *mayday* and control mice, a significant increase in virus load in heart tissue was observed in both homozygous and heterozygous *mayday* mutants, compared with the control mice (Fig. 4). We note that exaggerated CVB3 proliferation is observed even in heterozygous *mayday* mutant mice, whereas the deleterious effect of the *mayday* mutation (hypersensitivity to MCMV infection or LPS administration, leading to acute lethality) is strictly recessive (9). The cellular mechanism of the antiviral effect may therefore be quite different from the cellular mechanism of protection against coronary artery vasoconstriction, despite the likelihood that the same hetero-octameric channel complex mediates both phenomena.

Discussion

Our findings reveal that the evolutionarily conserved cardiac K_{ATP} channels play an essential role in the resistance to infection by the cardiotropic RNA virus FHV in *Drosophila*, through modulation of RNA interference. RNAi plays a major role in the regulation of several biological processes, including the control of infections. As such, it does not come as a surprise that RNA silencing must be regulated. Indeed, it was recently reported that molecules from the RNAi pathway, such as TRBP, AGO, or PIWI, can be regulated by phosphorylation, hydroxylation, or methylation (16). We now show that ion channels can also affect antiviral RNAi. It will be interesting in future studies to investigate whether potassium channels also regulate other RNAi pathways in the heart, such as the miRNA or the endosiRNA pathway, which may regulate heart physiology in the absence of viral infection (17).

K_{ATP} channels were previously shown to play a role in the survival to viral infection in mice, but through a different mechanism—namely, the modulation of the response to cytokines in coronary

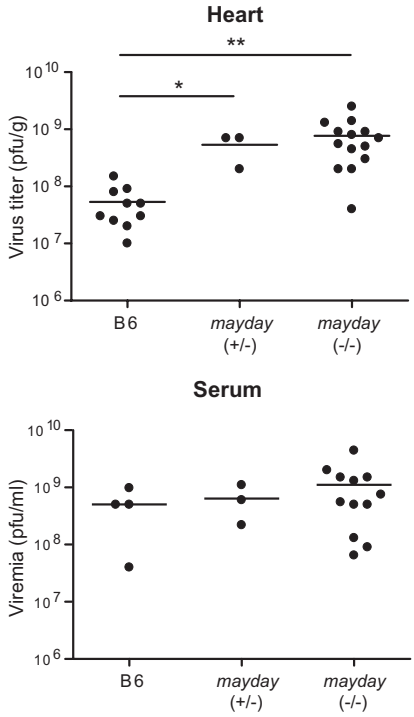

Fig. 4. Higher virus load in the heart of *Kcnj8* (*mayday*) mutant mice. Eight-wk-old *mayday* and C57BL/J control mice were infected with 500 pfu of CVB3 i.p. At 3 dpi, mice were bled for sera, and hearts were collected after perfusion. Virus titers were determined by the plaque assay on HeLa cells. $*P = 0.0001$, $**P = 0.0020$.

arteries (9, 11). This discrepancy may reflect the differences existing between insects and mammals both at the level of antiviral innate immunity (e.g., the prominent role of RNAi in flies vs. IFN-mediated inducible response in mammals) and host physiology (e.g., the important effect of inflammatory cytokines on the vasculature in mammals). An alternative hypothesis is that K_{ATP} channels may play a previously unnoticed dual role in virus–host interactions, modulating the effects of cytokines and also participating in the regulation of innate immunity mechanisms.

K^+ ions have previously been shown to regulate the induction of the NRLP3 inflammasome, which converts procaspase-1 into active caspase-1, an important aspect of the innate immune response (18). The inflammasome processes prointerleukin (IL)-1β into the active 17-kDa IL-1β inflammatory cytokine. One signal activating the NRLP3 inflammasome is the extracellular release of ATP, which activates the purinergic receptor P2X7R, leading to K^+ efflux and NRLP3 inflammasome activation. Treatment of cells with the K^+ ionophore toxin nigericin is sufficient to trigger the NRLP3 inflammasome, pointing to the important role of potassium ions in the regulation of the production of the essential inflammatory cytokine IL-1β. Interestingly, the sulfonyl urea drug glyburide (also known as glibenclamide), which functions like tolbutamide as an inhibitor of K_{ATP} channels, was recently reported to inhibit the NRLP3 inflammasome in bone marrow-derived macrophages (19). In a more direct connection to the context of viral infections, RIG-I appears to play a dual role upon recognition of RNA virus infection, activating on one hand the transcription factors of the NF-κB and IRF families through the signaling adaptor MAVS, and triggering inflammasome activation through the adaptor ASC on the other. Treatment of bone marrow-derived dendritic cells with glyburide completely abrogates vesicular stomatitis virus-induced secretion of IL-1β, providing further support for a role of K^+ ions in the regulation of antiviral innate immunity in mammals (20). In addition to the inflammasome, antiviral apoptosis can also be triggered by the voltage-dependent K^+ channels Kv2.1 in mammals (21). We now add RNA interference to the list of innate immunity mechanisms regulated by K^+ ions (Fig. S6). An intriguing question in all these cases pertains to the mechanism by which K^+ ions regulate these targets, and whether this function is directly regulated by K^+ ions, or indirectly through modified concentrations of other ions, such as Ca^{2+} or Na^+. Of note, inhibition of the sodium-potassium pump by cardiac glycosides was recently shown to block induction of IFN-β gene expression (22). This effect is mediated by the direct inhibition by Na^+ ions of the ATPase activity of RIG-I, an observation that is particularly interesting in light of the conservation of the DExD/H box helicase domains of RIG-I and Dcr-2 (23).

Potassium channels play an important role in cardiac repolarization both in flies and mammals (24, 25). An unexpected finding of our study is that FHV is a cardiotropic virus in *Drosophila*, providing a useful model to study virus–cardiomyocyte interaction in vivo in this genetically tractable model. Cardiotropic viruses play an important role in the onset of myocarditis in humans, which can lead to sudden death by cardiac arrest (26). However, the mechanisms leading to cardiomyopathy following viral infection in mammals are still poorly understood. One striking observation is that the cardiotropic viruses causing myocarditis are common and will be encountered by the vast majority of the population in their lifetime. However, only some 10% of the infected subjects will develop myocarditis (27, 28), which points to an important role for the genetic background and/or environmental factors in the onset of this disease. For example, defects in an antiviral immunity pathway may be associated with increased viral replication and tissue damage. Curiously, not much is known at this stage about antiviral host defense in cardiomyocytes, and the available data point to complex regulation (29–31). The fact that patients suffering from myocarditis do not appear to be particularly prone to other types of viral infections suggest that either heart-specific mechanisms of antiviral host defense are affected in these patients, or that certain heart-specific conditions regulate the interaction of the cardiomyocyte with the virus. Our findings in *Drosophila*, in conjunction with the established role of K^+ ions in the regulation of the inflammasome discussed above, suggest that control of K^+ ion efflux could be one such condition. Moreover, we observed a higher virus load in the hearts of both homozygous and heterozygous *mayday* mutant mice after CVB3 infection, although they did not show exaggerated viremia compared with control mice. These data are consistent with an ancestral antiviral function served by K_{ATP} channels, now retained in the mammalian heart, but not necessarily other tissues. Moreover, K_{ATP} channels appear to have been adapted to other functions, including the preservation of cardiovascular homeostasis during infection.

In summary, our data highlight a unique layer of complexity in the regulation of antiviral immunity. In addition to the general (e.g., type I IFN in mammals, or RNAi in invertebrates) and the tissue-specific [e.g., TLR-mediated gene induction in plasmacytoid dendritic cells in mammals (32) or *Vago* induction in the *Drosophila* fat body (23)] mechanisms of antiviral host defense, we describe here a tissue-specific regulation by the cellular environment of antiviral innate immunity. Our data indicate that genetic defects or drugs acting on this cellular environment, as opposed to direct effects on the virus or the immune system, can have major effects on the outcome of the infection. Therefore, the characterization of tissue-specific regulatory mechanisms of innate immunity represents an original and promising avenue of research for the development of novel therapeutics against infectious diseases.

Materials and Methods

***Drosophila* Strains and Infections.** w^- and *yw* flies were used as wild-type controls. Most mutant lines used in the experiments (UAS-dSUR RNAi lines; GMH5-Gal4 driver; UAS-RNA1 FHV; $Dcr2^{R416x}$, $AGO2^{414}$, and $r2d2^1$ mutants) have been previously described. SUR^{c04651} mutant flies and the deficiency Df (2L)Exel8024 were obtained from the Bloomington Stock Centre and the Exelixis Collection (Harvard Medical School), respectively. UAS-Ir (v28430 and v28431), UAS-Irk2 (v4341), and UAS-Irk3 (v3886) RNAi lines were purchased from the Vienna *Drosophila* RNAi Center (VDRC). All fly lines were tested for *Wolbachia* infection and cured whenever necessary. Raising of fly stocks and infections were done as previously described (5, 9). Two replicates of 10 flies were used for each treatment, and every assay was replicated three times.

Mice and Virus. $Kcnj8^{mayday/mayday}$ and $Kcnj8^{+/mayday}$ mice (C57BL/6J background) were used for Coxsackievirus B3 (CVB3) infection. Age-matched C57B/6J mice were used as controls. Mice were i.p. injected with 500 pfu of CVB3 (Woodruff strain), which was generously provided by L. Whitton (The Scripps Research Institute). Heart and serum were harvested at 3 dpi and subjected to virus titration by the conventional plaque assay on HeLa cells. All animal protocols were approved by The Scripps Research Institute Department of Animal Resources in compliance with Institutional Animal Care and Use Committee guidelines.

Drug Treatment. Stock solutions (1 M) of tolbutamide and pinacidil (Sigma) were initially prepared in dimethylsulfoxyde. Adult flies were fed on a 1% sucrose solution supplemented with tolbutamide or pinacidil (2 mM final concentration) for 3 h before infection with FHV.

RNA and Protein Analysis. Analysis of RNA expression was performed by real-time quantitative RT-PCR as previously described (23). For hemolymph protein analysis, hemolymph was collected from flies at various time points following infection using thin glass capillaries adjusted to the Nanoject II apparatus. Electrophoresis and immunoblot analysis, as well as immunostaining, were performed as described (23).

Median Tissue Culture Infective Dose Assays. Infected flies were homogenized in Schneider's *Drosophila* media (BioWest) and following centrifugation of fly parts, supernatants were filtered and dilutions of virus suspensions were used to infect *D. melanogaster* Kc167 cells in a 96-well plate format. The presence of virus was scored 24 h later by immunofluorescence.

Statistical Analysis. Data were analyzed using GraphPad Prism software. The mean values were compared by nonparametric unpaired *t* test. In all tests, $P < 0.05$ was considered significant.

ACKNOWLEDGMENTS. We thank E. Santiago and M. Yamba for excellent technical help; J. Kalschmidt for assistance with some experiments; N. Matt for advice and help for the confocal microscopy; M. Miehe for technical help for the electron microscopy; A. Schneeman for the anti-FHV antiserum; and D. Ferrandon, J. M. Reichhart, and P. Fornes for helpful discussions. Confocal microscopy was done at the Strasbourg Esplanade Cellular Imaging Facility (funded by Centre National de la Recherche Scientifique, Institut National de la Santé et de la Recherche Médicale, Université de Strasbourg, and Region Alsace). Electron microscopy was done at the Technical Platform of Imaging Facility at the Center of Neurochemistry (Strasbourg, France). This work was supported by National Institute of Health Grants PO1 AI070167 (to B.B., J.-L.I., and J.A.H.) and RO1 HL54732 (to R.B.), the Balzan Foundation (J.A.H.), and the Centre National de la Recherche Scientifique. K.O. was supported by a Scientist Development Award from the American Heart Association. S.C. acknowledges financial support from the Fondation pour la Recherche Médicale.

1. Beutler B, et al. (2007) Genetic analysis of resistance to viral infection. *Nat Rev Immunol* 7:753–766.
2. Fujita T (2009) A nonself RNA pattern: Tri-p to panhandle. *Immunity* 31:4–5.
3. Ding SW, Voinnet O (2007) Antiviral immunity directed by small RNAs. *Cell* 130: 413–426.
4. Kemp C, Imler JL (2009) Antiviral immunity in Drosophila. *Curr Opin Immunol* 21:3–9.
5. Galiana-Arnoux D, Dostert C, Schneemann A, Hoffmann JA, Imler JL (2006) Essential function in vivo for Dicer-2 in host defense against RNA viruses in drosophila. *Nat Immunol* 7:590–597.
6. van Rij RP, et al. (2006) The RNA silencing endonuclease Argonaute 2 mediates specific antiviral immunity in Drosophila melanogaster. *Genes Dev* 20:2985–2995.
7. Wang XH, et al. (2006) RNA interference directs innate immunity against viruses in adult Drosophila. *Science* 312:452–454.
8. Schneider DS, Ayres JS (2008) Two ways to survive infection: What resistance and tolerance can teach us about treating infectious diseases. *Nat Rev Immunol* 8: 889–895.
9. Croker B, et al. (2007) ATP-sensitive potassium channels mediate survival during infection in mammals and insects. *Nat Genet* 39:1453–1460.
10. Nichols CG (2006) KATP channels as molecular sensors of cellular metabolism. *Nature* 440:470–476.
11. Kane GC, et al. (2006) Gene knockout of the KCNJ8-encoded Kir6.1 K(ATP) channel imparts fatal susceptibility to endotoxemia. *FASEB J* 20:2271–2280.
12. Döring F, Wischmeyer E, Kühnlein RP, Jäckle H, Karschin A (2002) Inwardly rectifying K+ (Kir) channels in Drosophila. A crucial role of cellular milieu factors Kir channel function. *J Biol Chem* 277:25554–25561.
13. Wessells RJ, Fitzgerald E, Cypser JR, Tatar M, Bodmer R (2004) Insulin regulation of heart function in aging fruit flies. *Nat Genet* 36:1275–1281.
14. Kopek BG, Perkins G, Miller DJ, Ellisman MH, Ahlquist P (2007) Three-dimensional analysis of a viral RNA replication complex reveals a virus-induced mini-organelle. *PLoS Biol* 5:e220.
15. Akasaka T, et al. (2006) The ATP-sensitive potassium (KATP) channel-encoded dSUR gene is required for Drosophila heart function and is regulated by tinman. *Proc Natl Acad Sci USA* 103:11999–12004.
16. Heo I, Kim VN (2009) Regulating the regulators: Posttranslational modifications of RNA silencing factors. *Cell* 139:28–31.
17. Xin M, et al. (2009) MicroRNAs miR-143 and miR-145 modulate cytoskeletal dynamics and responsiveness of smooth muscle cells to injury. *Genes Dev* 23:2166–2178.
18. Martinon F, Mayor A, Tschopp J (2009) The inflammasomes: Guardians of the body. *Annu Rev Immunol* 27:229–265.
19. Lamkanfi M, et al. (2009) Glyburide inhibits the Cryopyrin/Nalp3 inflammasome. *J Cell Biol* 187:61–70.
20. Poeck H, et al. (2010) Recognition of RNA virus by RIG-I results in activation of CARD9 and inflammasome signaling for interleukin 1 beta production. *Nat Immunol* 11: 63–69.
21. Redman PT, et al. (2007) Apoptotic surge of potassium currents is mediated by p38 phosphorylation of Kv2.1. *Proc Natl Acad Sci USA* 104:3568–3573.
22. Ye J, Chen S, Maniatis T (2011) Cardiac glycosides are potent inhibitors of interferon-β gene expression. *Nat Chem Biol* 7:25–33.
23. Deddouche S, et al. (2008) The DExD/H-box helicase Dicer-2 mediates the induction of antiviral activity in drosophila. *Nat Immunol* 9:1425–1432.
24. Ocorr K, et al. (2007) Genetic control of heart function and aging in Drosophila. *Trends Cardiovasc Med* 17:177–182.
25. Sanguinetti MC, Tristani-Firouzi M (2006) hERG potassium channels and cardiac arrhythmia. *Nature* 440:463–469.
26. Andréoletti L, Lévêque N, Boulagnon C, Brasselet C, Fornes P (2009) Viral causes of human myocarditis. *Arch Cardiovasc Dis* 102:559–568.
27. Cooper LT, Jr. (2009) Myocarditis. *N Engl J Med* 360:1526–1538.
28. Esfandiarei M, McManus BM (2008) Molecular biology and pathogenesis of viral myocarditis. *Annu Rev Pathol* 3:127–155.
29. Deonarain R, Cerullo D, Fuse K, Liu PP, Fish EN (2004) Protective role for interferon-beta in coxsackievirus B3 infection. *Circulation* 110:3540–3543.
30. Fuse K, et al. (2005) Myeloid differentiation factor-88 plays a crucial role in the pathogenesis of Coxsackievirus B3-induced myocarditis and influences type I interferon production. *Circulation* 112:2276–2285.
31. Kumar H, et al. (2006) Essential role of IPS-1 in innate immune responses against RNA viruses. *J Exp Med* 203:1795–1803.
32. Kato H, et al. (2005) Cell type-specific involvement of RIG-I in antiviral response. *Immunity* 23:19–28.
33. Molina MR, Cripps RM (2001) Ostia, the inflow tracts of the Drosophila heart, develop from a genetically distinct subset of cardial cells. *Mech Dev* 109:51–59.

Supporting Information

Eleftherianos et al. 10.1073/pnas.1108926108

SI Materials and Methods

Quantitative and Semiquantitative RT-PCR. Primers used for quantitative real-time PCR were as follows: RpL32 forward, 5′-GACGCTTCAAGGGACAGTATCTG-3′, and reverse, 5′-AAACGCGGTTCTGCATGAG-3′; FHV1 forward, 5′-TTTAGAGCACATGCGTCCAG-3′, and reverse, 5′-CGCTCACTTTCTTCGGGATA-3′; FHV2 forward, 5′-CAACGTCGAACTTGATGCAG-3′, and reverse, 5′-GCTATACAGGGCATTTCCAA-3′; DCV forward, 5′-TCATCGGTATGCACATTGCT-3′, and reverse, 5′-CGCATAACCATGCTCTTCTG-3′. Gene expression was normalized to the expression of RNA encoding the "housekeeping" ribosomal protein L32 (RpL32), used as a loading control, and the data represented as the ratio $2^{CT(RpL32)}/2^{CT(FHV)}$.

For *dSUR*, *Ir*, and *Irk2* expression studies in *Drosophila*, single-step semiquantitative RT-PCR was performed with the Brilliant II RT-PCR Core Reagent Kit (Stratagene) as described previously (1). Sequences of primers used for semiquantitative RT-PCR were as follows: *dSUR* forward 5′- TCGCCAGCTATCCGTATTTC-3′, and reverse, 5′- TGCCACCGTACTGATCACAT-3′; *Ir* forward 5′- ACGCACACAATGATCTGGAG-3′, and reverse, 5′- ATGGTAGTGGGCCAGATGAA-3′; *Irk2* forward 5′- GGAGTGTCCACCTGAGTGGT-3′, and reverse, 5′- TCATGATGTGCTTCCAGTCC-3′. Amplifications were performed under the following cycling conditions: 45 °C for 30 min; 95 °C for 10 min; 25 cycles of 95 °C for 30 s, 64 °C for 1 min, and 72 °C for 30 s. PCR control reactions for RpL32 were performed at 20 cycles. PCR controls without template or reverse transcriptase were also included.

Median Tissue Culture Infective Dose Assays. Infected flies were homogenized in Schneider's *Drosophila* media (BioWest), and following centrifugation of fly parts, supernatants were filtered and dilutions of virus suspensions were used to infect *D. melanogaster* Kc167 cells plated out in wells of a 96-well plate (1.2×10^5 cells/well). Following incubation of infected cells at 23 °C for 1 d, cells were fixed in 8% formaldehyde solution for 10 min at room temperature, washed twice in PBS and 0.1% Triton X-100 (PBT) and blocked in blocking solution (PBS, 10% FBS; Thermo Scientific HyClone) for 30 min at room temperature. Cells were incubated with polyclonal antibodies to FHV capsid (1:500 dilution in blocking solution) for 2 h at room temperature, washed twice in PBT solution, and stained with goat anti-rabbit IgG FITC secondary antibodies (Invitrogen; 1:500 dilution in blocking solution) for 1 h at room temperature. Finally, cells were dried following washing in PBT solution and FHV titer was determined by fluorescence microscopy (Zeiss Axioscope 2).

1. Croker B, et al. (2007) ATP-sensitive potassium channels mediate survival during infection in mammals and insects. *Nat Genet* 39:1453–1460.

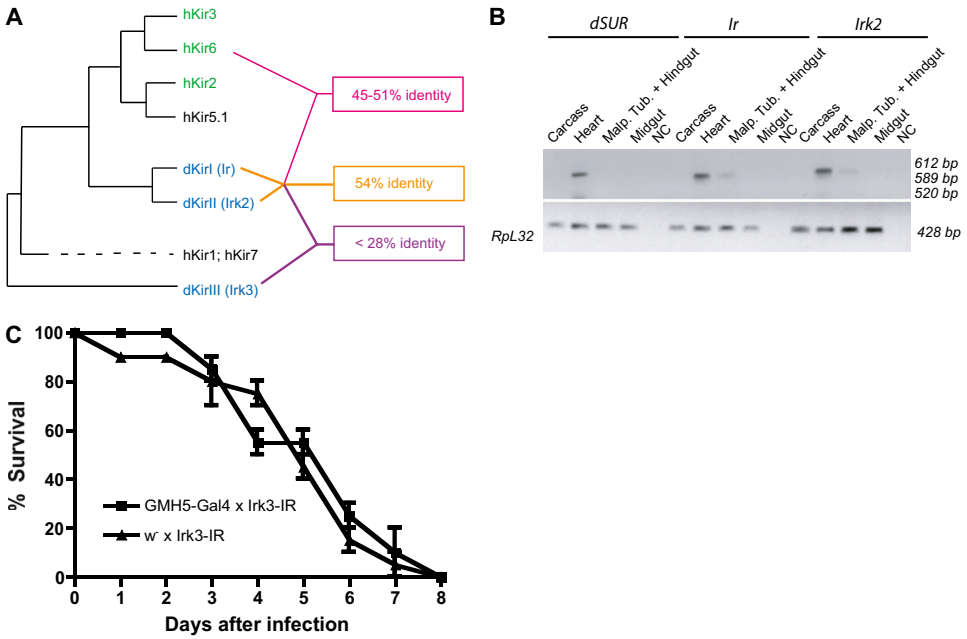

Fig. S1. *Drosophila Ir* and *Irk2* genes are orthologs to human *Kir6.x* genes, and are expressed in the heart. (*A*) Phylogenetic comparison of *Kir* genes in *Drosophila* and human. (*B*) Semiquantitative RT-PCR was used to analyze the expression of *dSUR*, *Ir*, and *Irk2* genes in different tissues dissected from wild-type flies. The sizes of the amplicons are 612 bp (*dSUR*), 589 bp (*Irk2*), and 520 bp (*Ir*). Note that *Ir* and *Irk2* are highly expressed in the *Drosophila* heart, like *dSUR*. The gene encoding the ribosomal protein RpL32 was used as a control. For *B*, data represent three independent experiments involving dissection of tissues from at least 50 flies. (*C*) Survival curves of flies obtained from crosses between UAS-Irk3 RNAi line (IR, inverted repeat) with the heart-specific GMH5-Gal4 driver and control flies (UAS-Irk3 RNAi line crossed with w^- flies) after infection with FHV. Data represent the mean ± SD of two independent experiments, each involving two groups of 10 flies.

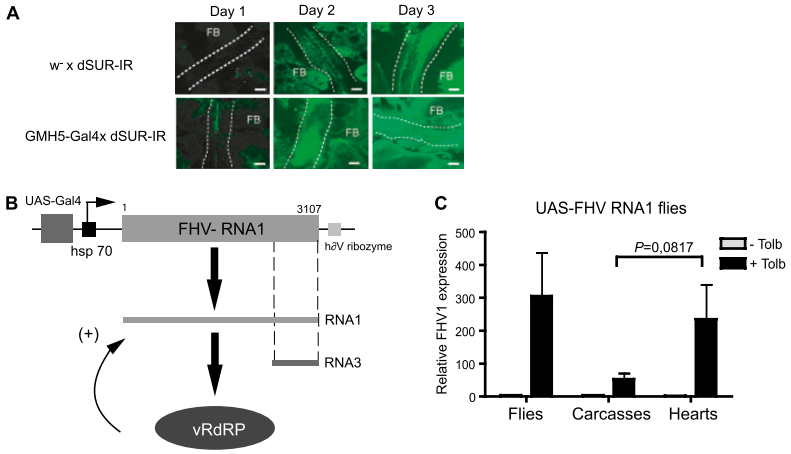

Fig. S2. Potassium channels regulate antiviral RNA interference in the *Drosophila* heart. (*A*) Immunostaining of heart and fat body tissue from dSUR-silenced flies and control flies with antibody to FHV capsid protein (green; Alexa Fluor 488) at different times after virus infection. Data are from one experiment representative of three with at least 10 flies for each treatment. (Scale bar: 35 μm.) FB, fat body. (*B*) RNA1 construct used for generating transgenic flies. RNA1- and subgenomic RNA3- encoded transcripts are shown. RNA1 encodes the viral RNA-dependent RNA polymerase (vRdRP). (*C*) Quantitative RT-PCR of FHV RNA1 levels in whole flies, carcasses, and hearts from 1-wk-old UAS-RNA1 transgenic flies treated or not with tolbutamide. For *C*, data represent the mean ± SD of three independent experiments each involving at least 30 flies.

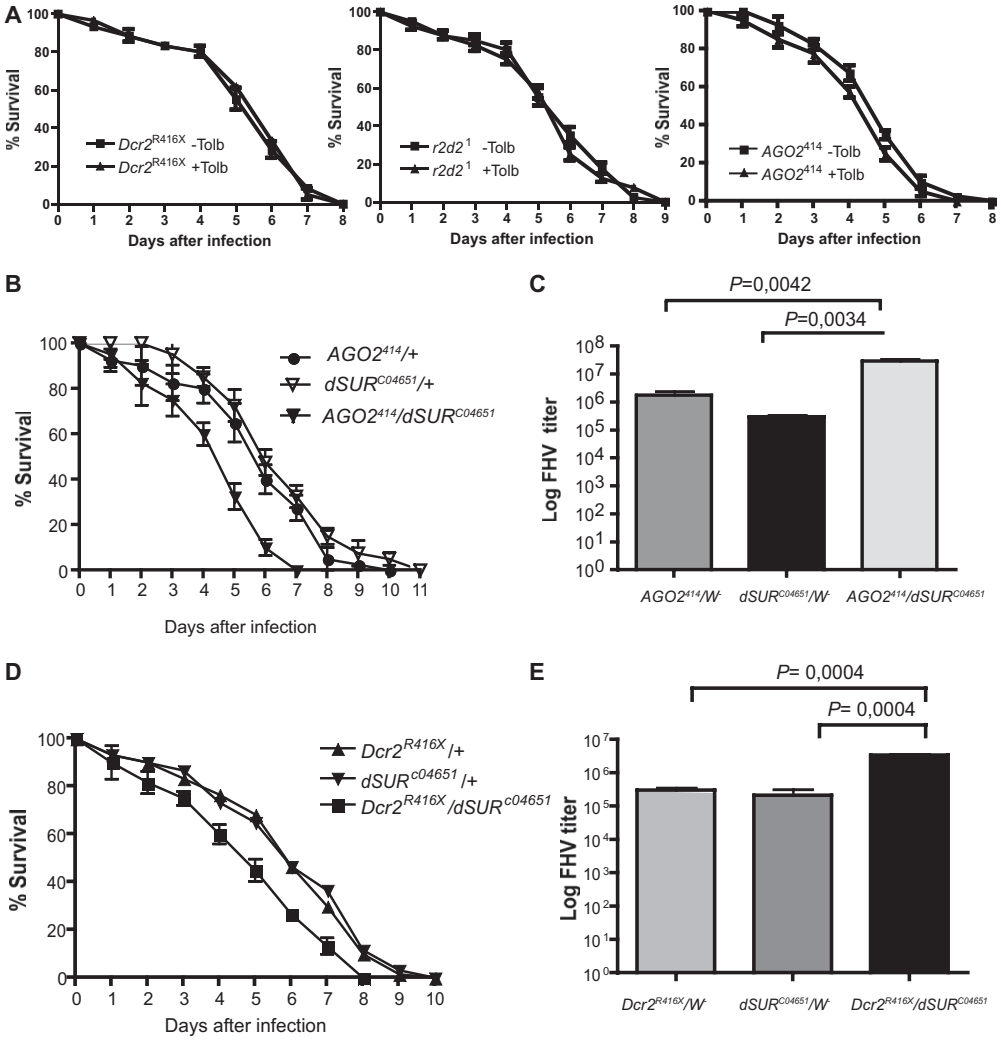

Fig. S3. Genetic interaction between *dSUR* and the antiviral RNAi pathway genes. (*A*) Survival curves of 1-wk-old *Dcr-2*, *r2d2*, and *AGO2* mutant flies with or without treatment with tolbutamide and following infection with FHV. (*B*) Survival curves of *AGO2*;*dSUR* double-heterozygote flies and control single-heterozygous flies after FHV infection. (*C*) FHV titers in *AGO2*;*dSUR* double-heterozygote flies compared with control single-heterozygous flies 3 d after FHV infection. (*D*) Survival curves of *Dcr-2*;*dSUR* double-heterozygote flies and control single-heterozygous flies after FHV infection. (*E*) FHV titers in *Dcr-2*;*dSUR* double-heterozygote flies compared with control single-heterozygous flies 3 d after FHV infection. Data represent the mean ± SD of three independent experiments, each involving at least two groups of 10 flies (survival) or 30 flies (viral load) per treatment.

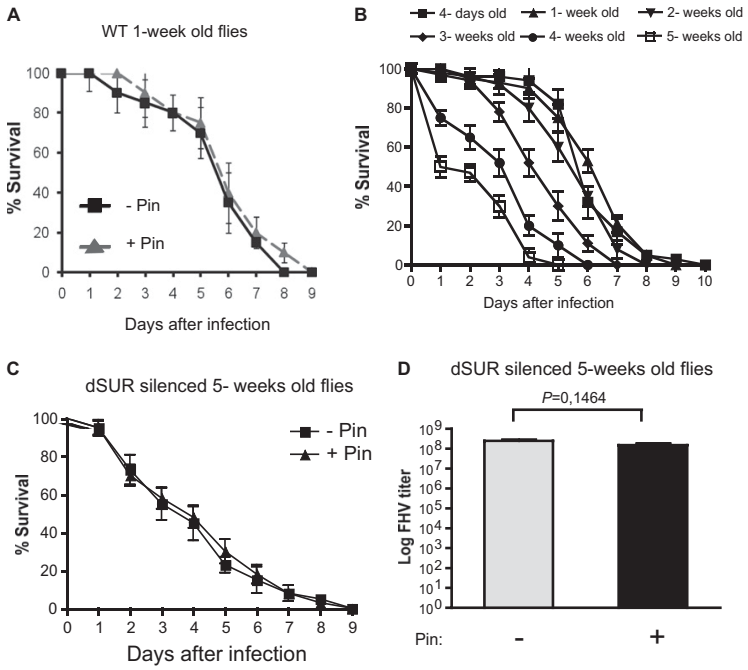

Fig. S4. The K_{ATP} channel agonist drug pinacidil does not protect old *dSUR* mutant flies against FHV infection. (*A*) Survival curves of 1-wk-old flies treated or not with pinacidil after FHV infection. (*B*) Survival curves of aging wild-type flies were determined after infection with FHV. Note the increased lethality in aged flies. (*C* and *D*) Survival curves (*C*) and viral load (*D*) of *dSUR*-silenced 5-wk-old flies fed on the K_{ATP} agonist pinacidil or on sucrose solution alone after infection with FHV. FHV titers in infected flies were estimated at 3 d following virus infection. Data represent the mean ± SD of three independent experiments, each containing two groups of 10 flies.

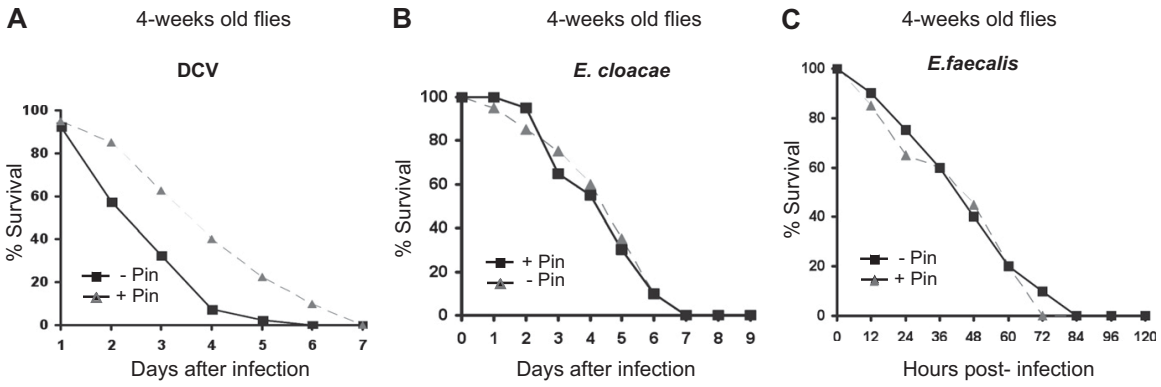

Fig. S5. The K_{ATP} channel agonist drug pinacidil does not significantly improve resistance of old flies to other infections. Survival curves of w^- wild-type 4-wk-old flies fed on the K_{ATP} agonist pinacidil or on sucrose solution alone after infection with DCV (*A*), the Gram-negative bacteria *Enterobacter cloacae* (*B*), and the Gram-positive bacteria *Enterococcus faecalis* (*C*). A representative experiment involving two groups of 10 flies per treatment is shown.

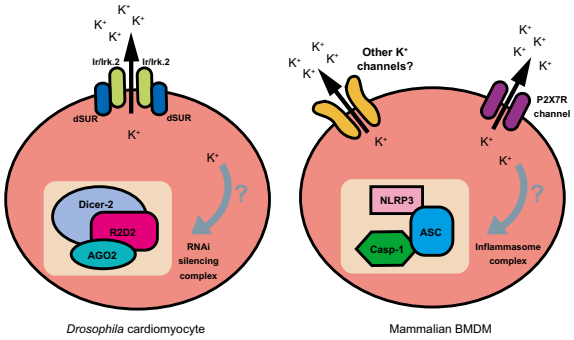

Fig. S6. A model for the evolutionary conserved role of K^+ ion efflux in the regulation of innate immunity in flies and mammals. See *Discussion* for more details. BMDM, bone-marrow derived macrophage.

5.2 The voltage-gated K^+ channel KCNQ also plays a role in resistance to FHV

We asked the question whether other potassium channels, which are involved in heart physiology under normal conditions, also regulate FHV infection. One such channel previously characterized in flies is KCNQ, a homologue of the human KCNQ1 channel, which functions as a voltage-dependent potassium channel involved in myocardial repolarization. KCNQ was previously shown to play an important role in the regulation of rhythmical contraction in the *Drosophila* heart [Ocorr et al., 2007]. We infected *KCNQ* mutant flies with FHV and observed that these flies were sensitive to infection with the virus (Figure 5.1A). *KCNQ* mutants were neither sensitive to infection with bacteria or fungi, nor with DCV (data not shown), suggesting that the phenotype observed with FHV is not due to the general weakness of the flies. In addition, we observed an increase of FHV viral RNAs in *KCNQ* mutant flies compared to wild-type controls at all time points analyzed (Figure 5.1B). The FHV infection titer was also increased in *KCNQ* mutant flies (data not shown).

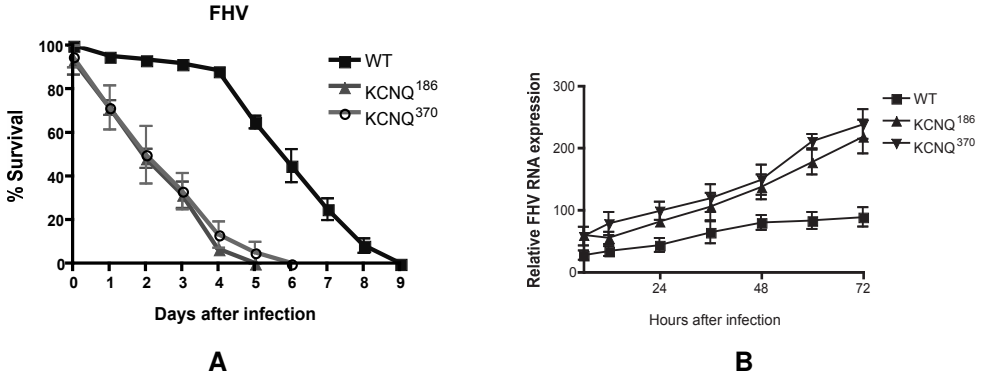

Figure 5.1: KNCQ channel mediate resistance to FHV infection . **A.** Survival curves of control (WT) and two KCNQ mutant lines ($KCNQ^{186}$ and $KCNQ^{370}$). Mean and error bars from 3 independent experiments, involving two groups of ten flies. **B.** qRT-PCR analysis of viral RNA accumulation at different times following infection with FHV. FHV RNA values were normalized to the expression of RNA encoding the 'housekeeping' ribosomal protein rp49, is used as a loading control.

Previously, we were able to show that K_{ATP} channels regulate the antiviral RNAi in the *Drosophila* heart. We next tested whether the KCNQ channel is also involved in the control of this antiviral pathway. We generated double heterozygote flies for *AGO2* and *KCNQ* and compared their resistance to FHV infection (survival and viral load) with flies heterozygous for *AGO2* and *KCNQ*. Flies heterozygote for *AGO2* and *KCNQ* died more rapidly (Figure 5.2A) and contain higher viral loads (Figure 5.2B) than single heterozygous flies, pointing to a genetic interaction between *AGO2* and *KCNQ*. Similar results were obtained for double heterozygote flies *Dcr-2* and *KCNQ* (data not shown).

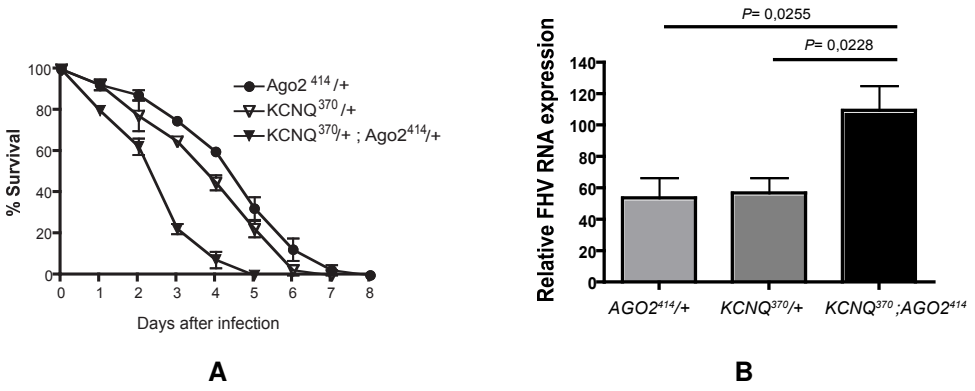

Figure 5.2: Regulation of antiviral RNAi by the voltage-gated potassium channel KCNQ . **A.** Survival curves of *AGO2;KCNQ* double heterozygote flies and single heterozygous flies (conrtols) after FHV infection. Mean and error bars from 3 indepandant experiments, involving two groups of ten flies. **B.** qRT-PCR analysis of viral RNA accumulation at different times following infection with FHV. FHV RNA values were normalized to the expression of RNA encoding the 'housekeeping' ribosomal protein rp49, is used as a loading control.

Our results indicate that in addition to the K_{ATP} channels, the voltage-dependent KCNQ channel also participates in the control of cardiotropic viral infection. Our findings point to a general implication of K^+ efflux in the tissue-specific regulation of antiviral immunity in *Drosophila*.

5.3 The *Drosophila* heart plays a central role in the resistance to FHV infection

The *Drosophila* heart is a favorite model for studying organogenesis. The mechanisms of cardiac formation were shown to be evolutionary conserved [Bodmer, 1995]. *Drosophila* was proposed as an emergent model system to study congenital heart disease and novel approaches that assess the cardiac function in flies have been developed [Bier and Bodmer, 2004]. The *Drosophila* heart is highly organized tube (Figure 5.3A, 5.3B) and its function might be examined by standardized measurements. Such methods can evaluate the rate of the heart beat frequency and arrhythmia, systole-diastole diameters and the rates of heart failure in response to electrical pacing [Bier and Bodmer, 2004, Fink et al., 2009] (Figure 5.3C).

Functionally, the *Drosophila* heart acts as a myogenic pump and allows the distribution of the hemolymph through the hemocoel of the fly [Medioni et al., 2009]. Interestingly, the main physiological function of the fly's heart remains mysterious. In contrast to the mammalian cardiovascular system, *Drosophila* has an open circulatory system and the oxygenation of the hemolymph occurs directly through the tracheal system, suggesting that the cardiac activity is dispensable for animal viability. This is supported by the fact that inactivation of Calmodulin or L-type Ca^{2+} channels specifically in the cardiac tissue results in arrested heart beats but otherwise viable and healthy animals [Medioni et al., 2009].

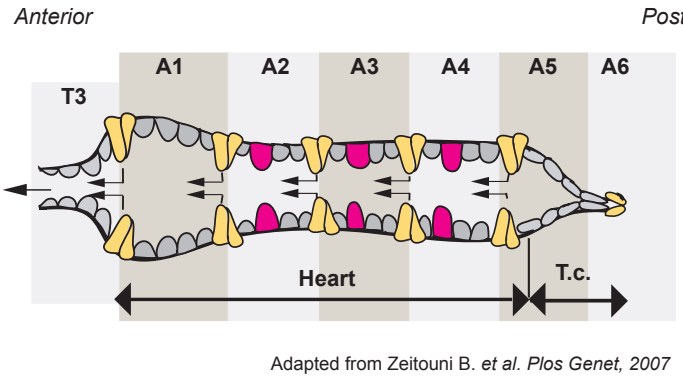

Adapted from Zeitouni B. *et al. Plos Genet, 2007*

A Schematic representation of the *Drosophila* cardiac tube

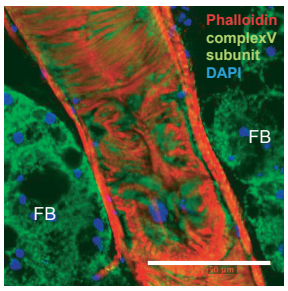

B Confocal picture of the adult heart

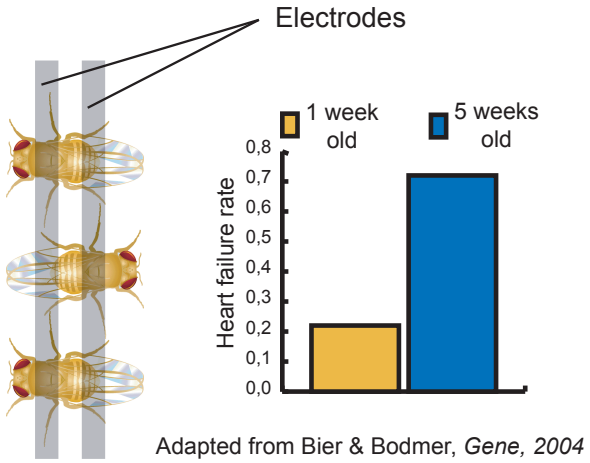

Adapted from Bier & Bodmer, *Gene, 2004*

C Example of heart performance assay in ageing flies

Figure 5.3: *Drosophila melanogaster* adult heart . **A.** The five inflow tracts (ostia) are represented in yellow. Contractile myocytes that allow tha autonomous rythmic activity of the heart in abdominal segments A1 to A4 are shown in grey. The three pairs of valves controlling the unidirectional flow of the hemolymph (from posterior to the anterior part) in segments A2 to A4 are shown in pink. The myocytes in the abdominal segment A5 form the terminal chamber (**T.c.**) of the heart. T3: thoracic segment 3. The arrows indicate the sens of the circulation of the hemolymph. **B.** The actin fibers are stained with Phalloidin, mitochondria are in green and nuclei in blue. Scale bar: 50 μm. **FB**: surrounding Fat body. **C.** Flies are arranged to touch two electrodes and the heart failure rate is mesured after 30 seconds of pacing at 6 Hz. We can notice the 3 to 4 fold increase of the heart failure rate with the age.

Because we identified the *Drosophila* heart as a major tissue controlling the resistance to infection with the cardiotropic virus FHV, we wondered whether viral infection affected the heart physiology. We also examined the role of the heart itself in the resistance to FHV infection by genetic ablation of this tissue. In collab-

oration of the group of Professor Rolf Bodmer at the Burnham Research Institute in San Diego, California, USA, we were able to show that infection with FHV was associated with an increase in the heart period, the arrhythmia index and changes in the pumping direction of the heart (I. Eleftherianos, K.Occor, unpublished data).

We took advantage of the UAS-Gal4 system in *Drosophila* and drove the expression of the proapoptotic factor Reaper specifically in cardiomyocytes by using the GMH5-Gal4 driver line [Wessells et al., 2004]. Interestingly, emerging adult flies were viable, without obvious health defects. We observed atrophied hearts in the GMH5-Gal4/UAS-Reaper flies, as illustrated on Figure 5.4A. These data are supported by the fact that the heart function is completely suppressed in GMH5-Gal4/UAS-Reaper flies (K.Occor, unpublished data). We quantified the atrophy and subsequently tested the susceptibility of these flies to virus infection (Figure 5.4D). Interestingly, we observed that flies with atrophied hearts became more resistant to infection with FHV, but not DCV (Figure 5.5A, 5.5B). The heart is the first target organ during infection with FHV, but the viral antigen becomes detecable in the fat body at later time points. Two mechanisms can account for this observation: *(i)* cardiomyocytes are the primary infected cells and multiplication in these cells lead to increased viremia and secondary infection of other tissues; *(ii)* the pumping activity of the heart may contribute to the spreading of the virus to other tissues. The absence of consequence of the heart ablation for resistance to DCV suggests that the main contribution of the heart is not the dissemination of the virus through the body cavity through its contractile activity, and supports the first hypothesis.

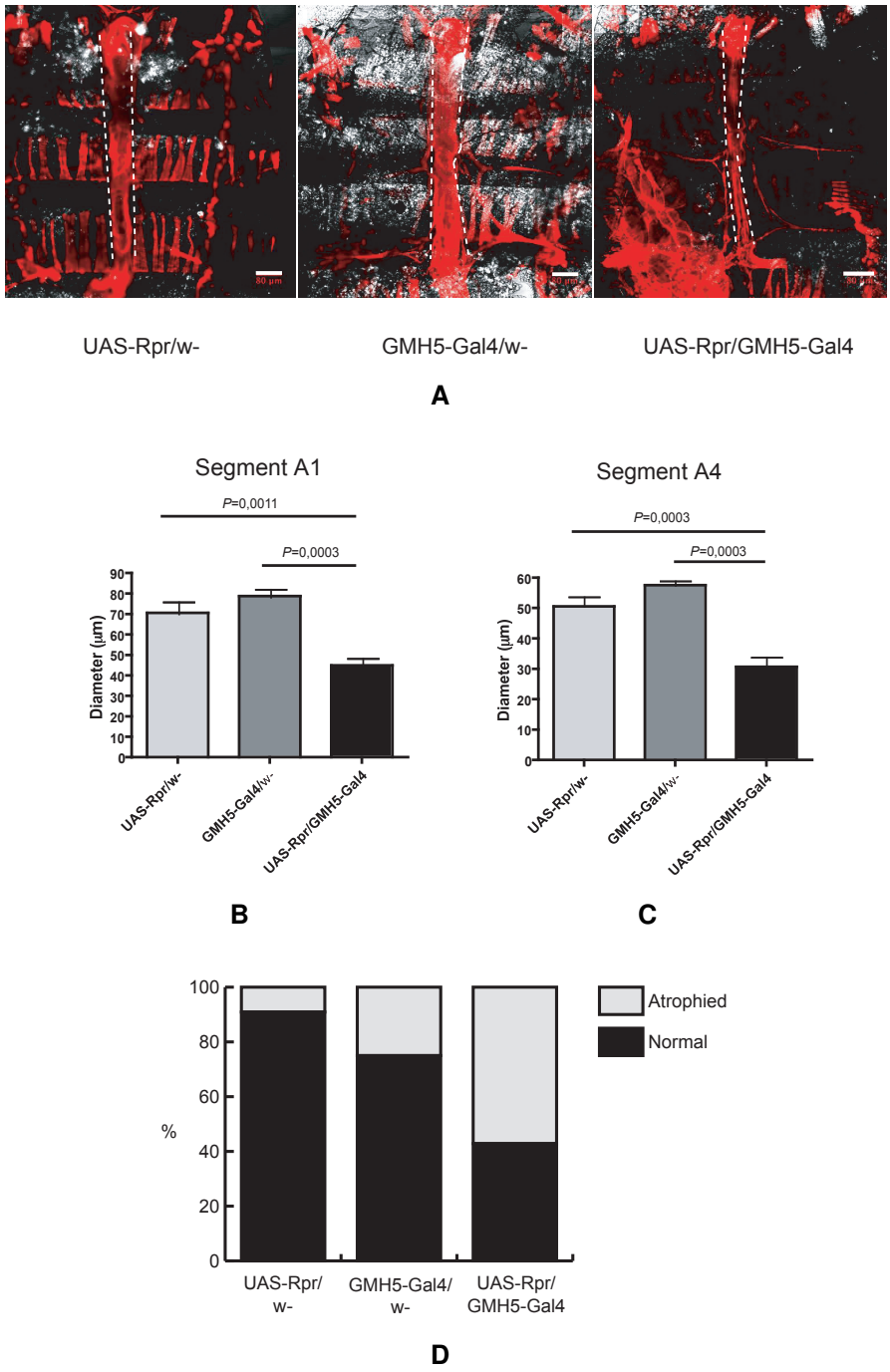

Figure 5.4: Reaper-triggered heart atrophy in *Drosophila* . A. Confocal microscope pictures of hearts, stained with Phalloidin-TaxasRed in UAS-Rpr/w-, GMH5-Gal4/w- (controls) and UAS-Rpr/GMH5-Gal4 flies. The heart atrophy is visible in UAS-Rpr/GMH5-Gal4 flies. Scale bar: 80 μm. **B.** Diameter of the heart at abdominal segment A1. **C.** Diameter of the heart at abdominal segment A4. **D.** Quantification of the heart atrophy. UAS-Rpr/w^-: n=11, GMH5-Gal4/w^-: n=12 and UAS-Rpr/GMH5-Gal4: n=14.

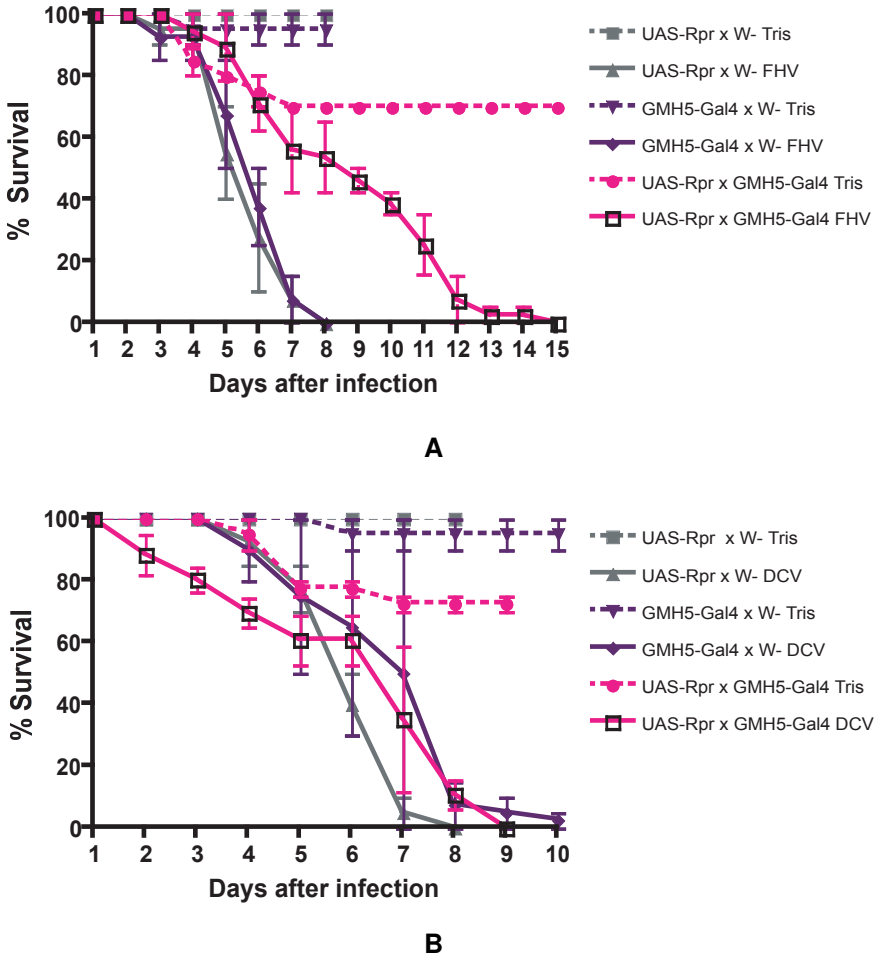

Figure 5.5: Heart atrophy confers protection against FHV . **A.** Protection against FHV infection of flies with atrophied hearts. Mean and error bars from 2 independant experiments. **B.** Flies with atrophied hearts show similar sensitivity to DCV.

5.4 *Ir*, *Irk2* and DCV infection

When looking at the effect of K_{ATP} channels on FHV infection, we always used DCV as a control. We did not observe consequences for DCV infection when dSUR was inhibited by Tolbutamide or its expression knocked-down [Croker et al., 2007]. Surprisingly, when we tested *Ir* and *Irk2*, we observed that flies silenced for these genes resisted better to DCV infection (Figure 5.6A, 5.6B). This suggests that Ir and Irk2 may function independently from dSUR and play a detrimental role in the context of DCV infection.

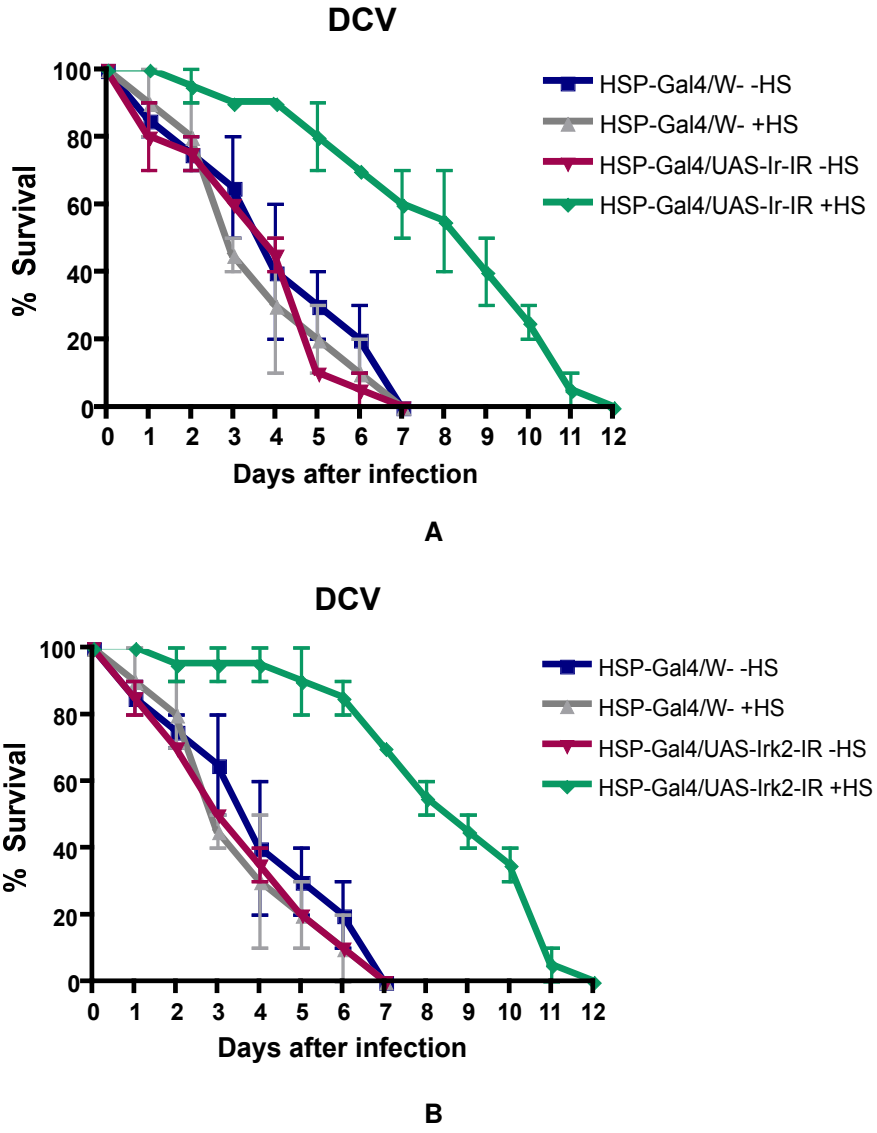

Figure 5.6: *Ir* and *Irk2* knock-downed flies are resistant to DCV . **A.** Ubiquitous knock down of *Ir*. Mean and error bars from 2 independant experiments, each involving two groups of ten flies. **B.** Ubiquitous knock down of *Irk2*. Mean and error bars from 2 independant experiments, each involving two groups of ten flies. +/- HS: with or without heat shock, IR: inverted repeat.

Chapter 6

Infection with the picorna-like virus DCV triggers an intestinal obstruction in *Drosophila*

We studied the transcriptional response of *Drosophila* after infection with three viruses with single strands RNA genomes of positive polarity, using genome-wide microarrays. The *Drosophila* C virus (DCV), the Flock House virus (FHV) and Sindbis (SINV) were used in this study. They belong to the *Dicistroviridae*, *Nodaviridae* and *Alphaviridae* families respectively. DCV and FHV are pathogenic to the flies, whereas injection of SINV is not lethal at the dose used, although the virus is able to replicate in *Drosophila* tissues. The analysis of the microarray study revealed that the number of induced genes by FHV largely exceeds the number of DCV and SINV induced genes. 487 genes were upregulated by a factor of at least two in FHV-infected flies, whereas DCV and SINV induced 166 and 201 genes, respectively [Kemp, 2011]. Strikingly, the comparison of the transcriptional profiles also revealed a major difference in the number of repressed genes: DCV represses the expression of more than 730 genes by at least two fold (Figure 6.1), whereas FHV and SINV repressed 250 and 189 genes respectively. To

further understand this phenomenon, we decided to analyze the DCV-repressed genes.

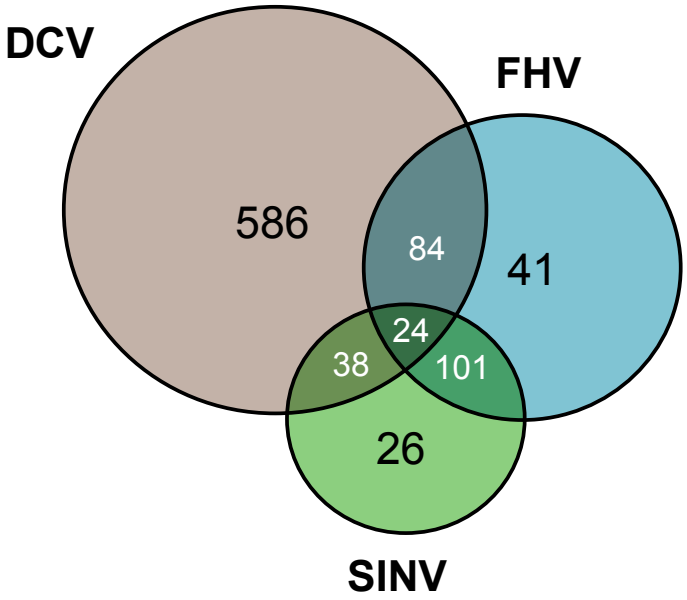

Figure 6.1: Microarray analysis of virus-infected flies . Venn diagram of virus-repressed genes after infection with DCV, FHV and SINV

6.1 DCV represses gene expression in the digestive tract

6.1.1 DCV represses expression of the gut-specific family of proteases Jonah

We first looked at the function (real or predicted) of the genes downregulated by DCV. The gene ontology analysis showed that about one third of them encode serine-proteases, mostly belonging to the Jonah family. We examined by Northern blot the expression of three members of the family: *Ser4*, *Jon25Biii* and *Jon99Ci* after challenge with DCV and FHV. We observed that the mRNA of these three genes became almost undetectable after 72 and 96 hours post-infection with DCV, but not FHV (Figure 6.2). Expression of a fourth member of the family,

Jon65Ai, was also repressed (Figure 6.3A). In order to analyze the consequence of this repression at the protein level, we produced an antibody recognizing a peptide from Jon65Ai. Western blot analysis showed that the antibody recognizes a band of 27 KDa, in good agreement with the predicted size of the protease in wild type flies, but not in the line Jon65Ai^{KG03203}, which contain a transposon inserted in the gene (Figure 6.3B and 6.3C). Infection by DCV led to a strong decrease in the expression of the Jon65Ai protease (Figure 6.3D).

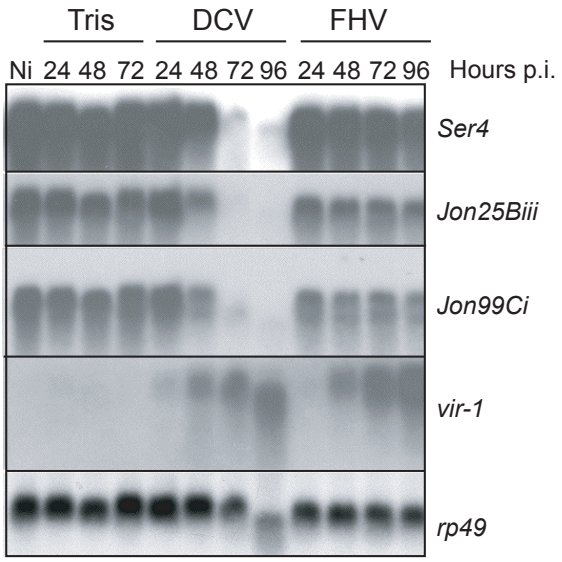

Figure 6.2: Quantitative validation of the microarray analysis for three members of the Jonah family of serine-proteases . 30 μg of total RNA from WT flies, extracted at different time points are analyzed by Northern blot. The probes are indicated at the right side of each blot. *Vir-1* is a marker gene, induced after viral infection and the RNA coding the ribosomal protein *Rp49* serves as loading control.

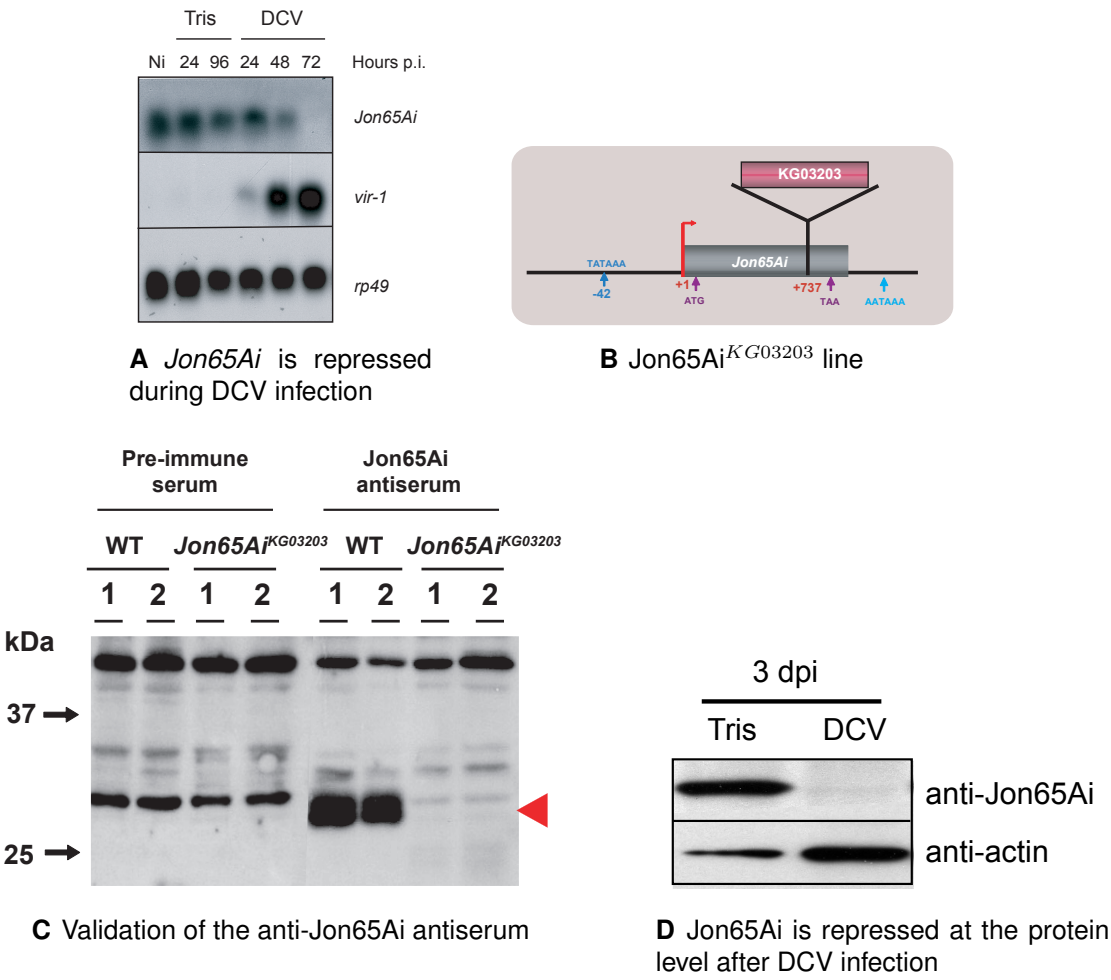

A *Jon65Ai* is repressed during DCV infection

B Jon65Ai^{KG03203} line

C Validation of the anti-Jon65Ai antiserum

D Jon65Ai is repressed at the protein level after DCV infection

Figure 6.3: Jon65Ai mRNA and protein analysis . **A.** Northern blot showing the repression of *Jon65ai* mRNA after DCV infection. **B.** Schematic representation of the transposon insertion in Jon65Ai^{KG03203} line, disturbing the coding sequence of the gene. **C.** Analysis of the anti-Jon65Ai serum. **D.** The protein Jon65Ai is strongly repressed after DCV infection.

6.1.2 The mechanism of gene repression

We asked whether DCV-induced gene repression occurs at the transcriptional or post-transcriptional level. We analyzed the 3'UTR sequences of several DCV-repressed genes for possible miRNA targets sites (http://www.targetscan.org/fly/). We were not able to identify miRNA target sites, suggesting that the repression occurs at transcriptional, rather than post-transcriptional level. To test this second hypothesis we generated transgenic lines, where we cloned the promoters of two of the DCV-repressed genes (*Jon65Ai* and *LysE*) upstream of the *LacZ* reporter

gene. We first determined the expression of the two reporters by X-Gal staining of dissected tissues. We detected the β-galactosidase activity in the anterior part of the midgut in LysE-LacZ line and posterior part of the midgut in Jon65Ai-LacZ. For Jon65Ai-LacZ, this result is consistent with the information provided by Flyatlas (www.flyatlas.org) [Chintapalli et al., 2007], in which *Jon65Ai* mRNA is detectable only in the midgut of *Drosophila* larvae and imago. No information is available on *LysE* mRNA expression in Flyatlas database, however this gene was previously shown to be expressed in the midgut [Daffre et al., 1994]. In agreement with this study, the *LysE* reporter gene was only expressed in the midgut (Figure 6.4).

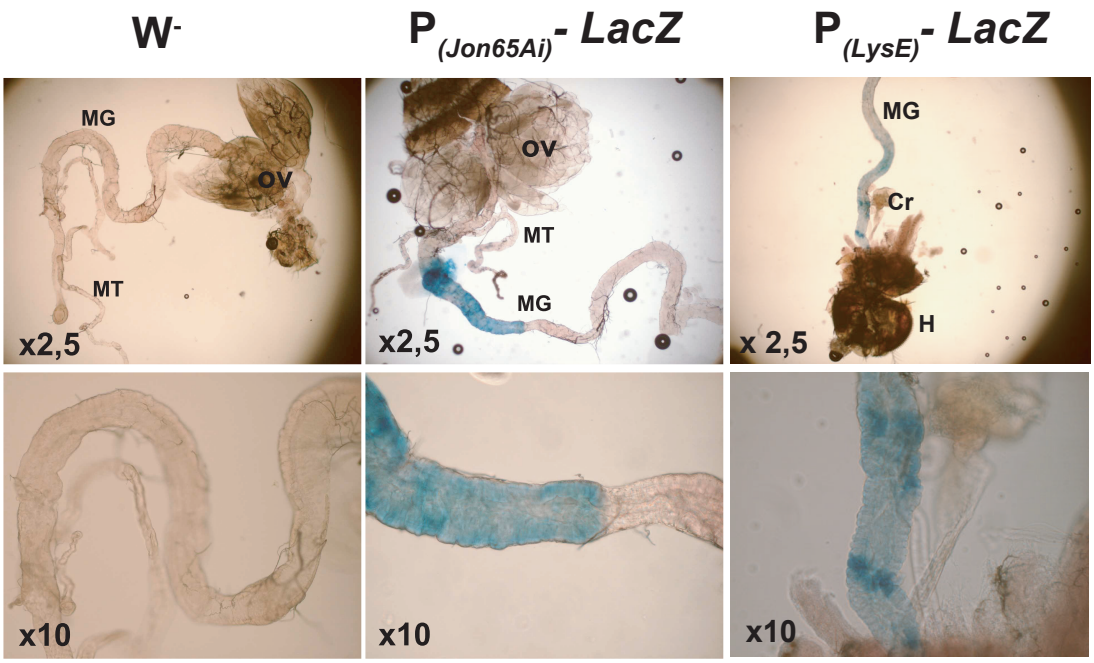

Figure 6.4: *Jon65Ai-LacZ* and *LysE-LacZ* are expressed in different parts of the adult midgut . X-Gal staining of dissected *Drosophila* tissues from w^- (negative controls), Jon65Ai-LacZ and LysE-LacZ flies. The β-galactosidase activity is detectable in the posterior part of the midgut of Jon65Ai-LacZ and anterior part of the midgut of LysE-LacZ line. Legend: **OV**: ovaries, **MT**: malpighian tubules, **MG**: midgut, **H**: head, **Cr**: crop.

We next measured the β-galactosidase activity after infection. We observed significant decrease in the reporter activity 3 days after infection with DCV for the two reporter lines. By contrast, the activity of the reporter transgene was not decreased, when flies were infected with FHV (Figure 6.5). For Jon65Ai-LacZ

we also measured the reporter activity after challenge with the Gram positive bacterium *Enteococcus faecalis* and the Gram negatif bacterium *Enterobacter cloacae*. We did not observe a repression after bacterial challenge and conclude that DCV, but not other infections represses *Jon65Ai* (Figure 6.6). These results suggest a transcriptional repression after DCV infection.

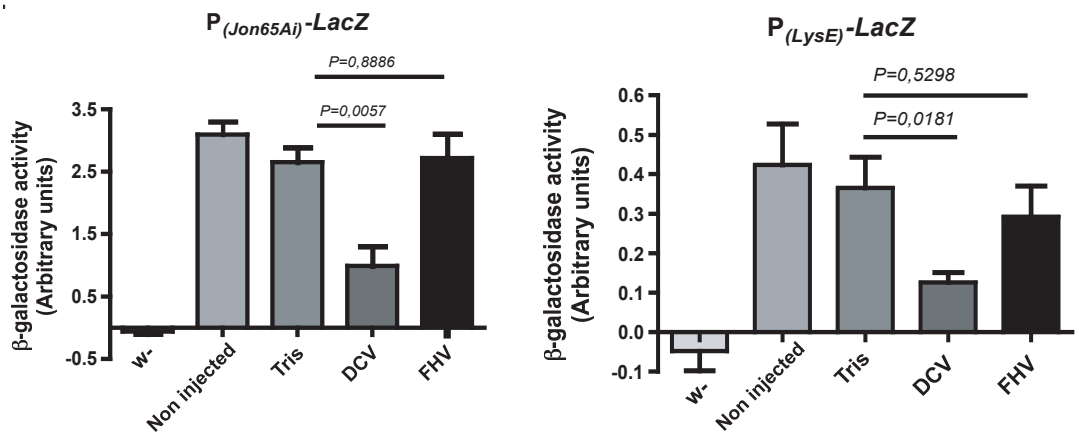

Figure 6.5: Transcriptional repression after DCV infection . The β-galactosidase activity significantly decreases 3 days after infection in DCV, but not FHV-infected reporter lines

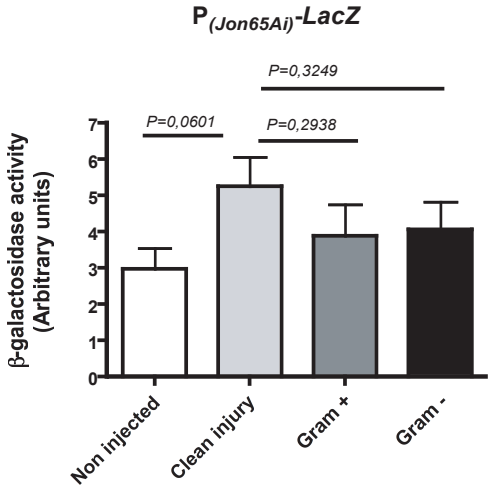

Figure 6.6: *Jon65Ai-LacZ* repoter gene is not repressed after bacterial challenge .

In order to identify a virus responsive element regulating the expression of *Jon65Ai* we generated truncated versions of the promoter region of *Jon65Ai* con-

taining 733, 483 ans 236 bp, placed upstream of the *LacZ* reporter gene. At least two lines of each construct were tested and the β-galactosidase activity was measured after infection with DCV. We detected the expression of β-galactosidase in all of the tested lines. Interestingly, the reporter activity was repressed in all the lines, suggesting that the first 236 bp of the promoter region are sufficient both for gene expression and repression by the virus (Figure 6.7).

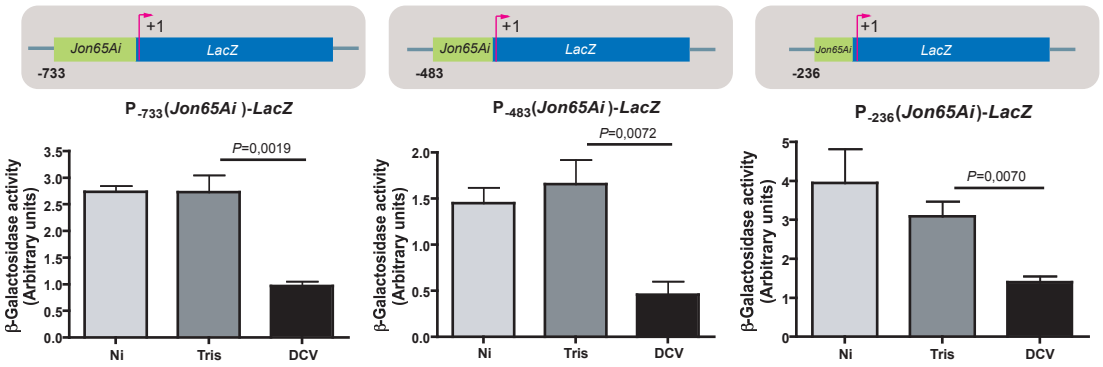

Figure 6.7: Analysis of *Jon65Ai* promoter region . Transgenic flies containing the *LacZ* gene under the control of truncated fragments of the *Jon65Ai* promoter were challenged with DCV, and β-galactosidase activity in single flies was measured 72 h later. Results correspond to the mean and error bars of three independent experiments. Representative result for at least two independent transgenic lines is shown

These results indicate that a regulatory sequence located in the 236 bp of the 5'UTR region is sufficient to drive expression. We compared a 250 bp sequence from the 5'UTR of *Jon65Ai* gene of *Drosophila melanogaster* with the same region of 7 other *Drosophila* species. We identify the starting codon ATG in all the sequences, as well as the TATA box, located upstream of the start codon (Figure 6.8). We observed three conserved regions between the 8 *Drosophila* species and found that two of them correspond to known transcription factor binding sites: GATA and Oct-11 (Figure 6.8) (gene-regulation.com). Interestingly, one GATA factor, dGATAe is involved in gut-specific gene expression in *Drosophila* larvae [Senger et al., 2006].

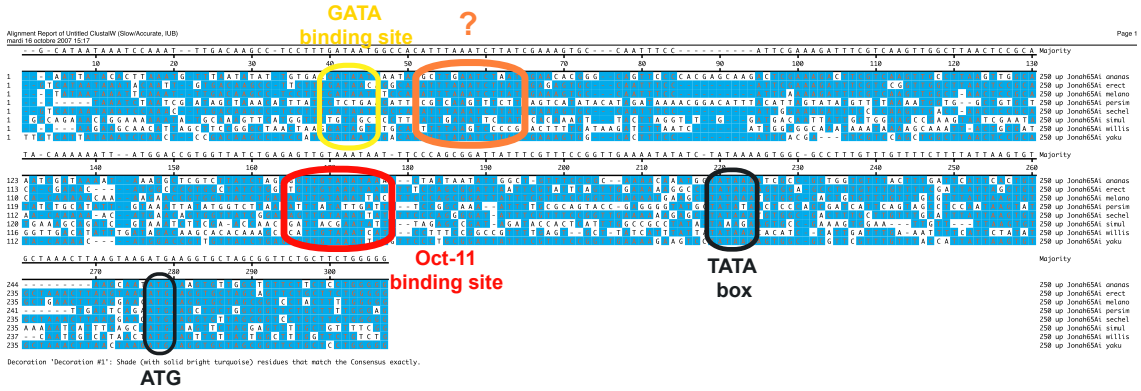

Figure 6.8: Analysis of *Jon65Ai* promoter region . Sequence alignement of the 250 bp of the 5'UTR region between eight *Drosophila* species. We notice the presence of conserved TATA box region. Three other regions of the promoter are strongly conserved between species and correspond to GATA, Oct-11 and unknown binding sites

6.1.3 Gene repression: physiological point of view

Genome wide microarray studies of *Drosophila* nutritional regulation showed that several members of the Jonah family of serine proteases were downregulated upon starvation [Bauer et al., 2006, Gronke et al., 2005]. This observation suggests that in the case of infection with DCV, the virus may trigger a nutritional stress and indirectly contribute to the gene repression. In order to verify this hypothesis we first analyzed the tissue distribution of the DCV-repressed genes. We used Flyatlas database (www.flyatlas.org) [Chintapalli et al., 2007] to analyse the tissue distribution of the one hundred most strongly repressed genes. We found that about 31% of them are specifically expressed in the midgut. Another 17% are also expressed in the midgut, although their expression is not restricted to this tissue. The list of the 30 most strongly repressed genes with their pattern of expression is shown in Table 6.1. We next compared the microarray data from DCV-infected and starved flies. We observed that 49,5% of the genes repressed by starvation, including Jonah proteases were also downregulated by DCV infection (Figure 6.9).

Repression factor (48h p.i.)	Gene	Function	Tissue pattern
18,76	***Ser4* (*Jon25Bi*)**	serine-type endopeptidase	midgut
12,23	**CG8869 (*Jon25Bii*)**	serine-type endopeptidase	midgut
7,47	**CG9466**	alpha-mannosidase	midgut
6,80	***Lsp2***	nutrient reservoir	head, eye, virgin spermatheca, adult carcass
6,32	***Sodh-1***	L-iditol 2-dehydrogenase	ubiquitous
5,93	**CG5973**	retinal binding	head, crop, eye, hindgut, heart, fat body, adult carcass
5,91	**CG8562**	metallocarboxypeptidase	midgut
5,41	**CG18180 (*Jon67Bi*)**	chymotrypsin	midgut
5,18	***Ser8***	trypsin activity	midgut
4,83	**CG9512**	choline dehydrogenase	head, tubule, adult carcass
4,75	**CG8871 (*Jon25Biii*)**	elastase	midgut
4,50	**CG11796**	4-hydroxyphenylpyruvate dioxygenase	head, eye, adult carcass
4,45	***Ser99Dc* (*Jon99Ci*)**	serine-type endopeptidase	midgut
4,41	**CG18030 (*Jon99Fi*)**	serine-type endopeptidase	midgut
4,28	**CG2736**	scavenger receptor	head, eye, heart, fat body, virgin spermatheca,mated spermatheca, adult carcass
4,26	**CG5804**	acyl-CoA binding	midgut
4,25	***Lectin-galC1***	sugar binding	heart, fat body, adult carcass
4,18	***Jheh3***	epoxide hydrolase	midgut, tubule, virgin spermatheca, mated spermatheca
4,14	**CG16749**	serine-type endopeptidase	midgut
4,11	**CG9468**	alpha-mannosidase	midgut
3,99	**CG7409**	chaperone	head,adult carcass
3,93	**CG3699**	oxidoreductase	head, midgut, tubule, heart, fat body, virgin spermatheca, adult carcass
3,88	**CG10475 (*Jon65Ai*)**	serine-type endopeptidase	midgut
3,86	***Obp57c***	odorant binding	head, eye, crop, hindgut, adult carcass
3,82	**CG7542 (*Jon74D*)**	chymotrypsin	midgut
3,81	***LysC***	lysozyme	?
3,81	***LvpL***	alpha-glucosidase	midgut
3,79	***Lsp1b***	nutrient reservoir	head, heart, fat body, virgin spermatheca, adult carcass
3,76	**CG6663**	serine-type endopeptidase inhibitor	male accessory glands
3,76	***MtnC***	metal ion binding	midgut

Table 6.1: DCV repressed genes and their tissue distribution . The thirty strongly repressed genes at 48h post-infection are shown. The tissue patterns are represented according to www.Flyatlas.org. The midgut specific genes are underlied in green.

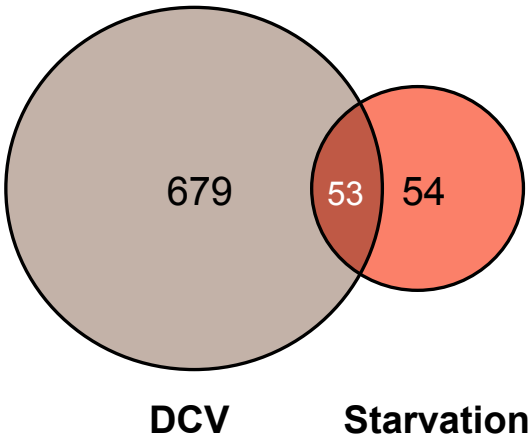

Figure 6.9: Transcriptome comparison between DCV-infected and starved flies . Venn diagrams showing the overlap of the downregulated genes between the DCV-infected and starved flies.

Altogether, our results suggest that DCV infection triggers a starvation-like shut down of midgut specific genes, possibly due to dysregulation of nutritional status of the fly.

6.2 DCV triggers a starvation-like state in *Drosophila*

We compared the β-galactosidase reporter activity in Jon65Ai-LacZ transgenic flies after DCV infection and starvation (Figure 6.10A). We observed that both DCV-infection and starvation downregulate the reporter activity. Studies on the *Drosophila* larval metabolism showed that during starvation, lipid stores are efficiently mobilized from larval fat body to hepatocyte-like cells, called the oenocytes [Gutierrez et al., 2007]. We wondered whether DCV also triggers such a phenomenon in adult flies. The staining of dissected carcasses with the Oil red O dye revealed that lipids were mobilized from the fat body to the oenocytes of about 90% of the adult flies 3 days post-infection (dpi) with DCV. By contrast, no such mobilization was observed in the case of the other RNA virus, FHV (Figure 6.10B, 6.10C). Surprisingly, we did not observe a strong mobilization of the lipid stores in flies 24 or 48 hours after starvation (data not shown). We looked by immunofluorescence if the oenocytes are infected by DCV. We observed that these cells are infected although the labelling is detected at later time points than in the fat body, after the manifestation of the first symptoms of infection (Figure 6.11). Therefore, we do not believe that the oenocytes play a role in the onset of the pathology. Overall, our results indicate that *(i)* differences exist in the physiological response to starvation in adults and larvae, and *(ii)* the effect of DCV infection may not simply reflect food deprivation.

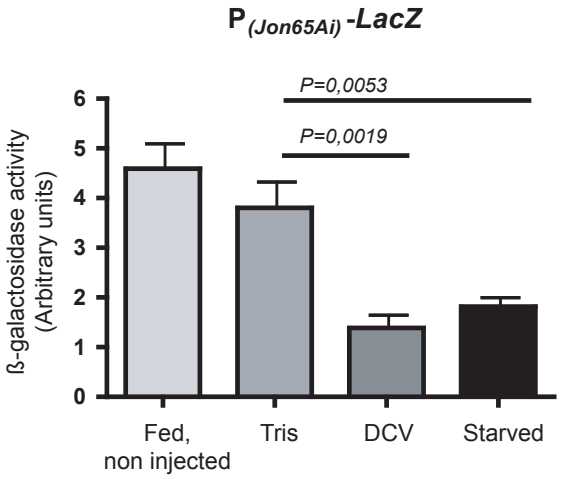

A *Jon65Ai-LacZ* reporter activity is repressed after DCV infection and starvation

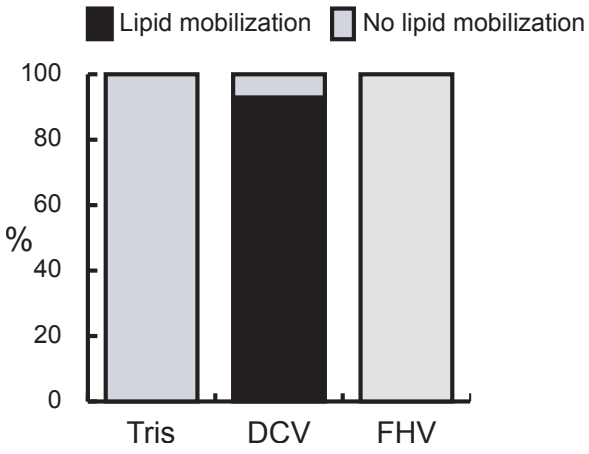

B Quantification of lipid mobilization

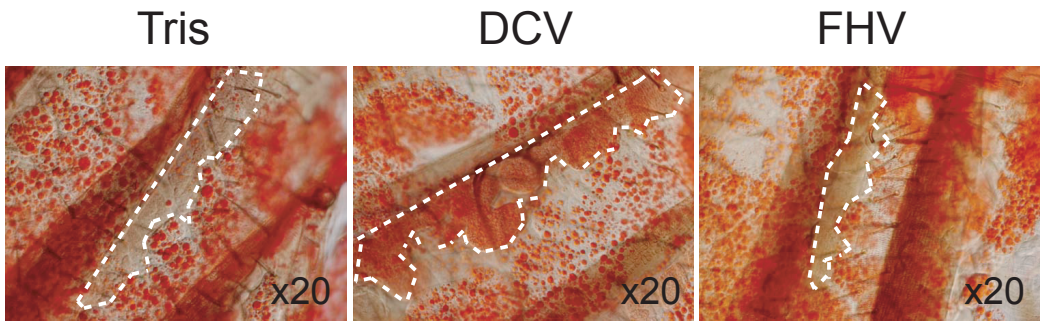

C Oil red O staining of neutral lipids in virus-infected flies

Figure 6.10: Similarities between DCV-infected and starved flies . **A.** DCV infection and starvation downregulate the reporter gene *Jon65Ai-LacZ*. (**B**), (**C**) Lipid mobilization from fat body to oenocytes in adults 3 days after infection with DCV,but not FHV, similar to starved *Drosophila* larvae. The oenocytes are limitted with the dotted lines. Tris: n=15, DCV: n=14, FHV: n=14

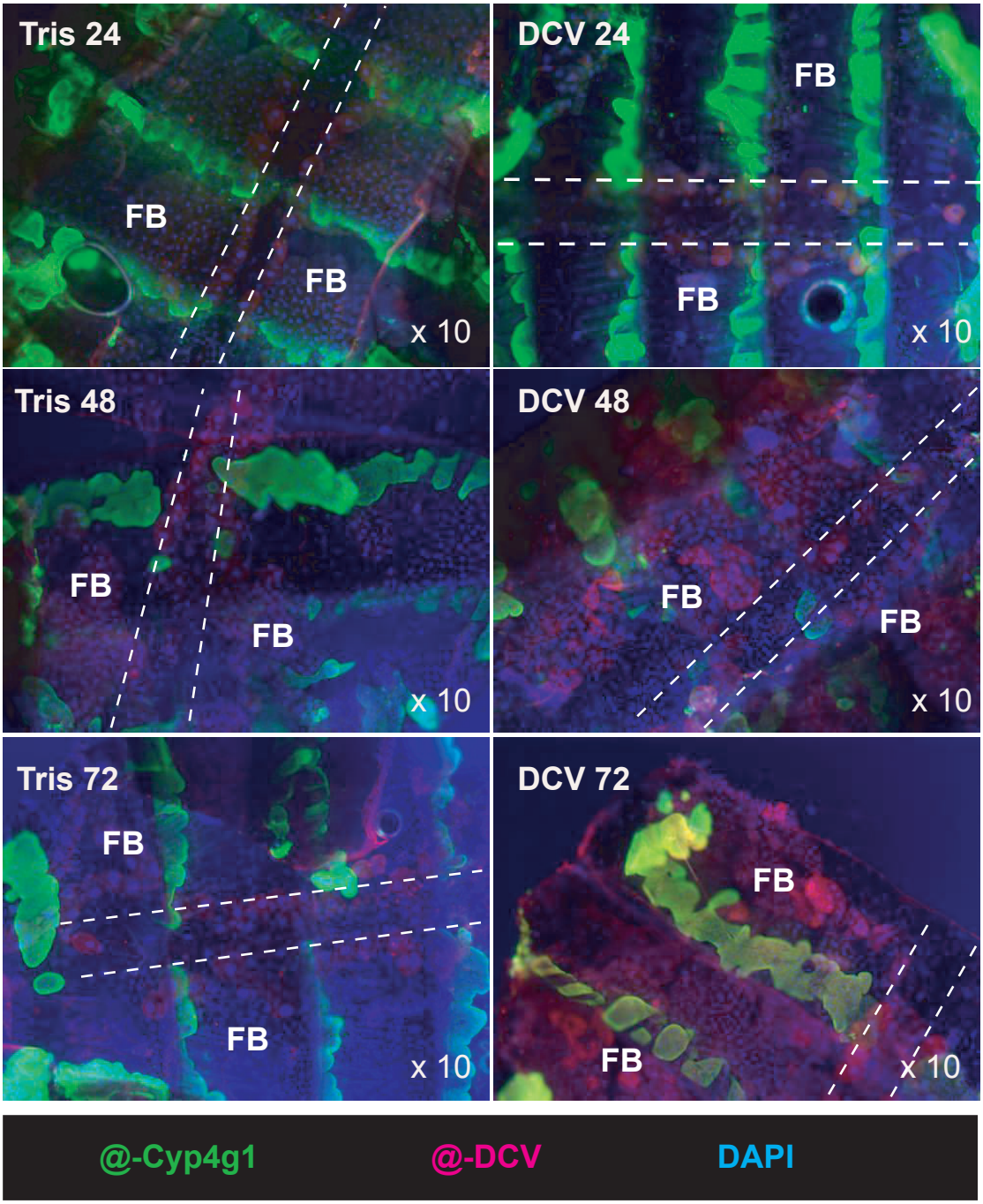

Figure 6.11: DCV infects *Drosophila* oenocytes at late time points . Double immunostaining of dissected carcasses. The virus (red) colocalizes with the Cyp4g1, expressed in oenocytes (green) at 72h post-infection. We detect the viral capsid in the fat body cells already at 48h post-infection. The cardiac tube is limitted with the dotted lines. Legend: **FB**: fat body

6.3 Does DCV induce a nutritional stress in *Drosophila*?

We hypothesized that infection with DCV will trigger a decrease in the body weight of the flies, as is the case when flies are food-deprived. We measured the body weight of DCV, FHV and starved flies and observed a significant decrease 2 days after starvation, as expected (Figure 6.12A). Surprisingly, DCV infected flies gain, rather then lose weight, compared to Tris or FHV- injected flies. The increase become significant 4 days following infection, and was accompanied with abdominal swelling (Figure 6.12B).

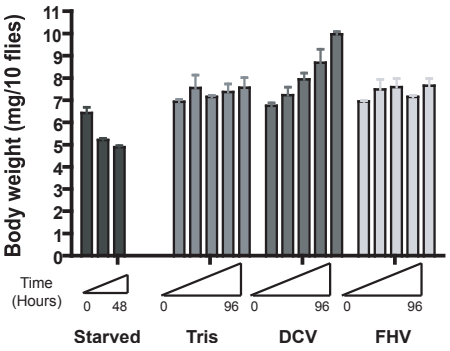

	DCV	FHV	Starvation
0h	*P*=0,3594	*P*=0,8891	*P*=0,1270
24h	*P*=0,6601	*P*=0,9352	*P*=0,0516
48h	*P*=0,0606	*P*=0,3364	***P=0,0002***
72h	*P*=0,1342	*P*=0,5930	/
96h	***P=0,0073***	*P*=0,8721	/

A

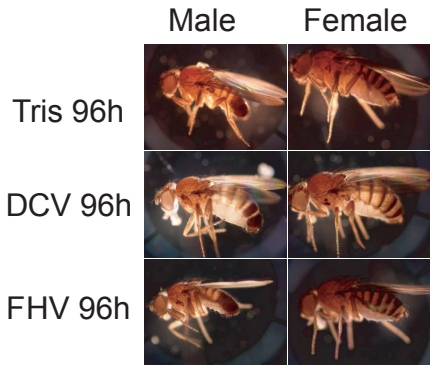

B

Figure 6.12: Increased body weight in DCV-infected flies . **A.** Groups of 10 flies (5 males and 5 females) were weighted at different time points at intervals of 24 hours after starvation or injection with Tris (control), DCV or FHV. The *P*-values from statistical analysis (Student's *t*-test) are shown on the table. **B.** Abdominal swelling in DCV-infected flies.

We next measured the triglycerides and glucose levels in infected flies. Triglycerides were significantly reduced in DCV and FHV infected flies 72 and 96 hours post-infection, with levels comparable to those of starved flies (Figure 6.13A). However, the glucose levels were only reduced 96h post-infection and in a similar manner for DCV and FHV infected flies (Figure 6.13B).

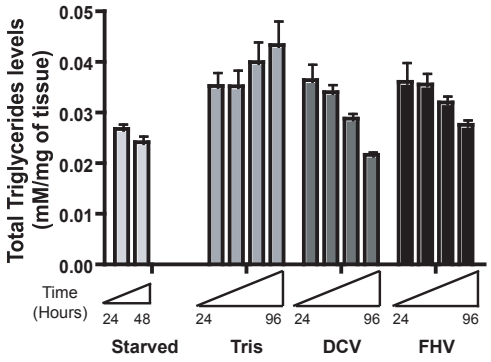

	DCV	FHV	Starvation
24h	*P*=0,5634	*P*=0,4788	***P=0,0006***
48h	*P*=0,6403	*P*=0,8743	***P=0,0073***
72h	***P=0,0025***	***P=0,0105***	/
96h	***P=0,0008***	***P=0,0039***	/

A Triglycerides levels in virus-infected flies

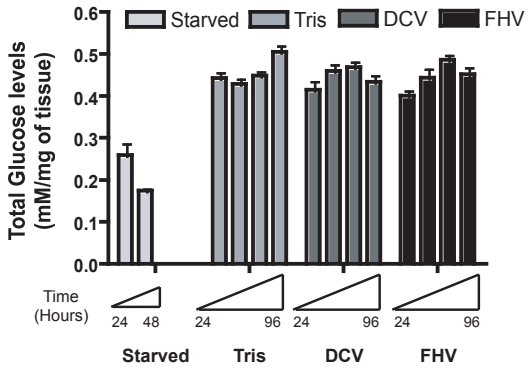

	DCV	FHV	Starvation
24h	*P*=0,1665	*P*=0,0561	***P=0,0003***
48h	***P=0,0397***	*P*=0,2954	***P<0,0001***
72h	*P*=0,3789	*P*=0,2544	/
96h	***P=0,0067***	***P=0,0386***	/

B Glucose levels in virus-infected flies

Figure 6.13: Total triglycerides and glucose levels in virus-infected flies . Total triglyceride (**A**) and glucose (**B**) levels were measured in groups of five flies at different time points at intervals of 24 hours after starvation, injection with Tris (control), DCV or FHV. The graphs represent the mean and error bars from three independent experiments, each performed in triplicates. The *P*-values from statistical analysis (Student's *t*-test) are shown on the tables.

Finally, we examined whether infected flies continue to feed and assessed the food ingestion by a colorimetric assay in which flies feed on 0,1% Bromophenol blue and 0,5% Xylene cyanol-containing medium ("tracking" medium) [Ayres and Schneider, 2009]. We observed a significant increase in the staining intensity of DCV, but not Tris- or FHV-infected flies (Figure 6.14A). This could be

due either to increased food uptake or to decreased excretion. To test whether the increase of the body weight is due to decreased defecation rates, we monitored the quantity of feces deposited as blue spots on the sides on the culture vial. We observed that DCV infection was associated with a decrease in the defecation rate (Figure 6.14B), in contrast to control or FHV-infected flies.

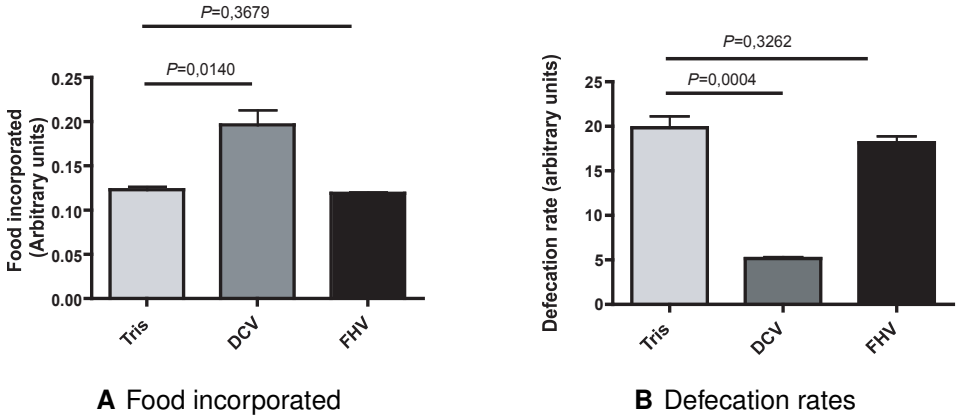

A Food incorporated **B** Defecation rates

Figure 6.14: Food incorporated and defecation rates in infected flies . **A.** Groups of 10 flies were injected with Tris, DCV or FHV and kept on Tracking medium. 4 dpi flies were homogenized in TE-0,1% Triton-X100 buffer and the O.D$_{614nm}$ of the supernatants, corresponding to the incorporated food was measured. **B.** Groups of 10 flies were injected with Tris, DCV or FHV and kept on Tracking medium. 3 dpi flies were transferred in empty vials and blue spots corresponding to excretion rates were measured 5h later. (**A**) and (**B**) The graphs represent the mean and error bars from three independent experiments, each performed in triplicates.

Overall, our data indicate that DCV infection is accompanied by wasting symptoms (decreased triglycerides and glucose levels). However, this wasting is also observed for FHV and probably reflects a general consequence of viral infection on the flies. Furthermore, DCV infection does not induce a dramatic cessation of food uptake that could explain the similar repression of gut specific genes observed in DCV-infected and starved flies.

The apparent descripancy between the starvation-like status of DCV-infected flies and their increasing body weight suggests a dysregulation of the homeostatic mechanisms regulating energy storage. The hormone AKH, which is produced by CC cells in response to food deprivation, normally triggers release of stored nutrients in the fat body to guarantee survival [Baker and Thummel, 2007]. Inter-

estingly, AKH release by the CC cells is regulated by the K_{ATP} channel composed of Ir and dSUR [Kim and Rulifson, 2004]. Because we observed that Ir appeared to play a role during DCV infection (Figure 5.6A), we tested if the CC played a role in the resistance to DCV infection. Tissue-specific knock down of *Ir* and *dSUR* in the CC did not affect the resistance to DCV infection (Figure 6.15A, 6.15B).

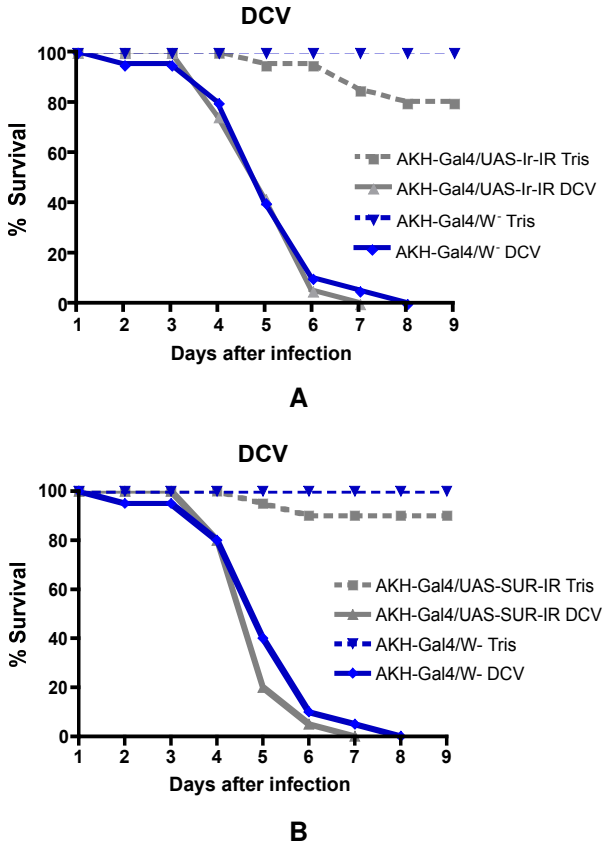

Figure 6.15: The *Corpus cardiacum*-specific knock down of *Ir* (A) and *dSUR* (B) does not affect resistance to DCV infection . IR: inverted repeat

To completely exclude a role of the CC in the control of DCV infection, we next genetically ablated this organ by forced expression of the pro-apoptotic gene *reaper* using an AKH-Gal4 driver (Figure 6.16A, 6.16B). Neither the survival of the flies, nor the mobilization of triglycerides to the oenocytes following DCV infection were affected in CC-ablated flies (Figure 6.17A, 6.17B). We concluded that AKH-producing cells are not involved in the pathology caused by DCV.

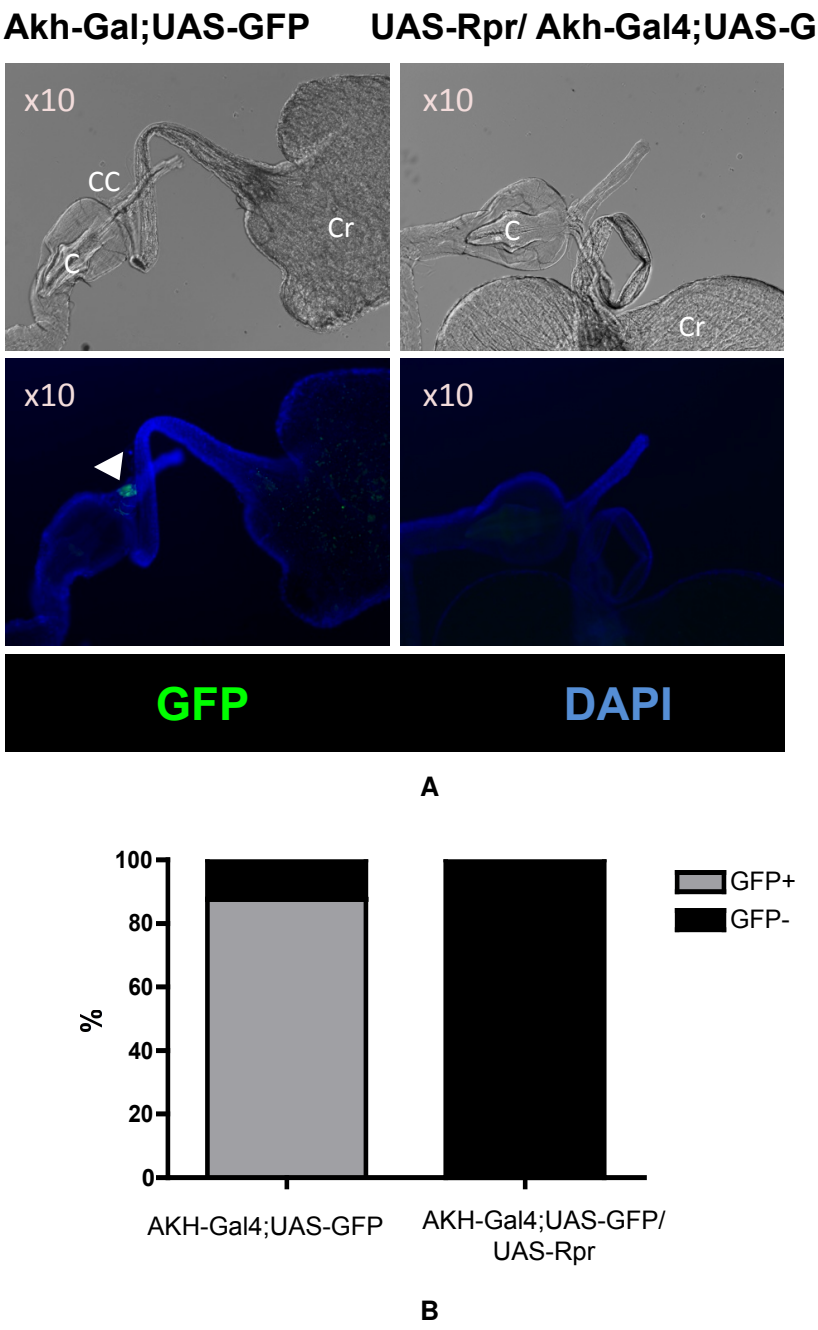

Figure 6.16: ***Reaper*-triggered ablation of CC cells** . **A.** Detection of GFP-expressing AKH-producing cells, located at the level of the cardia (white arrowhead). We notice the abscence of GFP in reaper-triggered ablation of these cells. **B.** Quantification of the CC cells ablation. AKH-Gal4: n=8, UAS-Rpr/AKH-Gal4: n=14

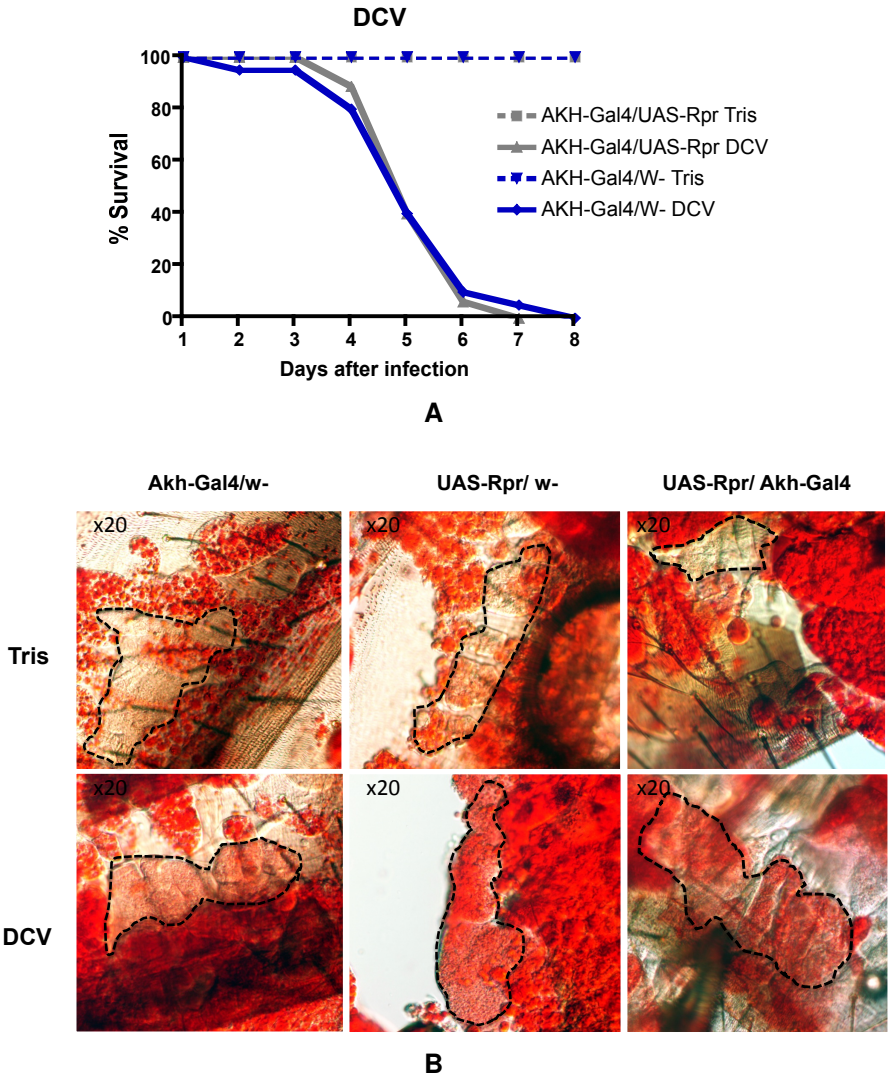

Figure 6.17: *Reaper*-triggered ablation of CC cells does not affect the outcome of DCV infection . **A.** Survival curves of control and CC-ablated flies. **B.** Similar lipid mobilization from the fat body to the oenocytes in control and CC-ablated flies. The oenocytes are limitted with the dotted lines.

6.4 DCV induces intestinal obstruction in *Drosophila*

The fact that DCV infection is associated with an increase in the incorporated food and a decrease in the defecation rates, suggests that the food might be retained in the digestive tract of the flies. We dissected the digestive tracts of control, DCV and FHV-infected flies, kept on blue "tracking" medium, and observed a strong accumulation in the food-storage organ, called the crop, and the

anterior part of the midgut (Figure 6.18A). By contrast, the posterior part of the midgut and the hindgut of DCV-infected flies is not stained. This result provides an explanation for the fact that DCV infected flies defecate less than the controls. The colorimetric assay measures the total amount of food incorporated in the digestive tract of the fly, but does not quantify the amount of food uptaken. To measure the exact volume of food uptake in DCV infected flies we used the Capillary Feeder (CAFE) assay [Ja et al., 2007]. We observed that DCV-infected flies ingested a significant amount of food (more than 1.2 μL of nutritional solution per 24h), confirming that DCV infection does not induce cessation of feeding (Figure 6.18B). However, DCV-infected flies ingested slightly less food than healthy controls. This confirms that the ingested food is retained in the digestive tract of DCV-infected flies.

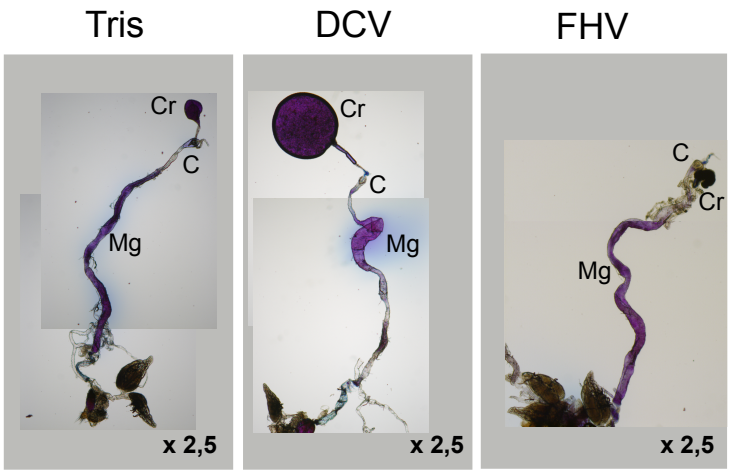

A Food retention in the digestive tract of DCV-infected flies

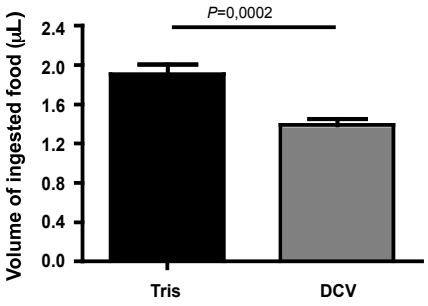

B Quantification of the volume of ingested food

Figure 6.18: Food incorporated and CAFE assay . **A.** Dissected digestive tracts from Tris, DCV and FHV injected flies, kept on 'tracking' medium. The blue dye is equally distributed through the whole gut of Tris controls and FHV-infected flies. The blue food accumulates preferentially in the crop and anterior part of the midgut in DCV-infected flies. Legend: **Cr**: crop, **C**: cardia, **Mg**: midgut. **B.** Measurement of the ingested volume of food in Tris controls and DCV-infected flies. Mean and error bars from two independent experiments.

When observing the anterior midgut of DCV-infected flies by contrast phase microscopy, we noticed the presence of invaginated membranous material in the lumen (Figure 6.19). This could correspond to disorganized peritrophic matrix, the protective extracellular membranous material that lines the midgut epithelium.

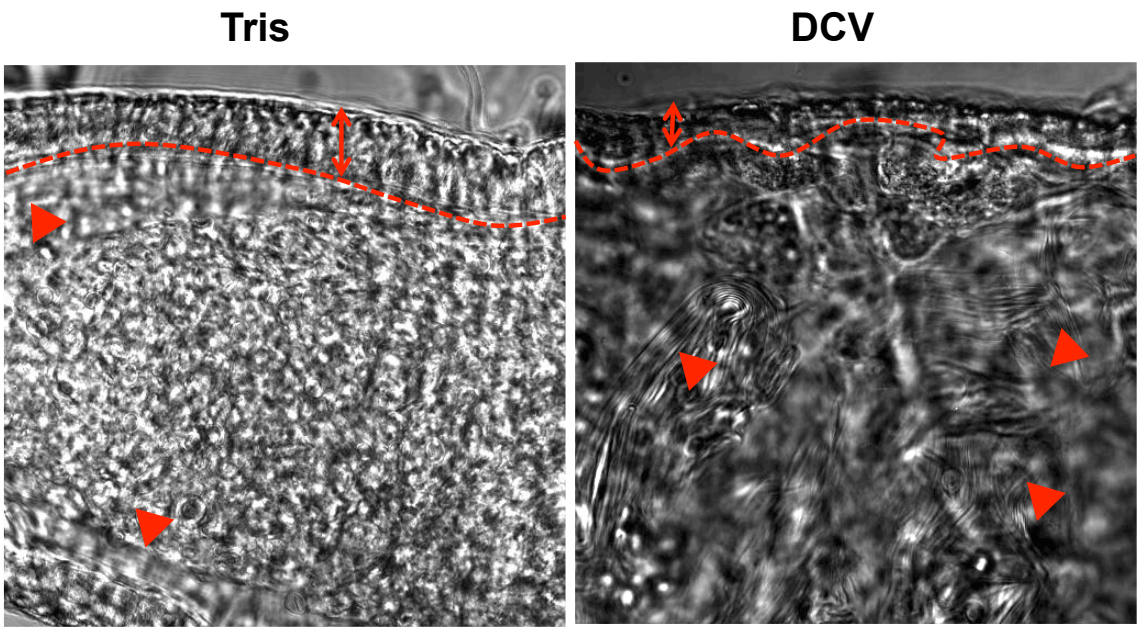

Figure 6.19: Accumulation of membranous material in the *Drosophila* gut after DCV infection . Digestive tracts were dissected 3 dpi from Tris and DCV-infected flies. The peritrophic matrix is indicated with the arrowheads. Invaginations are visible in the lumen of the gut of DCV-infected flies.

Calcofluor is a dye that specifically stains chitin, which is the major component of the peritrophic matrix in *Drosophila* midgut. When the dye is administrated by feeding to control flies, it stains the whole midgut. By contrast, in DCV-infected flies, only the crop and the anterior midgut are stained by Calcofluor (Figure 6.20A, 6.20B). These results indicate that DCV infection induces an obstruction in the digestive tract of the fly, possibly by disorganized peritrophic matrix. The results obtained from the "tracking" medium-fed and calcofluor-fed flies show staining in the anterior part of the midgut. This observation suggests that one part of the food bolus can pass trough the cardia. However, the ingested food can not be further processed and this might explain the downregulation of midgut specific genes, in particular the proteases involved in digestion.

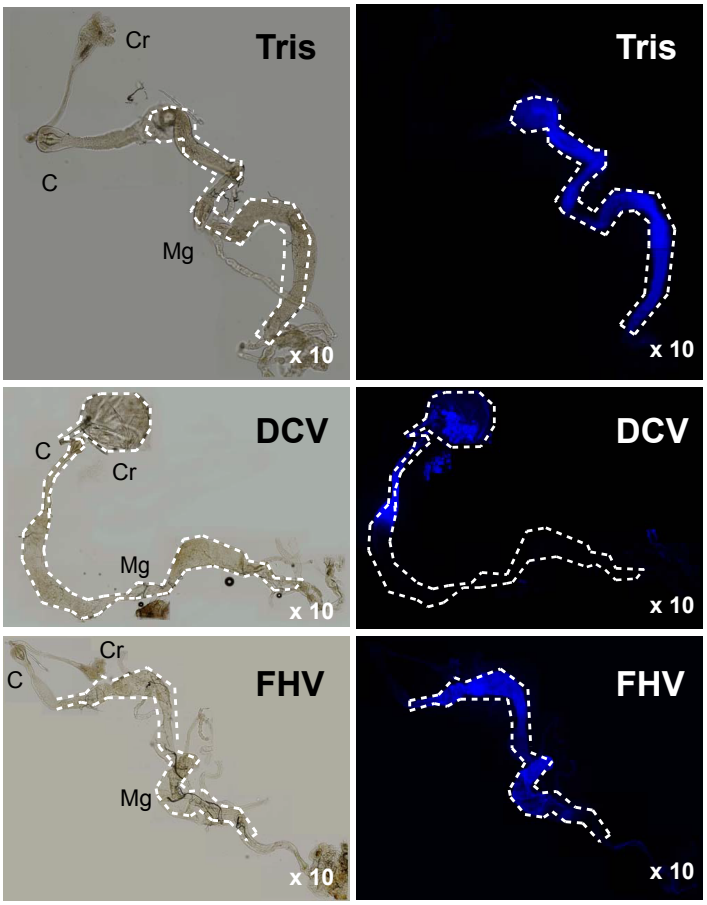

A Ingested Calcofluor dye is retained in the crop and anterior midgut of DCV-infected flies

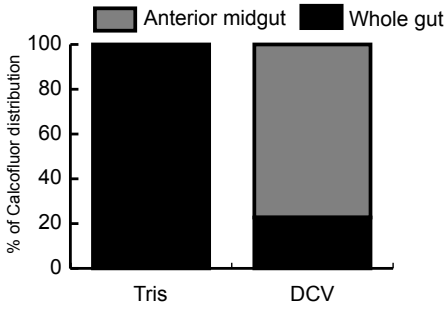

B Quantification of the intestinal obstruction

Figure 6.20: DCV induces intestinal obstruction in *Drosophila* . A. Dissected digestive tracts from Tris, DCV and FHV injected flies, fed for 6h on on Calcofluor. The dye is equally distributed through the whole gut of Tris controls and FHV-infected flies. The blockage in the gut does not allow the normal passage of food through the digestive tract. The midguts are limitted with the dotted lines. Legend: **Cr**: crop, **C**: cardia, **Mg**: midgut. **B.** Quantification of the intestinal obstruction of Tris-injected, DCV-infected flies. Tris: n=19, DCV: n=22.

These results suggest that DCV infection triggers modifications at the level of

the anterior part of the midgut. We noticed a very clear alteration of the morphology of the cardia (Figure 6.21) in DCV-infected flies, with a characteristic swelling of its posterior part. The swelling becomes apparent 3 dpi, and is visible in all flies 5 dpi.

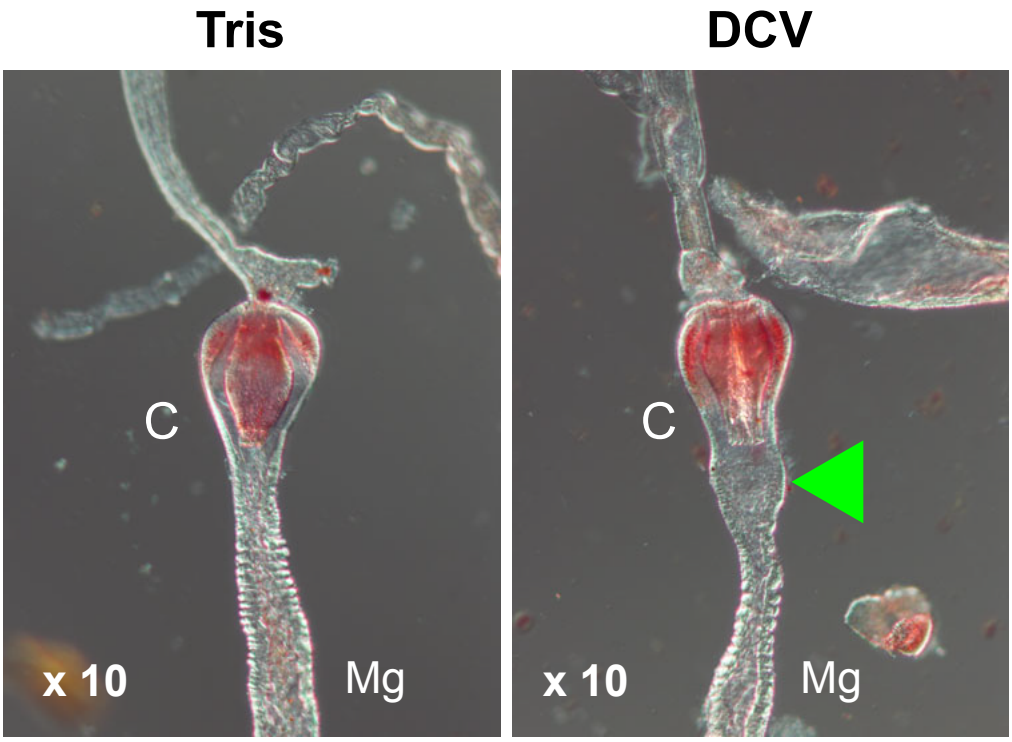

Figure 6.21: Morphological changes of the *Drosophila* cardia during DCV infection . Digestive tracts were dissected 3 dpi from Tris and DCV-infected flies. We notice the swallen posterior part of the cardia in DCV-infected flies (arrowhead). Legend: **Mg**: Midgut, **C**: cardia

We analyzed by electron microscopy the digestive tracts from DCV-infected flies, focusing on the most anterior part of the midgut, the cardia (Figure 6.22), see also Figure 3.4A. Our preliminary results show several abnormalities: *(i)* the inner (IR) and recurrent (RL) layers are much thinner following DCV infection, *(ii)* the hilus (H) size is considerably increased, *(iii)* the lumen of the oesophagus is filled with a fibrous material in which some yeasts are trapped (Figure 6.23).

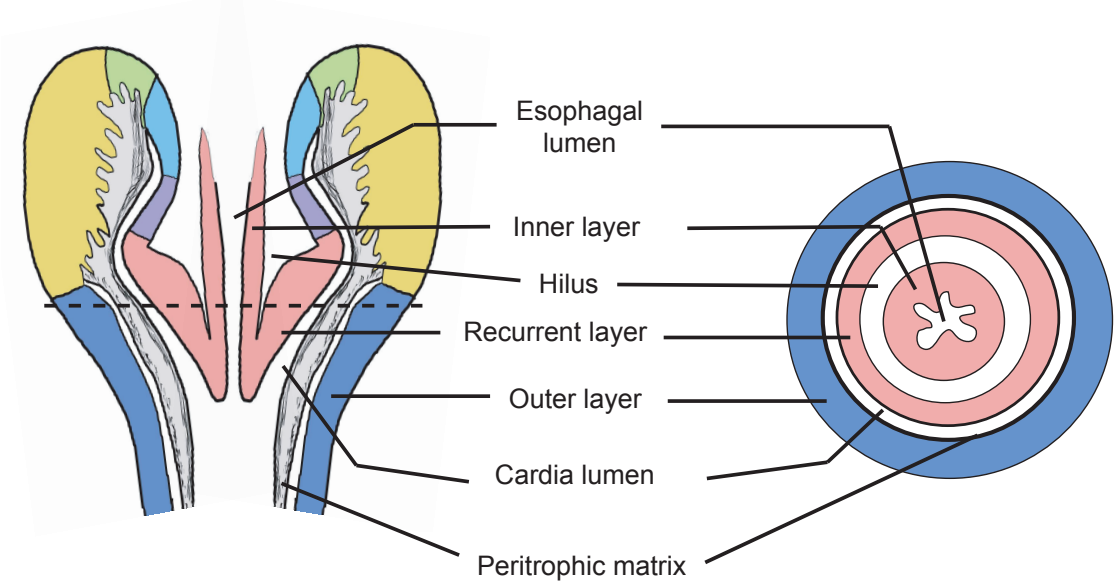

Adapted from D.G. King *(Journal of morphology, 196:253-282, 1988)*

Figure 6.22: Schematic representation of the *Drosophila* cardia. . Longitudinal and transversal sections of the cardia.

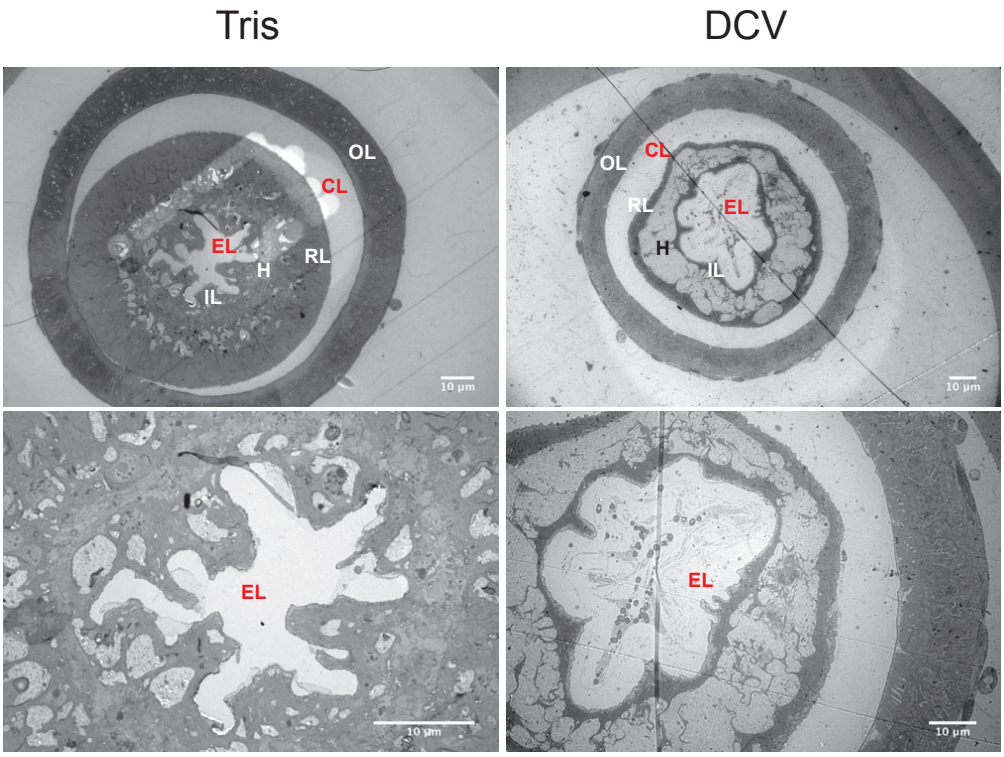

Figure 6.23: Electron micrographs of transversal sections of the *Drosophila* cardia in controls (Tris) and DCV-infected flies . Disturbed organization of the cardia in DCV-infected flies. We notice the presence of yeast in the esophagal lumen of DCV-infected flies. Legend: **EL**: oesophagal lumen, **IL**: inner layer, **H**: hilus, **RL**: reccurent layer, **CL**: cardia lumen, **OL**: outer layer. Scalebar: 10 μm

6.5 The DCV-induced pathology is not due to the activation of the host immune response

To test whether the symptoms observed in DCV-infected flies were a consequence of the host immune response or a direct consequence of virus infection we analyzed the pathology associated with DCV infection in *Drosophila* mutants for the antiviral immune pathways. RNA interference is major antiviral mechanism and was shown to play an essential role in the resistance to a wide range of viruses [Galiana-Arnoux et al., 2006, Wang et al., 2006, van Rij et al., 2006, Zambon et al., 2006] and [Kemp, 2011]. The JAK/STAT, Toll and Imd pathways also participate to antiviral host defense [Zambon et al., 2005, Dostert et al., 2005, Costa et al., 2009, Avadhanula et al., 2009]. We first analyzed the DCV-induced pathology in flies mutant for Dcr-2, a key component of the RNAi pathway. We measured the repression of the endogenous Jon65Ai protein in dissected digestive tracts of *yw* (WT) and *Dcr-2* mutants and observed no difference in the repression of Jon65Ai (Figure 6.24).

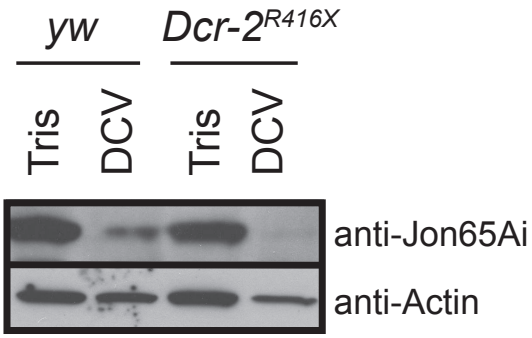

Figure 6.24: Jon65Ai is repressed in the gut of *Dcr-2* mutants . Western blot analysis of proteins extracted from the guts of Tris- and DCV-injected flies, 72h post-infection.

We also measured the body weight, lipid mobilization and incorporated food in *Dcr-2* deficient flies, and did not observe differences with the wild type controls. *Dcr-2* mutants mobilize their lipid stores (Figure 6.25), and their body weight in-

creases significantly 72h after infection with DCV (Figure 6.26A). At this time point, the body weight of the wild type controls is not significantly increased, indicating faster developement of the symptoms in *Dcr-2* mutant flies. The colorimetric assay for food incorporation showed similar increase in the staining intensity in WT and *Dcr-2* deficient flies infected with DCV (Figure 6.26B). Therefore we conclude that the DCV induced pathology does not depend on the siRNA pathway. If anything, the symptoms appear earlier or are stronger in the *Dcr-2* mutant flies, which may reflect the more rapid accumulation of DCV in the mutant flies. Similar experiments with flies mutant for the genes *hopscotch* (JAK/STAT pathway), *Dif* (Toll pathway) and *imd* (IMD pathway) yielded similar results (Table 6.2). Therefore, we conclude that the observed symptoms do not result from the adverse effect of the host immune response, but rather reflect a direct effect of the virus on its host.

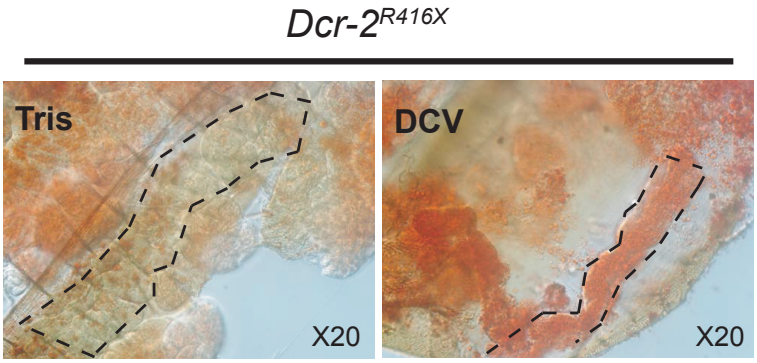

Figure 6.25: Lipid mobilization from fat body to oenocytes in *Dcr-2* mutant flies . Oil red O staining of dissected carcasses form *Dcr-2* flies. The oenocytes are limitted with the dotted lines.

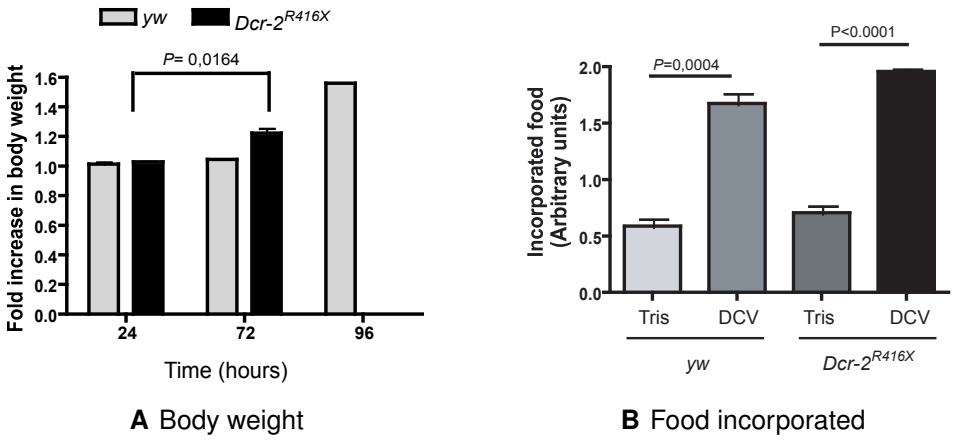

A Body weight **B** Food incorporated

Figure 6.26: Increased body weight and incorporated food in *Dcr-2* mutants . **A.** Increased body weight in *Dcr-2* mutant flies after infection with DCV. **B.** Increase of the incorporated food in *Dcr-2* mutants after infection with DCV

Mutant	Survival after DCV infection	Jon65Ai expression	Body weight	Food incorporated	Lipid mobilization
Hopscotch	Sensitive	Decreases	n.d.	n.d.	yes
Dif^{1}	Sensitive	Decreases	Increases	Increases	yes
Imd^{Shadok}	Sensitive	Decreases	Increases	Increases	yes

Table 6.2: DCV-induced pathology in other antiviral immune pathway mutants .

6.6 The closely related Cricket paralysis virus does not induce the same pathology as DCV

To test whether the pathology associated with DCV infection is specific to this virus or is a common for other members of the *Dicistroviridae* family, we compared the pathology between DCV and Cricket paralysis virus (CrPV). DCV and CrPV are closely related and their genomic RNAs share a high percentage of homology (Figure 6.27). The main difference between the two viruses resides in

their supressors of RNAi, which are not structurally related and function differently (see 2.1.3). When injected to flies, DCV and CrPV kill their host within a few days.

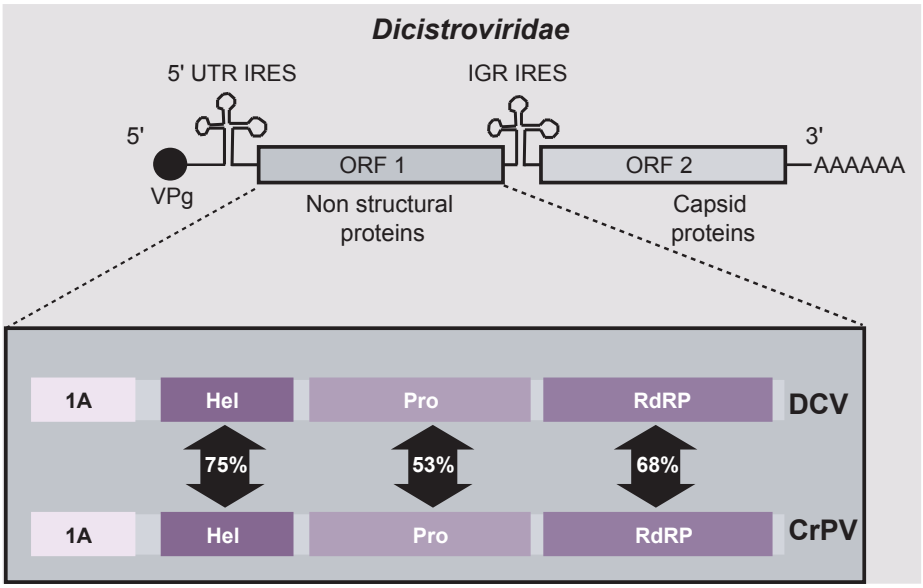

Figure 6.27: Schematic representation of the genome structure of two Dicistroviruses: DCV and CrPV . The translation of viral proteins is regulated by two IRES sites. The percentage of identity between three non-structural genes encoded by ORF1 is shown. The variable N-terminal domain of the polyprotein encoded by ORF1 in DCV and CrPV plays a role in supression of host RNAi. Legend: **Hel**: helicase, **Pro**: protease, **RdRP**: RNA-dependen RNA polymerase.

We first measured the reporter activity in Jon65Ai-LacZ flies, infected with the two viruses. We observed the repression of the β-galactosidase activity in Jon65Ai-LacZ flies after challenge with DCV, but not CrPV (Figure 6.28A). In addition, CrPV infected flies did not show an increase in the body weight 4 days post-infection, as is the case after DCV infection (Figure 6.28B). Finally, CrPV infection did not trigger an increased retention of the food, as measured with the food incorporation colorimetric assay (Figure 6.28C). The only similarity observed between CrPV and DCV infected flies is a decrease in the defecation rate (Figure 6.29). We conclude that, with the exception of defecation, DCV triggers a specific set of symptoms.

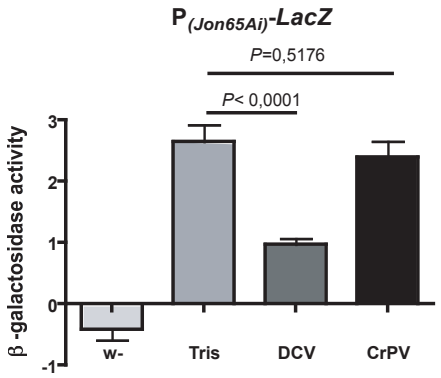

A β-galactosidase activity in DCV and CrPV-infected Jon65Ai-LacZ flies

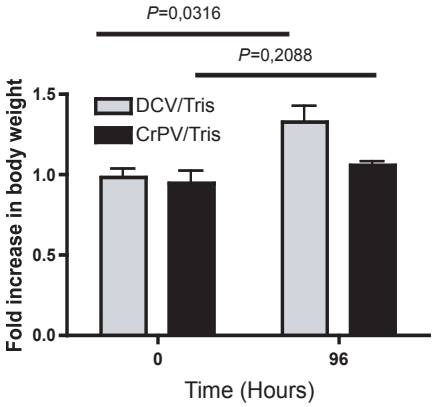

B Body weight of DCV and CrPV-infected flies

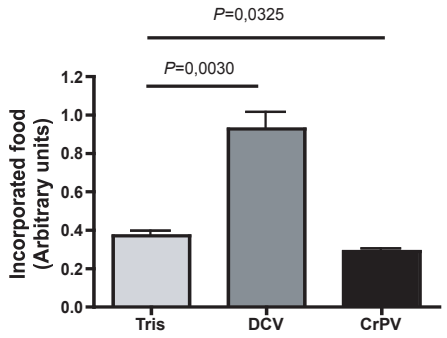

C Food incorporation after DCV and CrPV infection

Figure 6.28: DCV-induced pathology is not phenocopied in CrPV-infected flies
.

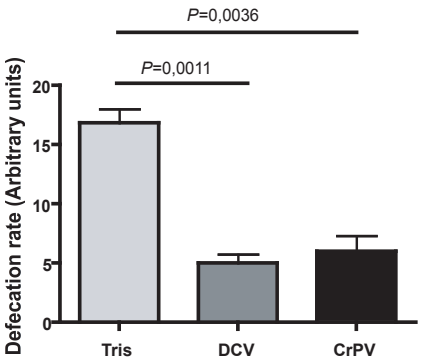

Figure 6.29: Defecation rates in CrPV-infected flies, similar to DCV-infected *Drosophila* .

In order to understand the difference between the symptoms caused by the two viruses, we compared the tissue tropism of DCV and CrPV by *in situ* hy-

bridization. We observed a clear labelling for DCV RNA in the fat bodies of infected flies (Figure 6.30B), but not in other tissues. This result is in agreement with previous studies indicating that the fat body is a major site of replication for DCV. CrPV RNA is also detected in the fat body (Figure 6.30B). In addition, we detected CrPV RNA in the cardiac tube and the visceral muscles surrounding the gut (Figure 6.30A, 6.30B). We hypothesized that infection of those muscles by CrPV might affect the peristaltic activity of the gut and result in the observed decrease in defecation rates.

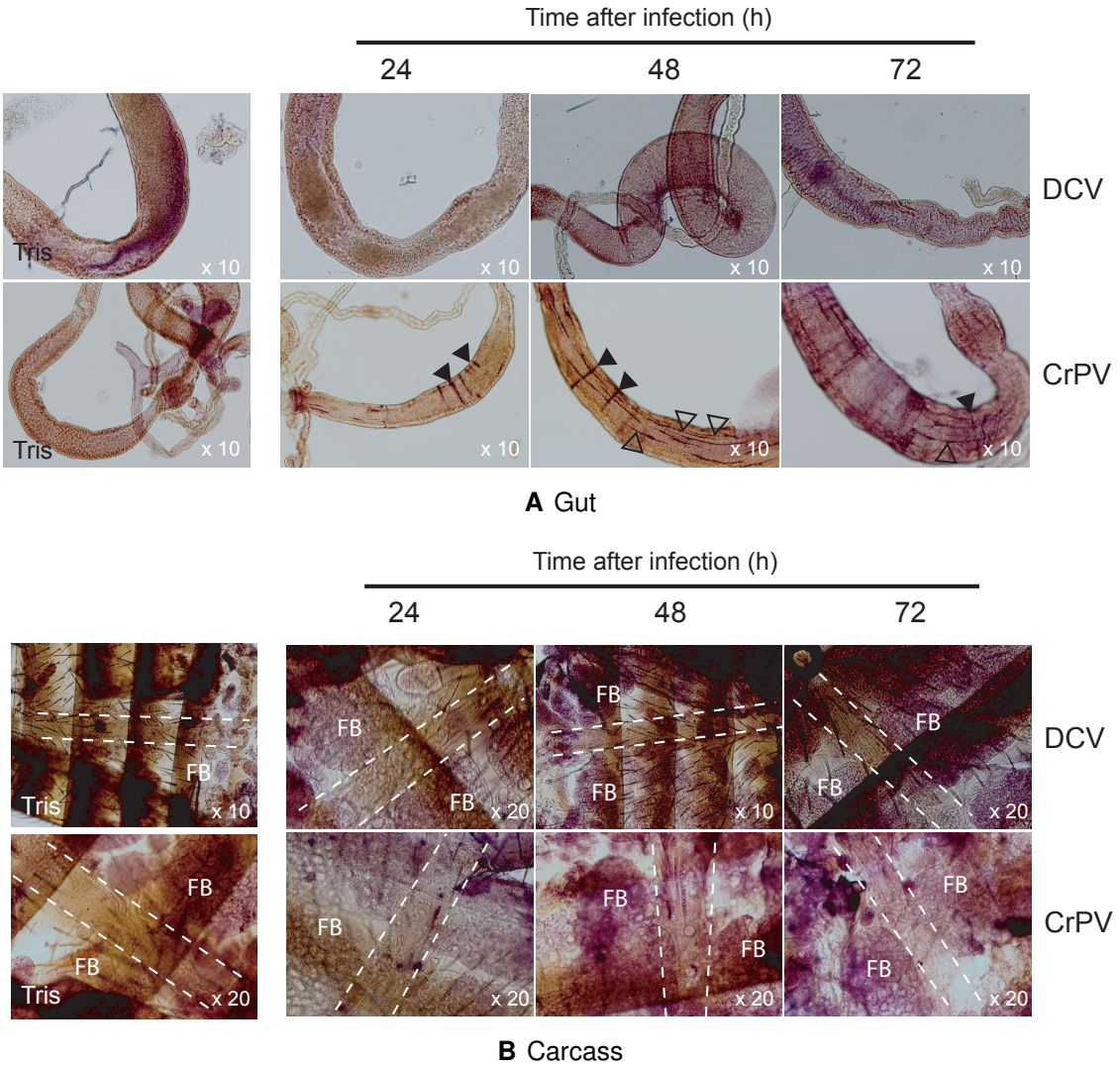

Figure 6.30: ***In situ*** **hybridization detecting DCV and CrPV RNAs** . **A.** CrPV RNA is detectable in the visceral muscle surrounding the gut. The filled and empty arrowheads indicate the circular longitudinal fibers, respectively. **B.** Accumulation of DCV RNA in the fat body of infected flies. CrPV RNA is detectable in the fat body, as well as in the heart of infected flies. The heart is limitted with the dotted lines.

Unfortunately, we could not identify by *in situ* hybridization tissues specifically targetted by DCV compared to CrPV, which could have provided a hint for the cause of the DCV-induced symptoms. This might reflect a technical limitation of the technique used, which did not allow us to detect DCV RNA in the tissues where it replicates at a lower level than in the fat body. Indeed, we did not detect DCV RNA in the periovarian sheath, which is a known target tissue for DCV [Sabatier et al., 2003, Cherry and Perrimon, 2004], or in the oenocytes, where we detected DCV by immunofluorescence (Figure 6.11).

6.7 What are the tissues involved in the DCV-induced pathology?

The DCV pathology is caracterized by an intestinal obstruction at the level of the anterior midgut, accompagnied by a swelling of the posterior region of the cardia. Two hypothesis could account for this phenomenon: DCV could affect either the neurons regulating the opening of the stomodeal valve or the contraction of the smooth muscles of the cardia. In a first attempt to discriminate between these two hypothesis, we looked for the presence of virus in these tissues. We repeatedly failed to detect DCV in the digestive tract using immunofluorescence, which may be due to the high background observed for this tissue in control, non-infected flies (data not shown). Therefore, we dissected flies and looked by western blot for the presence of DCV in the fat body, the brain and the cardia (Figure 6.31). We observed a strong signal for the cardia, indicating that DCV is present in this tissue. DCV was also detected in the brain, although at a lower level. Further studies, using immunofluorescence, or in the case of the cardia, electron microscopy will be required to identify the cell types infected by DCV, which my contribute to the pathology.

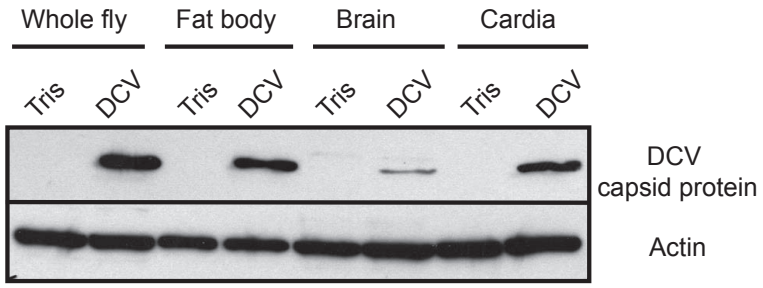

Figure 6.31: DCV is detectable in *Drosophila* cardia and brain . Western blot analysis of proteins extracted 3 dpi from dissected tissues of Tris or DCV-infected flies.

6.8 DCV-induced patholgy: why do infected flies die?

Our first hypothesis was that DCV-infected flies die from starvation. However, several experimental facts argue that this is not the case. For example, the glucose levels do not decrease as rapidly and strongly as in the case of starvation (Figure 6.13B). Furthermore, we could not increase the survival of the flies with injection of glucose (data not shown). The decreased expression of midgut proteases in DCV-infected flies may result in an amino acid starvation [Bauer et al., 2006]. However, flies can survive for long period on sucrose diet (V. Barbier, personnal communication), indicating that amino acid starvation is likely not the cause of the death.

An alternative hypothesis is that DCV infection triggers the production or accumulation of toxic compounds. For example, mobilization of lipid stores during fasting in mammals leads to the production of ketone bodies, which can lead to a decrease in the blood pH and have toxic effects (ketoascidosis). In order to monitor the pH of the hemolymph of DCV-infected flies, we crushed in a preliminary experiment whole flies on pH paper. Strikingly, we observed that several DCV-infected flies had an acidic pH. By contrast, all control flies had a neutral pH (data

not shown). To confirm this result, we extracted hemolymph from the thorax of control and DCV-infected flies and dotted it on pH paper. In this case we did not observe an acidification (data not shown). We reasoned that the acid pH might come from the abdomen, which is swollen in DCV-infected flies. Indeed, when we extracted the content of the abdomen and dotted it on pH paper, we observed an acidification in all DCV-infected flies. By contrast, the abdominal pH remained neutral in Tris-injectd flies (Figure 6.32). Because the abdomen of DCV-infected flies is filled with the largely expanded crop, this result suggest that the content of the crop is strongly acid. The cause of this acidification could be the fermentation of the yeast retained in the crop. Indeed, we observed an accumulation of mCherry-expressing fluorescent yeast in the crop of DCV-infected flies (Figure 6.33).

Figure 6.32: Acidification in *Drosophila* abdomen after infection with DCV . The content of the abdomen of a single fly was dotted on pH paper. According to the pH scale, we notice acidification in DCV-infected flies.

Acid release by the crop , possibly caused by its rupture, might be the cause of the death of the flies. However, we did not detect acid pH in the hemolymph taken from the thorax, even at late time points of infection (data not shown). Furthermore in a preliminary experiment we did not detect fluorescent yeast circulating in the hemolymph of DCV-infected flies.

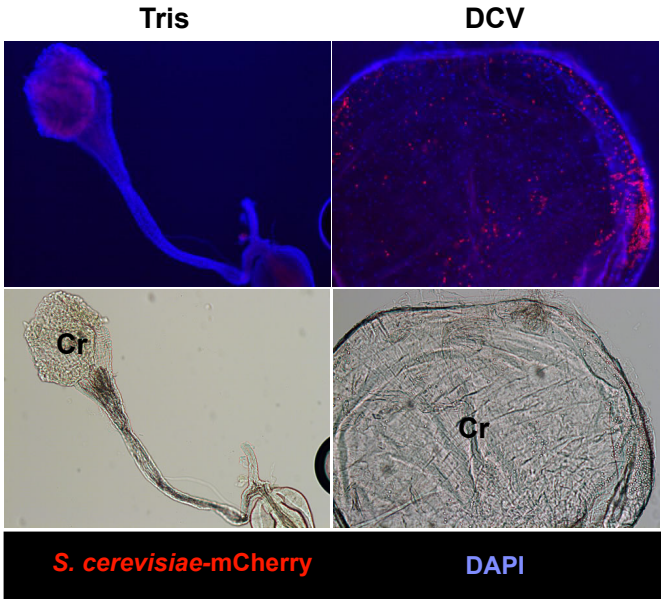

Figure 6.33: mCherry-expressing fluorescent yeast accumulates in the crop of DCV-infected flies .

Experiments are under way to confirm these results. We also plan to perform hemolymph transfer experiments to see if a circulating toxin is involved in the killing of the DCV-infected flies.

Part IV

Discussion and perspectives

Chapter 7

Discussion and perspectives

During this PhD thesis, we have attempted to understand the pathogenesis triggered by two RNA viruses in *Drosophila*. For a long time, *Drosophila* has successfully been used to decipher the mechanisms of innate immunity using model microorganisms, and simple assays such as survival, microbial load and induction of markers. These assays have proved very valuable in dissecting the basic molecular and cellular biology driving host-defense in *Drosophila*, in particular with regards to the humoral immune response [Lemaitre and Hoffmann, 2007]. One caveat of these studies, however, is that they ignore what is happening in the flies between the time when the microorganism is injected and the time when induction of molecular markers or microbial load are measured, or when death occurs. In other words, these experiments do not take into account the pathology triggered by the microbial infection, and the effects of homeostasis mechanisms on the ability of the fly to withstand the effects of this pathology. As a result, the cause of death triggered by infection in *Drosophila* remains unknown, although clues have been provided in some cases [Dionne et al., 2006, Liehl et al., 2006, Nehme et al., 2007]. For this reason, studies on immunity in *Drosophila* have focused on the resistance to microbial infection, and the endurance aspect has been largely ignored until recently, although

it contributes to a large extent to the final outcome of the infection, at least in mammals [Shirasu-Hiza and Schneider, 2007].

Studies on antiviral defense so far have been constructed on the same scheme, and have focused on the monitoring of survival, viral titer and characterization of the profiles of small RNAs produced by the RNAi machinery, or the induction of marker genes. We have decided four years ago to obtain a better understanding of the pathology associated with viral infections in *Drosophila*. We selected as viruses DCV and FHV, which resemble each other by many aspects, such as their single stranded RNA genome of positive polarity; their small, non-enveloped capsid; their rapid replication in *Drosophila* cells; their intense replication in cells from the fat body; their sensitivity to the siRNA pathway [Huszar and Imler, 2008]. Yet, these viruses also exhibit some differences such as the fact that DCV is a natural pathogen of *Drosophila*, whereas FHV was not identified in wild populations of flies; the strength of their RNA suppressor (FHV-B2 is more potent than DCV-1A). The IRES-dependent translation in the case of DCV; the replication of viral RNA on mitochondrial membranes for FHV versus COPI-dependent vesicle for DCV. These differences could impinge on the response of the host. Indeed, we observed significant differences between the transcriptomes of DCV- and FHV-infected flies [Dostert et al., 2005, Kemp, 2011], suggesting that these two viruses were triggering different pathologies in *Drosophila*. In this PhD thesis, we have begun to unravel the molecular and cellular consequences of infection by these two viruses. As detailed below, the results are rich in learning, and reveal that FHV and DCV induce very different, organ-specific, pathologies in flies.

7.1 Lessons from FHV: *in vivo* impact of ion channels on antiviral immunity

The approach of unbiased genetic screens played a key role in the identification of the important role of K_{ATP} channels in the control of viral infections. Although this type of approach is a favorite among *Drosophila* geneticists, in this case the screen was conducted in mice, and showed that the gene *Kcnj8*, encoding a component of K_{ATP} channels, is required to survive infection by the DNA virus MCMV. Because K_{ATP} channels are conserved in evolution, we looked for a virus-susceptibility phenotype in flies deficient for dSUR, the regulatory subunit of K_{ATP} channels. Somewhat surprisingly, we found that these flies were susceptible to FHV, but not to the other viruses we tested (DCV, SINV, VSV) [Croker et al., 2007]. This observation provided us with a unique opportunity to study the interaction of *Drosophila* with FHV.

Our results show that K_{ATP} channels are required for an efficient RNAi antiviral response to occur in the heart of *Drosophila*. This raises the question of the mechanism involved. Another component of innate immunity, the inflammasome, is regulated by K^+ ion efflux in mammalian cells. It is possible to activate the inflammasome in tissue culture cells by either increasing the consentration of K^+ ions in the medium, or treating the cells with ionomycine [Petrilli et al., 2007, Perregaux and Gabel, 1994]. We have tried to establish a tissue culture model to study the role of K^+ ion efflux on antiviral RNAi, by culturing cells with increased concentration of potassium or in the presence of nigericin, but did not obtain reproducible results. The variability of our data probably results from the toxicity of these treatments. Indeed, 30 minutes are sufficient to detect secretion of IL-1β, the readout of inflammasome activation, whereas in our case 6 to 8 hours are required to monitor FHV replication. Another possibility to identify the mechanism involved would be to analyze the profiles of FHV derived small

RNAs from the heart of flies treated or not with Tolbutamide. If dicing is affected, a reduction in the number of siRNA should be seen. Alternatively, if loading of the siRNA on AGO2 is affected, the siRNA should not be methylated by Hen1, and thus should be sensitive to β-elimination following oxidation [Aliyari et al., 2008]. We constructed libraries of small RNA prepared from dissected hearts from 200 FHV infected flies treated or not by tolbutamide. The libraries were sequenced, but did not give interpretable results: indeed, we observed a strong bias for some small RNAs, suggesting that sequence enrichment occured during the PCR amplification steps of the preparation of the library. One last possibility would be to perform *in vitro* dicing and RISC loading assays [Nayak et al., 2010], in the presence of increasing concentrations of potassium or other ions. Interestingly, this type of *in vitro* approach was used by Maniatis and colleagues to understand the effect of the Na^+/K^+ ATPase on IFN induction. Their work showed that the effect of the Na^+/K^+ pump is mediated by Na^+ ions, which interfere with the helicase activity of RIG-I [Ye et al., 2011]. It will be very interesting in future studies to test whether the helicase activity of Dcr-2, which is phylogenetically related to that of RIG-I, can also be inhibited by K^+, Na^+ or other ions.

Whatever the mechanism, our results reveal a previously unknown contribution of potassium channels to antiviral immunity in a particular tissue, the heart. Interestingly, this effect is not limited to K_{ATP} channels, and we also observed that flies mutant for the *KCNQ* gene, encoding another evolutionarily conserved voltage-dependent K^+ channel are also sensitive to FHV infection. It will be interesting to test other channels in both *Drosophila* and mice. It would also be interesting to investigate the presence of polymorphisms in the genes encoding K_{ATP} channels in patients suffering from virus-induced myocarditis. If such polymorphisms could be associated with this disease, better prophylaxis and therapy could be envisioned. The *Kcnj8* mutant mice characterized by Bruce Beutler and his collaborators represent an interesting tool to better understand how K_{ATP}

channels contribute to the control of viral load in the heart of mammals. In particular, it would be interesting to know if the function of the inflammasome or the production of type I IFN is affected in the heart of *Kcnj8* mutant mice.

Overall, our studies on FHV have unraveled a novel critical aspect of immunity, namely the fact that some potassium channels can regulate the antiviral immune response in the heart. Thus, patients with a perfectly fit immune system may be susceptible to cardiotropic viral infections if the activity of these channels is affected. Conversely, drugs acting on these channels, rather than on the virus or on the immune system, may affect the course of the infection, and allow the infected host to survive, as we showed as proof of principle with pinacidil on FHV infected flies. This work has also revealed that FHV can be a valuable tool to study the regulation of heart physiology in *Drosophila*. Work is now on the way in the laboratory of Karen Occor and Rolf Bodmer in La Jolla, USA, to understand how FHV affects heart performance.

7.2 Lessons from DCV: towards a better understanding of the biology of the cardia

The study was more complex than for FHV, and it took us some time and many experiments to figure out what was happening in DCV-infected flies. We initially started from the observation that DCV, but not FHV, represses the expression of a large number of proteases. Because DCV is a natural pathogen of *Drosophila*, which co-evolved with its host and may have learned how to ward off some of its defense mechanisms, we considered the possibility that these proteases could be part of an intrinsic mechanism of antiviral host defense [Bieniasz, 2004]. However, we quickly came to realize that this was not the case as *(i)* these proteases are specifically expressed in the midgut, where we did not detect DCV;

(ii) Jon65Ai mutant flies were not susceptible to virus infection; (iii) many of these proteases are also repressed by starvation.

We next considered the possibility that DCV infection was causing a metabolic syndrom, as reported in mammals in cases of chronic inflammation affecting the physiology and metabolism of the host [Hotamisligil and Erbay, 2008]. We were misled in this direction by the observation that the transcriptome of the DCV-infected flies and the mobilization of lipid reserves from fat body to oenocytes were evocative of starvation, while the body weight and the stained food incorporation assays indicated that the flies were not suffering from anorexia or excessive wasting, but were actually gaining weight and appeared to overeat. We were also misled by the fact that while using DCV as control to study the contribution of K_{ATP} channels to the resistance to FHV infection we inadvertently observed that flies silenced for *Ir* and *Irk2* exhibited enhanced resistance to DCV infection. This suggested that K_{ATP} channels, which play a role in glucose sensing and AKH secretion by the corpora cardiaca in *Drosophila* [Kim and Rulifson, 2004] played a detrimental role in the resistance to DCV infection. However, we found that *(i)* neither mutation of *dSUR* nor Tolbutamide treatment affected the resistance to DCV infection; *(ii)* the cells from the *corpora cardiaca* are not infected by DCV; *(iii)* silencing of *Ir*, *Irk2* or *dSUR* in the corpora cardiaca, or genetic ablation of this tissue by expression of the pro-apoptotic gene *reaper*, did not affect the resistance to DCV. Thus, even though the analysis of the role of *Ir* and *Irk2* in the context of DCV infection undoubtly deserves further investigation, we did not pursue this hypothesis.

We finally came to the conclusion that DCV infection triggers an intestinal obstruction. We believe that this obstruction is a direct consequence of virus replication in the cardia, although we cannot completely rule out that it results from an effect on the neurons controlling the function of this organ. Further experiments will be required to fully understand what happens in the cardia upon infection by

DCV. The continuation of this work will be important since the cardia is a poorly understood structure, playing a very important role in host-pathogen interactions in insects. Indeed, it synthesizes the peritrophic matrix, which lines the surface of the midgut, and protects the gut epithelium from infections. Our results suggest that the cells involved in the secretion and folding of the peritrophic matrix are affected by DCV infection. Thus, DCV appears as a valuable tool to better understand the function of the cardia in normal and pathological situations.

Viruses have in the past proved to be valuable tools to decipher the molecular biology of the cell (e.g. discovery of enhancers, introns, nuclear localization signals). Our studies with FHV and DCV illustrate how viruses can also be very useful to gain insight on the physiology of critical organs such as the heart and the cardia, respectively.

7.3 Confronting the real world: how do virus-infected flies die?

In spite of our efforts, we have to admit that we still do not know the cause of death of FHV- and DCV- infected flies. When we obtained our first results with FHV and the heart, indicating that FHV infection causes arrhythmias, we believed that we had found the cause of death. However, overexpression of ORK1, a two-pore domain K^+ channel, completely prevent heart beating in transgenic flies, without affecting the viability [Lalevee et al., 2006]. This indicates that flies can live without a functional heart. We confirmed this finding by showing that flies in which cardiomyocytes were genetically ablated were viable, and resisted better to FHV infection than wild-type flies. This shows that it is not a dysfunction of the heart following FHV infection that leads to death of the flies. The heart however, plays a critical role as a primary site of replication of the virus, which can then spread to other tissues. Alternatively, the heart, which regulates the circulation of

the hemolymph in the insect body cavity, could be important for the dissemination of the virus in the organism. Curiously, the genetic ablation of the heart did not affect resistance to DCV, suggesting that the heart is not absolutely required for the spreading of this virus. May be the reduced spreading of the virus is compensated by a reduced circulation of compounds involved in the antiviral response, such as cytokines (e.g. Upd-2 and -3) [Kemp, 2011] or viral dsRNA released from dying cells [Saleh et al., 2009]. It would be interesting to test the resistance of heart-ablated flies against bacteria or fungi, for which the humoral response involving the secretion of a cocktail of antimicrobial peptides reaching a concentration higher than 500μM, plays a well documented role [Imler and Bulet, 2005]. So, even though we made some interesting progress regarding the pathology of FHV infection, we still do not know what is ultimately causing the death of the flies and, incidentally, the function of the heart in adult flies.

Similarly, the cause of death in the case of DCV remains uncertain. We have ruled out that flies die from starvation. Two other causes of death could be the accumulation of toxins, or dehydratation. The toxin production could result from the intense fermentation of yeasts in the crop, a hypothesis that can be tested by feeding flies on another source of food. Water absorption occurs in the midgut and hindgut, and could be affected by the intestinal obstruction caused by DCV. In support of this hypothesis, we noticed that DCV infected flies spontaneously gather around water when placed in a small Petri dishes, whereas non infected flies, or flies infected by FHV or CrPV only occasionally do so. In addition, we observed that DCV infected flies spent most of their time attached to the extremity of the liquid filled capillary in the CAFE assay. Finally, we note that two of the water channels expressed in the Malpighian tubules (CG4019, CG17664) are down-regulated in DCV-infected flies, but not in FHV or SINV-infected flies, suggesting that flies try to save water. Further experiments monitoring the osmolarity of the hemolymph in DCV-infected flies are required to validate this hy-

pothesis. A metabolomic analysis [Sreekumar et al., 2009, Reitman et al., 2011] of the hemolymph of the flies infected by DCV, or FHV, may represent a powerful way to progress in our understanding of the cause of death of the flies. Such an approach was just initiated in the group with FHV in tissue culture cells.

An interesting issue concerning the cause of death is whether it results from a direct effect of the virus on a vital tissue, or from an adverse effect of the host reaction to the infection. In vertebrates, the adverse effects of the inflammatory response and the famous "cytokine storm" are well documented [Hotchkiss and Karl, 2003]. In flies, there is so far little evidence that the immune response contributes to the pathology. One study reported that flies mutant for the gene *eiger*, which encodes a TNF ortholog, resist better than wild-type flies to *Salmonella* infections, suggesting that *eiger* is involved in an immune response that causes pathology [Brandt et al., 2004]. Alternatively, it is possible that *eiger* is required for the endurance of the flies to this type of infection. In the case of virus infection, there is some evidence that the immune response may be toxic. For example, investigators were initially perplexed by the fact that *hopscotch* mutant flies contain more virus than wild-type flies, but do not die more rapidly. They reasoned that if the immune response was associated to some adverse effects, the decreased inducible response in *hopscotch* mutant flies could compensate for the increased viral load. Indeed, when lower doses of DCV were injected, *hopscotch* mutant flies were found to die more rapidly than wild-type control [Dostert et al., 2005]. Along the same lines, it was observed that *Dcr-2* mutant flies die more rapidly than controls following FHV infection, even though the increased viral titer was only moderately increased. Furthermore, the *vir-1* gene was induced more strongly in *Dcr-2* mutant flies, suggesting that in the absence of the RNAi response, the inducible response contributed to the lethality of the flies [Galiana-Arnoux et al., 2006]. Clearly, it will be interesting to investigate further the issue of the detrimental effects of the immune response on the host.

7.4 Concluding remarks

In conclusion, this work has improved our understanding on the pathologies caused by two RNA viruses in *Drosophila*, DCV and FHV. This work will be pursued to determine how these viruses kill flies, a question that needs to be answered in order to fully understand the pathophysiology of the infection and the role of the immune system. Overall, this work leads for three major perspectives. First, we expect that this type of work could lead to a new subfield of insect physiology, using viruses to decipher essential physiological mechanisms such as regulation of heart beating and secretion of the peritrophic matrix. Importantly, all our studies were done with an injection model of infection, which bypasses the natural defenses of barrier epithelia. It will also be important in future work to develop natural infection models for DCV and possibly FHV. This may reveal additional tissues associated with the pathophysiology of the infection. Second, these studies may have relevance for mammalian models, as exemplified by the identification of a role for K_{ATP} channels in the control of cardiac infection with CVB3 in mice. Third, the work reported here is rich in learning for future studies on the transmission of mosquito-borne viruses to mammals. Indeed, very little is known regarding the interaction of viruses such as Dengue, West-Nile or Chikungunya with their mosquito vector. The identification of tissues or organs playing a critical role in the multiplication of the virus or the resistance/endurance of the mosquito to the infection, such as the heart or the cardia for FHV and DCV, respectively, holds promise for the development of novel prophylactic strategies aimed at decreasing the transmission of the viruses to vertebrates.

Bibliography

[Agaisse and Perrimon, 2004] Agaisse, H. and Perrimon, N. (2004). The roles of JAK/STAT signaling in Drosophila immune responses. Immunol Rev *198*, 72–82.

[Agaisse et al., 2003] Agaisse, H., Petersen, U. M., Boutros, M., Mathey-Prevot, B. and Perrimon, N. (2003). Signaling Role of Hemocytes in Drosophila JAK/STAT-Dependent Response to Septic Injury. Dev Cell *5*, 441–50.

[Akasaka et al., 2006] Akasaka, T., Klinedinst, S., Ocorr, K., Bustamante, E. L., Kim, S. K. and Bodmer, R. (2006). The ATP-sensitive potassium (KATP) channel-encoded dSUR gene is required for Drosophila heart function and is regulated by tinman. Proc Natl Acad Sci U S A *103*, 11999–2004.

[Aliyari et al., 2008] Aliyari, R., Wu, Q., Li, H. W., Wang, X. H., Li, F., Green, L. D., Han, C. S., Li, W. X. and Ding, S. W. (2008). Mechanism of induction and suppression of antiviral immunity directed by virus-derived small RNAs in Drosophila. Cell Host Microbe *4*, 387–97.

[Ambrose et al., 2009] Ambrose, R. L., Lander, G. C., Maaty, W. S., Bothner, B., Johnson, J. E. and Johnson, K. N. (2009). Drosophila A virus is an unusual RNA virus with a T=3 icosahedral core and permuted RNA-dependent RNA polymerase. J Gen Virol *90*, 2191–2200.

[Ammar el et al., 2009] Ammar el, D., Tsai, C. W., Whitfield, A. E., Redinbaugh, M. G. and Hogenhout, S. A. (2009). Cellular and molecular aspects of rhabdovirus interactions with insect and plant hosts. Annu Rev Entomol *54*, 447–68.

[Apidianakis and Rahme, 2011] Apidianakis, Y. and Rahme, L. G. (2011). Drosophila melanogaster as a model for human intestinal infection and pathology. Dis Model Mech *4*, 21–30.

[Avadhanula et al., 2009] Avadhanula, V., Weasner, B. P., Hardy, G. G., Kumar, J. P. and Hardy, R. W. (2009). A novel system for the launch of alphavirus RNA synthesis reveals a role for the Imd pathway in arthropod antiviral response. PLoS Pathog *5*, e1000582.

[Ayres and Schneider, 2009] Ayres, J. S. and Schneider, D. S. (2009). The role of anorexia in resistance and tolerance to infections in Drosophila. PLoS Biol *7*, e1000150.

[Baker and Thummel, 2007] Baker, K. D. and Thummel, C. S. (2007). Diabetic larvae and obese flies-emerging studies of metabolism in Drosophila. Cell Metab *6*, 257–266.

[Bauer et al., 2006] Bauer, M., Katzenberger, J. D., Hamm, A. C., Bonaus, M., Zinke, I., Jaekel, J. and Pankratz, M. J. (2006). Purine and folate metabolism as a potential target of sex-specific nutrient allocation in Drosophila and its implication for lifespan-reproduction tradeoff. Physiol Genomics *25*, 393–404.

[Best, 2008] Best, S. M. (2008). Viral subversion of apoptotic enzymes: escape from death row. Annu Rev Microbiol *62*, 171–92.

[Bieniasz, 2004] Bieniasz, P. D. (2004). Intrinsic immunity: a front-line defense against viral attack. Nat Immunol *5*, 1109–15.

[Bier and Bodmer, 2004] Bier, E. and Bodmer, R. (2004). Drosophila, an emerging model for cardiac disease. Gene *342*, 1–11.

[Bodmer, 1995] Bodmer, R. (1995). Heart development in Drosophila and its relationship to vertebrates. Trends Cardiovasc Med *5*, 21–8.

[Bonning and Miller, 2010] Bonning, B. C. and Miller, W. A. (2010). Dicistroviruses. Annu Rev Entomol *55*, 129–50.

[Brandt et al., 2004] Brandt, S. M., Dionne, M. S., Khush, R. S., Pham, L. N., Vigdal, T. J. and Schneider, D. S. (2004). Secreted Bacterial Effectors and Host-Produced Eiger/TNF Drive Death in aSalmonella-Infected Fruit Fly. PLoS Biol *2*, e418.

[Buch and Pankratz, 2009] Buch, S. and Pankratz, M. J. (2009). Making metabolic decisions in Drosophila. Fly (Austin) *3*, 74–77.

[Bucheton, 1995] Bucheton, A. (1995). The relationship between the flamenco gene and gypsy in Drosophila: how to tame a retrovirus. Trends Genet *11*, 349–53.

[Buchon et al., 2009] Buchon, N., Broderick, N. A., Chakrabarti, S. and Lemaitre, B. (2009). Invasive and indigenous microbiota impact intestinal stem cell activity through multiple pathways in Drosophila. Genes Dev *23*, 2333–44.

[Carre-Mlouka et al., 2007] Carre-Mlouka, A., Gaumer, S., Gay, P., Petitjean, A. M., Coulondre, C., Dru, P., Bras, F., Dezelee, S. and Contamine, D. (2007). Control of sigma virus multiplication by the ref(2)P gene of Drosophila melanogaster: an in vivo study of the PB1 domain of Ref(2)P. Genetics *176*, 409–19.

[Castorena et al., 2007] Castorena, K. M., Weeks, S. A., Stapleford, K. A., Cadwallader, A. M. and Miller, D. J. (2007). A functional heat shock protein 90 chaperone is essential for efficient flock house virus RNA polymerase synthesis in Drosophila cells. J Virol *81*, 8412–8420.

[Cevallos and Sarnow, 2010] Cevallos, R. C. and Sarnow, P. (2010). Temperature protects insect cells from infection by cricket paralysis virus. J Virol *84*, 1652–1655.

[Chao et al., 2005] Chao, J. A., Lee, J. H., Chapados, B. R., Debler, E. W., Schneemann, A. and Williamson, J. R. (2005). Dual modes of RNA-silencing suppression by Flock House virus protein B2. Nat Struct Mol Biol *12*, 952–957.

[Chatterjee and Ip, 2009] Chatterjee, M. and Ip, Y. T. (2009). Pathogenic stimulation of intestinal stem cell response in Drosophila. J Cell Physiol *220*, 664–71.

[Cherry et al., 2005] Cherry, S., Doukas, T., Armknecht, S., Whelan, S., Wang, H., Sarnow, P. and Perrimon, N. (2005). Genome-wide RNAi screen reveals a specific sensitivity of IRES-containing RNA viruses to host translation inhibition. Genes Dev *19*, 445–52.

[Cherry et al., 2006] Cherry, S., Kunte, A., Wang, H., Coyne, C., Rawson, R. B. and Perrimon, N. (2006). COPI activity coupled with fatty acid biosynthesis is required for viral replication. PLoS Pathog *2*, e102.

[Cherry and Perrimon, 2004] Cherry, S. and Perrimon, N. (2004). Entry is a rate-limiting step for viral infection in a Drosophila melanogaster model of pathogenesis. Nat Immunol *5*, 81–7.

[Chintapalli et al., 2007] Chintapalli, V. R., Wang, J. and Dow, J. A. (2007). Using FlyAtlas to identify better Drosophila melanogaster models of human disease. Nat Genet *39*, 715–20.

[Chotkowski et al., 2008] Chotkowski, H. L., Ciota, A. T., Jia, Y., Puig-Basagoiti, F., Kramer, L. D., Shi, P. Y. and Glaser, R. L. (2008). West Nile virus infection of Drosophila melanogaster induces a protective RNAi response. Virology *377*, 197–206.

[Corby-Harris et al., 2007] Corby-Harris, V., Habel, K. E., Ali, F. G. and Promislow, D. E. (2007). Alternative measures of response to Pseudomonas aeruginosa infection in Drosophila melanogaster. J Evol Biol *20*, 526–33.

[Costa et al., 2009] Costa, A., Jan, E., Sarnow, P. and Schneider, D. (2009). The Imd pathway is involved in antiviral immune responses in Drosophila. PLoS One *4*, e7436.

[Costantino et al., 2008] Costantino, D. A., Pfingsten, J. S., Rambo, R. P. and Kieft, J. S. (2008). tRNA-mRNA mimicry drives translation initiation from a viral IRES. Nat Struct Mol Biol *15*, 57–64.

[Croker et al., 2007] Croker, B., Crozat, K., Berger, M., Xia, Y., Sovath, S., Schaffer, L., Eleftherianos, I., Imler, J. L. and Beutler, B. (2007). ATP-sensitive potassium channels mediate survival during infection in mammals and insects. Nat Genet *39*, 1453–60.

[Cronin et al., 2009] Cronin, S. J., Nehme, N. T., Limmer, S., Liegeois, S., Pospisilik, J. A., Schramek, D., Leibbrandt, A., Simoes Rde, M., Gruber, S., Puc, U., Ebersberger, I., Zoranovic, T., Neely, G. G., von Haeseler, A., Ferrandon, D. and Penninger, J. M. (2009). Genome-wide RNAi screen identifies genes involved in intestinal pathogenic bacterial infection. Science *325*, 340–3.

[Crosnier et al., 2006] Crosnier, C., Stamataki, D. and Lewis, J. (2006). Organizing cell renewal in the intestine: stem cells, signals and combinatorial control. Nat Rev Genet *7*, 349–59.

[Daffre et al., 1994] Daffre, S., Kylsten, P., Samakovlis, C. and Hultmark, D. (1994). The lysozyme locus in Drosophila melanogaster: an expanded gene family adapted for expression in the digestive tract. Mol Gen Genet *242*, 152–162.

[Dasgupta et al., 2003] Dasgupta, R., Cheng, L. L., Bartholomay, L. C. and Christensen, B. M. (2003). Flock house virus replicates and expresses green fluorescent protein in mosquitoes. J Gen Virol *84*, 1789–97.

[Dasgupta et al., 2007] Dasgupta, R., Free, H. M., Zietlow, S. L., Paskewitz, S. M., Aksoy, S., Shi, L., Fuchs, J., Hu, C. and Christensen, B. M. (2007). Replication of flock house virus in three genera of medically important insects. J Med Entomol *44*, 102–10.

[Debiasi, 2011] Debiasi, R. L. (2011). West Nile Virus Neuroinvasive Disease. Curr Infect Dis Rep *z*, z.

[Deddouche et al., 2008] Deddouche, S., Matt, N., Budd, A., Mueller, S., Kemp, C., Galiana-Arnoux, D., Dostert, C., Antoniewski, C., Hoffmann, J. A. and Imler, J. L. (2008). The DExD/H-box helicase Dicer-2 mediates the induction of antiviral activity in drosophila. Nat Immunol *9*, 1425–32.

[den Boon et al., 2010] den Boon, J. A., Diaz, A. and Ahlquist, P. (2010). Cytoplasmic viral replication complexes. Cell Host Microbe *8*, 77–85.

[Ding, 2010] Ding, S. W. (2010). RNA-based antiviral immunity. Nat Rev Immunol *10*, 632–44.

[Ding and Voinnet, 2007] Ding, S. W. and Voinnet, O. (2007). Antiviral immunity directed by small RNAs. Cell *130*, 413–26.

[Dionne et al., 2003] Dionne, M. S., Ghori, N. and Schneider, D. S. (2003). Drosophila melanogaster is a genetically tractable model host for Mycobacterium marinum. Infect Immun *71*, 3540–50.

[Dionne et al., 2006] Dionne, M. S., Pham, L. N., Shirasu-Hiza, M. and Schneider, D. S. (2006). Akt and FOXO dysregulation contribute to infection-induced wasting in Drosophila. Curr Biol *16*, 1977–85.

[Dostert et al., 2005] Dostert, C., Jouanguy, E., Irving, P., Troxler, L., Galiana-Arnoux, D., Hetru, C., Hoffmann, J. A. and Imler, J. L. (2005). The Jak-STAT signaling pathway is required but not sufficient for the antiviral response of drosophila. Nat Immunol *6*, 946–53.

[Ekstrom et al., 2011] Ekstrom, J.-O., Habayeb, M. S., Srivastava, V., Kieselbach, T., Wingsle, G. and Hultmark, D. (2011). Drosophila Nora virus capsid proteins differ from those of other picorna-like viruses. Virus Res *in press*, in press.

[El Chamy et al., 2008] El Chamy, L., Leclerc, V., Caldelari, I. and Reichhart, J. M. (2008). Sensing of 'danger signals' and pathogen-associated molecular patterns defines binary signaling pathways 'upstream' of Toll. Nat Immunol *9*, 1165–70.

[Fagegaltier et al., 2009] Fagegaltier, D., Bouge, A. L., Berry, B., Poisot, E., Sismeiro, O., Coppee, J. Y., Theodore, L., Voinnet, O. and Antoniewski, C. (2009). The endogenous siRNA pathway is involved in heterochromatin formation in Drosophila. Proc Natl Acad Sci U S A *106*, 21258–63.

[Ferrandon et al., 2007] Ferrandon, D., Imler, J. L., Hetru, C. and Hoffmann, J. A. (2007). The Drosophila systemic immune response: sensing and signalling during bacterial and fungal infections. Nat Rev Immunol *7*, 862–74.

[Fink et al., 2009] Fink, M., Callol-Massot, C., Chu, A., Ruiz-Lozano, P., Izpisua Belmonte, J. C., Giles, W., Bodmer, R. and Ocorr, K. (2009). A new method for detection and quantification of heartbeat parameters in Drosophila, zebrafish, and embryonic mouse hearts. BioTechniques *46*, 101–13.

[Fire et al., 1998] Fire, A., Xu, S., Montgomery, M. K., Kostas, S. A., Driver, S. E. and Mello, C. C. (1998). Potent and specific genetic interference by double-stranded RNA in Caenorhabditis elegans. Nature *391*, 806–811.

[Fleuriet, 1981] Fleuriet, A. (1981). Effect of overwintering on the frequency of flies infected by the rhabdovirus sigma in experimental populations of Drosophila melanogaster. Arch Virol *69*, 253–60.

[Flynt et al., 2009] Flynt, A., Liu, N., Martin, R. and Lai, E. C. (2009). Dicing of viral replication intermediates during silencing of latent Drosophila viruses. Proc Natl Acad Sci U S A *106*, 5270–5.

[Galiana-Arnoux et al., 2006] Galiana-Arnoux, D., Dostert, C., Schneemann, A., Hoffmann, J. A. and Imler, J. L. (2006). Essential function in vivo for Dicer-2 in host defense against RNA viruses in drosophila. Nat Immunol *7*, 590–7.

[Gateff et al., 1980] Gateff, E., Gissmann, L., Shresta, R., Plus, N., Pfister, H., Schr$\surd\partial$der, J. and Zur Hausen, H. (1980). Characterization of two tumorous blood cell lines of Drosophila melanogaster and the viruses they contain. In Invertebrate systems in vitro, (Kurstak, E., Maramorosch, K. and D$\surd^{o}$bendorfer, A., eds), pp. 517–533. Elsevier/North Holland Biomedical Press Amsterdam.

[Ghildiyal et al., 2008] Ghildiyal, M., Seitz, H., Horwich, M. D., Li, C., Du, T., Lee, S., Xu, J., Kittler, E. L., Zapp, M. L., Weng, Z. and Zamore, P. D. (2008). Endogenous siRNAs derived from transposons and mRNAs in Drosophila somatic cells. Science *320*, 1077–81.

[Ghildiyal and Zamore, 2009] Ghildiyal, M. and Zamore, P. D. (2009). Small silencing RNAs: an expanding universe. Nat Rev Genet *10*, 94–108.

[Go et al., 2006] Go, E. P., Wikoff, W. R., Shen, Z., O'Maille, G., Morita, H., Conrads, T. P., Nordstrom, A., Trauger, S. A., Uritboonthai, W., Lucas, D. A., Chan, K. C., Veenstra, T. D., Lewicki, H., Oldstone, M. B., Schneemann, A. and Siuzdak, G. (2006). Mass spectrometry reveals specific and global molecular transformations during viral infection. J Proteome Res *5*, 2405–2416.

[Gottar et al., 2006] Gottar, M., Gobert, V., Matskevich, A. A., Reichhart, J. M., Wang, C., Butt, T. M., Belvin, M., Hoffmann, J. A. and Ferrandon, D. (2006). Dual detection of fungal infections in Drosophila via recognition of glucans and sensing of virulence factors. Cell *127*, 1425–37.

[Gottar et al., 2002] Gottar, M., Gobert, V., Michel, T., Belvin, M., Duyk, G., Hoffmann, J. A., Ferrandon, D. and Royet, J. (2002). The Drosophila immune response against Gram-negative bacteria is mediated by a peptidoglycan recognition protein. Nature *416*, 640–4.

[Griffin, 1976] Griffin, D. E. (1976). Role of the immune response in age-dependent resistance of mice to encephalitis due to Sindbis virus. J Infect Dis *133*, 456–464.

[Gronke et al., 2005] Gronke, S., Mildner, A., Fellert, S., Tennagels, N., Petry, S., Muller, G., Jackle, H. and Kuhnlein, R. P. (2005). Brummer lipase is an evolutionary conserved fat storage regulator in Drosophila. Cell Metab *1*, 323–30.

[Gutierrez et al., 2007] Gutierrez, E., Wiggins, D., Fielding, B. and Gould, A. P. (2007). Specialized hepatocyte-like cells regulate Drosophila lipid metabolism. Nature *445*, 275–80.

[Ha et al., 2005] Ha, E. M., Oh, C. T., Bae, Y. S. and Lee, W. J. (2005). A direct role for dual oxidase in Drosophila gut immunity. Science *310*, 847–50.

[Habayeb et al., 2009] Habayeb, M. S., Cantera, R., Casanova, G., Ekstrom, J. O., Albright, S. and Hultmark, D. (2009). The Drosophila Nora virus is an enteric virus, transmitted via feces. J Invertebr Pathol *101*, 29–33.

[Habayeb et al., 2006] Habayeb, M. S., Ekengren, S. K. and Hultmark, D. (2006). Nora virus, a persistent virus in Drosophila, defines a new picorna-like virus family. J Gen Virol *87*, 3045–51.

[Habayeb et al., 2009] Habayeb, M. S., Ekstrom, J. O. and Hultmark, D. (2009). Nora virus persistent infections are not affected by the RNAi machinery. PLoS One *4*, e5731.

[Hamilton and Baulcombe, 1999] Hamilton, A. J. and Baulcombe, D. C. (1999). A species of small antisense RNA in posttranscriptional gene silencing in plants. Science *286*, 950–952.

[Hedges et al., 2008] Hedges, L. M., Brownlie, J. C., O'Neill, S. L. and Johnson, K. N. (2008). Wolbachia and virus protection in insects. Science *322*, 702.

[Hegedus et al., 2009] Hegedus, D., Erlandson, M., Gillott, C. and Toprak, U. (2009). New insights into peritrophic matrix synthesis, architecture, and function. Annu Rev Entomol *54*, 285–302.

[Heinz, 1985] Heinz, P. (1985). Comperhensive insect physiology pp. 371–406. Oxford: Pergamon press.

[Hoffmann, 2003] Hoffmann, J. (2003). The immune response of Drosophila. Nature , *426*, 33–38.

[Hotamisligil and Erbay, 2008] Hotamisligil, G. S. and Erbay, E. (2008). Nutrient sensing and inflammation in metabolic diseases. Nat Rev Immunol , *8*, 923–934.

[Hotchkiss and Karl, 2003] Hotchkiss, R. S. and Karl, I. E. (2003). The pathophysiology and treatment of sepsis. N Engl J Med , *348*, 138–150.

[Huszar and Imler, 2008] Huszar, T. and Imler, J. L. (2008). Drosophila viruses and the study of antiviral host-defense. Adv Virus Res , *72*, 227–65.

[Imler and Bulet, 2005] Imler, J. L. and Bulet, P. (2005). Antimicrobial peptides in Drosophila: structures, activities and gene regulation. Chem Immunol Allergy , *86*, 1–21.

[Irving et al., 2001] Irving, P., Troxler, L., Heuer, T. S., Belvin, M., Kopczynski, C., Reichhart, J. M., Hoffmann, J. A. and Hetru, C. (2001). A genome-wide analysis of immune responses in Drosophila. Proc Natl Acad Sci U S A , *98*, 15119–24.

[Ja et al., 2007] Ja, W. W., Carvalho, G. B., Mak, E. M., de la Rosa, N. N., Fang, A. Y., Liong, J. C., Brummel, T. and Benzer, S. (2007). Prandiology of Drosophila and the CAFE assay. Proc Natl Acad Sci U S A , *104*, 8253–6.

[Jackson et al., 1987] Jackson, A. C., Moench, T. R., Griffin, D. E. and Johnson, R. T. (1987). The pathogenesis of spinal cord involvement in the encephalomyelitis of mice caused by neuroadapted Sindbis virus infection. Lab Invest , *56*, 418–423.

[Janeway, 2005] Janeway, C. (2005). Immunobiology : the immune system in health and disease. Garland Science.

[Jiang and Edgar, 2009] Jiang, H. and Edgar, B. A. (2009). EGFR signaling regulates the proliferation of Drosophila adult midgut progenitors. Development *136*, 483–93.

[Jiang et al., 2009] Jiang, H., Patel, P. H., Kohlmaier, A., Grenley, M. O., McEwen, D. G. and Edgar, B. A. (2009). Cytokine/Jak/Stat signaling mediates regeneration and homeostasis in the Drosophila midgut. Cell *137*, 1343–55.

[Jousset et al., 1977] Jousset, F. X., Bergoin, M. and Revet, B. (1977). Characterization of the Drosophila C virus. J Gen Virol *34*, 269–83.

[Jousset et al., 1972] Jousset, F. X., Plus, N., Croizier, G. and Thomas, M. (1972). [Existence in Drosophila of 2 groups of picornavirus with different biological and serological properties]. C R Acad Sci Hebd Seances Acad Sci D *275*, 3043–6.

[Kampmueller and Miller, 2005] Kampmueller, K. M. and Miller, D. J. (2005). The cellular chaperone heat shock protein 90 facilitates Flock House virus RNA replication in Drosophila cells. J Virol *79*, 6827–6837.

[Kemp, 2011] Kemp, C. e. a. (2011). Manuscript in preparation. . ., .

[Kim and Rulifson, 2004] Kim, S. K. and Rulifson, E. J. (2004). Conserved mechanisms of glucose sensing and regulation by Drosophila corpora cardiaca cells. Nature *431*, 316–320.

[King and Moore, 1988] King, L. and Moore, N. (1988). Evidence for the presence of a genome-linked protein in two insect picornaviruses, cricket paralysis virus and Drosophila C virus. FEMS Microbiology Letters *50*, 41–44.

[Kopek et al., 2007] Kopek, B. G., Perkins, G., Miller, D. J., Ellisman, M. H. and Ahlquist, P. (2007). Three-dimensional analysis of a viral RNA replication complex reveals a virus-induced mini-organelle. PLoS Biol *5*, e220.

[Kraaijeveld and Godfray, 1997] Kraaijeveld, A. R. and Godfray, H. C. (1997). Trade-off between parasitoid resistance and larval competitive ability in Drosophila melanogaster. Nature *389*, 278–280.

[Kuhnlein, 2010] Kuhnlein, R. P. (2010). Energy homeostasis regulation in Drosophila: a lipocentric perspective. Results Probl Cell Differ *52*, 159–173.

[LaJeunesse et al., 2010] LaJeunesse, D. R., Johnson, B., Presnell, J. S., Catignas, K. K. and Zapotoczny, G. (2010). Peristalsis in the junction region of the Drosophila larval midgut is modulated by DH31 expressing enteroendocrine cells. BMC Physiol *10*, 14.

[Lalevee et al., 2006] Lalevee, N., Monier, B., Senatore, S., Perrin, L. and Semeriva, M. (2006). Control of cardiac rhythm by ORK1, a Drosophila two-pore domain potassium channel. Curr Biol *16*, 1502–1508.

[Lannan et al., 2007] Lannan, E., Vandergaast, R. and Friesen, P. D. (2007). Baculovirus caspase inhibitors P49 and P35 block virus-induced apoptosis downstream of effector caspase DrICE activation in Drosophila melanogaster cells. J Virol *81*, 9319–30.

[Lee et al., 2004] Lee, Y. S., Nakahara, K., Pham, J. W., Kim, K., He, Z., Sontheimer, E. J. and Carthew, R. W. (2004). Distinct roles for Drosophila Dicer-1 and Dicer-2 in the siRNA/miRNA silencing pathways. Cell *117*, 69–81.

[Lemaitre and Hoffmann, 2007] Lemaitre, B. and Hoffmann, J. (2007). The host defense of Drosophila melanogaster. Annu Rev Immunol *25*, 697–743.

[Lemaitre et al., 1995] Lemaitre, B., Meister, M., Govind, S., Georgel, P., Steward, R., Reichhart, J. M. and Hoffmann, J. A. (1995). Functional analysis and regulation of nuclear import of dorsal during the immune response in Drosophila. Embo J *14*, 536–45.

[Lemaitre et al., 1996] Lemaitre, B., Nicolas, E., Michaut, L., Reichhart, J. and Hoffmann, J. (1996). The dorsoventral regulatory gene cassette sp√§tzle/Toll/cactus controls the potent antifungal response in Drosophila adults. Cell *86*, 973–983.

[Li et al., 2002] Li, H., Li, W. X. and Ding, S. W. (2002). Induction and suppression of RNA silencing by an animal virus. Science *296*, 1319–21.

[Lichty et al., 2004] Lichty, B. D., Power, A. T., Stojdl, D. F. and Bell, J. C. (2004). Vesicular stomatitis virus: re-inventing the bullet. Trends Mol Med *10*, 210–6.

[Liehl et al., 2006] Liehl, P., Blight, M., Vodovar, N., Boccard, F. and Lemaitre, B. (2006). Prevalence of local immune response against oral infection in a Drosophila/Pseudomonas infection model. PLoS Pathog *2*, e56.

[Lin et al., 2008] Lin, G., Xu, N. and Xi, R. (2008). Paracrine Wingless signalling controls self-renewal of Drosophila intestinal stem cells. Nature *455*, 1119–23.

[Markowitz and Bertagnolli, 2009] Markowitz, S. D. and Bertagnolli, M. M. (2009). Molecular origins of cancer: Molecular basis of colorectal cancer. N Engl J Med *361*, 2449–60.

[Marques et al., 2010] Marques, J. T., Kim, K., Wu, P.-H., Alleyne, T. M., Jafari, N. and Carthew, R. W. (2010). Loqs and R2D2 act sequentially in the siRNA pathway in Drosophila. Nat Struct Mol Biol *17*, 24–30.

[Matzke and Matzke, 2004] Matzke, M. A. and Matzke, A. J. M. (2004). Planting the seeds of a new paradigm. PLoS Biol *2*, E133.

[Mauricio, 2000] Mauricio, R. (2000). Natural selection and the joint evolution of toleranceand resistance as plant defenses. Evolutionary Ecology *14*, 491–507.

[Medioni et al., 2009] Medioni, C., Senatore, S., Salmand, P. A., Lalevee, N., Perrin, L. and Semeriva, M. (2009). The fabulous destiny of the Drosophila heart. Curr Opin Genet Dev *19*, 518–25.

[Medzhitov and Janeway, 1997] Medzhitov, R. and Janeway, C. A., J. (1997). Innate immunity: the virtues of a nonclonal system of recognition. Cell *91*, 295–8.

[Melcher and Pankratz, 2005] Melcher, C. and Pankratz, M. J. (2005). Candidate gustatory interneurons modulating feeding behavior in the Drosophila brain. PLoS Biol *3*, e305.

[Micchelli and Perrimon, 2006] Micchelli, C. A. and Perrimon, N. (2006). Evidence that stem cells reside in the adult Drosophila midgut epithelium. Nature *439*, 475–9.

[Moreira et al., 2009] Moreira, L. A., Iturbe-Ormaetxe, I., Jeffery, J. A., Lu, G., Pyke, A. T., Hedges, L. M., Rocha, B. C., Hall-Mendelin, S., Day, A., Riegler, M., Hugo, L. E., Johnson, K. N., Kay, B. H., McGraw, E. A., van den Hurk, A. F., Ryan, P. A. and O'Neill, S. L. (2009). A Wolbachia symbiont in Aedes aegypti limits infection with dengue, Chikungunya, and Plasmodium. Cell *139*, 1268–1278.

[Moret and Schmid-Hempel, 2001] Moret, Y. and Schmid-Hempel, P. (2001). Immune defence in bumble-bee offspring. Nature *414*, 506.

[Moser et al., 2010] Moser, T. S., Jones, R. G., Thompson, C. B., Coyne, C. B. and Cherry, S. (2010). A kinome RNAi screen identified AMPK as promoting poxvirus entry through the control of actin dynamics. PLoS Pathog *6*, e1000954.

[Mueller et al., 2010] Mueller, S., Gausson, V., Vodovar, N., Deddouche, S., Troxler, L., Perot, J., Pfeffer, S., Hoffmann, J. A., Saleh, M. C. and Imler, J. L. (2010). RNAi-mediated immunity provides strong protection against the negative-strand RNA vesicular stomatitis virus in Drosophila. Proc Natl Acad Sci U S A *107*, 19390–5.

[Myles et al., 2008] Myles, K. M., Wiley, M. R., Morazzani, E. M. and Adelman, Z. N. (2008). Alphavirus-derived small RNAs modulate pathogenesis in disease vector mosquitoes. Proc Natl Acad Sci U S A *105*, 19938–19943.

[Nakagoshi, 2005] Nakagoshi, H. (2005). Functional specification in the Drosophila endoderm. Dev Growth Differ *47*, 383–392.

[Nayak et al., 2010] Nayak, A., Berry, B., Tassetto, M., Kunitomi, M., Acevedo, A., Deng, C., Krutchinsky, A., Gross, J., Antoniewski, C. and Andino, R. (2010). Cricket paralysis virus antagonizes Argonaute 2 to modulate antiviral defense in Drosophila. Nat Struct Mol Biol *17*, 547–54.

[Nehme et al., 2007] Nehme, N. T., Liegeois, S., Kele, B., Giammarinaro, P., Pradel, E., Hoffmann, J. A., Ewbank, J. J. and Ferrandon, D. (2007). A model of bacterial intestinal infections in Drosophila melanogaster. PLoS Pathog *3*, e173.

[Novoa et al., 2005] Novoa, R. R., Calderita, G., Arranz, R., Fontana, J., Granzow, H. and Risco, C. (2005). Virus factories: associations of cell organelles for viral replication and morphogenesis. Biol Cell *97*, 147–72.

[Ocorr et al., 2007] Ocorr, K., Reeves, N. L., Wessells, R. J., Fink, M., Chen, H.-S. V., Akasaka, T., Yasuda, S., Metzger, J. M., Giles, W., Posakony, J. W. and Bodmer, R. (2007). KCNQ potassium channel mutations cause cardiac arrhythmias in Drosophila that mimic the effects of aging. Proc Natl Acad Sci U S A *104*, 3943–3948.

[Ohlstein and Spradling, 2006] Ohlstein, B. and Spradling, A. (2006). The adult Drosophila posterior midgut is maintained by pluripotent stem cells. Nature *439*, 470–4.

[Olivieri et al., 2010] Olivieri, D., Sykora, M. M., Sachidanandam, R., Mechtler, K. and Brennecke, J. (2010). An in vivo RNAi assay identifies major genetic and cellular requirements for primary piRNA biogenesis in Drosophila. EMBO J *29*, 3301–3317.

[Pannebakker et al., 2007] Pannebakker, B. A., Loppin, B., Elemans, C. P. H., Humblot, L. and Vavre, F. (2007). Parasitic inhibition of cell death facilitates symbiosis. Proc Natl Acad Sci U S A *104*, 213–215.

[Parrish et al., 2000] Parrish, S., Fleenor, J., Xu, S., Mello, C. and Fire, A. (2000). Functional anatomy of a dsRNA trigger: differential requirement for the two trigger strands in RNA interference. Mol Cell *6*, 1077–1087.

[Pelisson et al., 2007] Pelisson, A., Sarot, E., Payen-Groschene, G. and Bucheton, A. (2007). A novel repeat-associated small interfering RNA-mediated silencing pathway downregulates complementary sense gypsy transcripts in somatic cells of the Drosophila ovary. J Virol *81*, 1951–60.

[Perregaux and Gabel, 1994] Perregaux, D. and Gabel, C. A. (1994). Interleukin-1 beta maturation and release in response to ATP and nigericin. Evidence that potassium depletion mediated by these agents is a necessary and common feature of their activity. J Biol Chem *269*, 15195–15203.

[Petrilli et al., 2007] Petrilli, V., Papin, S., Dostert, C., Mayor, A., Martinon, F. and Tschopp, J. (2007). Activation of the NALP3 inflammasome is triggered by low intracellular potassium concentration. Cell Death Differ *14*, 1583–1589.

[Plus et al., 1975a] Plus, N., Croizier, G., Duthoit, J. L., David, J., Anxolabxh-re, D. and Pxriquet, G. (1975a). [The discovery, in Drosophila, of viruses belonging to three new groups]. C R Acad Sci Hebd Seances Acad Sci D *280*, 1501–1504.

[Plus et al., 1975b] Plus, N., Croizier, G., Jousset, F. X. and David, J. (1975b). Picornaviruses of laboratory and wild Drosophila melanogaster: geographical distribution and serotypic composition. Ann Microbiol (Paris) *126*, 107–17.

[Plus et al., 1976] Plus, N., Croizier, G., Veyrunes, J. C. and David, J. (1976). A comparison of buoyant density and polypeptides of Drosophila P, C and A viruses. Intervirology *7*, 346–350.

[Prud'homme et al., 1995] Prud'homme, N., Gans, M., Masson, M., Terzian, C. and Bucheton, A. (1995). Flamenco, a gene controlling the gypsy retrovirus of Drosophila melanogaster. Genetics *139*, 697–711.

[Ramirez and Dimopoulos, 2010] Ramirez, J. L. and Dimopoulos, G. (2010). The Toll immune signaling pathway control conserved anti-dengue defenses across diverse Ae. aegypti strains and against multiple dengue virus serotypes. Dev Comp Immunol *34*, 625–629.

[Reinganum C, 1970] Reinganum C, O,ÄôLoughlin GT, H. T. (1970). A nonoccluded virus of the field crickets Teleogryllus aceanicus and T. commodu (Orthoptera: Gryllidae). J. Invertebr. Pathol. *16*, 220,Äì314.

[Reitman et al., 2011] Reitman, Z. J., Jin, G., Karoly, E. D., Spasojevic, I., Yang, J., Kinzler, K. W., He, Y., Bigner, D. D., Vogelstein, B. and Yan, H. (2011). Profiling the effects of isocitrate dehydrogenase 1 and 2 mutations on the cellular metabolome. Proc Natl Acad Sci U S A *108*, 3270–3275.

[Roberts et al., 1998] Roberts, A., Kretzschmar, E., Perkins, A. S., Forman, J., Price, R., Buonocore, L., Kawaoka, Y. and Rose, J. K. (1998). Vaccination with a recombinant vesicular stomatitis virus expressing an influenza virus hemagglutinin provides complete protection from influenza virus challenge. J Virol *72*, 4704–4711.

[Roignant et al., 2003] Roignant, J. Y., Carre, C., Mugat, B., Szymczak, D., Lepesant, J. A. and Antoniewski, C. (2003). Absence of transitive and systemic pathways allows cell-specific and isoform-specific RNAi in Drosophila. Rna *9*, 299–308.

[Rorsman et al., 2008] Rorsman, P., Salehi, S. A., Abdulkader, F., Braun, M. and MacDonald, P. E. (2008). K(ATP)-channels and glucose-regulated glucagon secretion. Trends Endocrinol Metab *19*, 277–284.

[Rulifson et al., 2002] Rulifson, E. J., Kim, S. K. and Nusse, R. (2002). Ablation of insulin-producing neurons in flies: growth and diabetic phenotypes. Science *296*, 1118–1120.

[Rust et al., 2001] Rust, R. C., Landmann, L., Gosert, R., Tang, B. L., Hong, W., Hauri, H. P., Egger, D. and Bienz, K. (2001). Cellular COPII proteins are involved in production of the vesicles that form the poliovirus replication complex. J Virol *75*, 9808–9818.

[Rutschmann et al., 2000] Rutschmann, S., Jung, A., Hetru, C., Reichhart, J., Hoffmann, J. and Ferrandon, D. (2000). The Rel protein DIF mediates the Toll-dependent antifungal response in Drosophila. Immunity *12*, 569–580.

[Sabatier et al., 2003] Sabatier, L., Jouanguy, E., Dostert, C., Zachary, D., Dimarcq, J., Bulet, P. and Imler, J. (2003). Pherokine-2 and -3: Two Drosophila molecules related to pheromone/odor-binding proteins induced by viral and bacterial infections. Eur J Biochem *270*, 3398–3407.

[Sabin et al., 2009] Sabin, L. R., Zhou, R., Gruber, J. J., Lukinova, N., Bambina, S., Berman, A., Lau, C. K., Thompson, C. B. and Cherry, S. (2009). Ars2 regulates both miRNA- and siRNA- dependent silencing and suppresses RNA virus infection in Drosophila. Cell *138*, 340–51.

[Saleh et al., 2009] Saleh, M. C., Tassetto, M., van Rij, R. P., Goic, B., Gausson, V., Berry, B., Jacquier, C., Antoniewski, C. and Andino, R. (2009). Antiviral immunity in Drosophila requires systemic RNA interference spread. Nature *458*, 346–50.

[Schneider, 2000] Schneider, D. (2000). Using Drosophila as a model insect. Nat Rev Genet *1*, 218–26.

[Schwartz, 2005] Schwartz, R. H. (2005). Natural regulatory T cells and self-tolerance. Nat Immunol *6*, 327–330.

[Scotti et al., 1983] Scotti, P. D., Dearing, S. and Mossop, D. W. (1983). Flock House virus: a nodavirus isolated from Costelytra zealandica (White) (Coleoptera: Scarabaeidae). Arch Virol *75*, 181–9.

[Senger et al., 2006] Senger, K., Harris, K. and Levine, M. (2006). GATA factors participate in tissue-specific immune responses in Drosophila larvae. Proc Natl Acad Sci U S A *103*, 15957–15962.

[Sengupta and MacDonald, 2007] Sengupta, N. and MacDonald, T. T. (2007). The role of matrix metalloproteinases in stromal/epithelial interactions in the gut. Physiology (Bethesda) *22*, 401–9.

[Senti and Brennecke, 2010] Senti, K. A. and Brennecke, J. (2010). The piRNA pathway: a fly's perspective on the guardian of the genome. Trends Genet *26*, 499–509.

[Serbus et al., 2008] Serbus, L. R., Casper-Lindley, C., Landmann, F. and Sullivan, W. (2008). The genetics and cell biology of Wolbachia-host interactions. Annu Rev Genet *42*, 683–707.

[Settles and Friesen, 2008] Settles, E. W. and Friesen, P. D. (2008). Flock house virus induces apoptosis by depletion of Drosophila inhibitor-of-apoptosis protein DIAP1. J Virol *82*, 1378–88.

[Shanbhag and Tripathi, 2009] Shanbhag, S. and Tripathi, S. (2009). Epithelial ultrastructure and cellular mechanisms of acid and base transport in the Drosophila midgut. J Exp Biol *212*, 1731–44.

[Shelly et al., 2009] Shelly, S., Lukinova, N., Bambina, S., Berman, A. and Cherry, S. (2009). Autophagy is an essential component of Drosophila immunity against vesicular stomatitis virus. Immunity *30*, 588–98.

[Shirasu-Hiza and Schneider, 2007] Shirasu-Hiza, M. M. and Schneider, D. S. (2007). Confronting physiology: how do infected flies die? Cell Microbiol *9*, 2775–2783.

[Siviter et al., 2000] Siviter, R. J., Coast, G. M., Winther, A. M., Nachman, R. J., Taylor, C. A., Shirras, A. D., Coates, D., Isaac, R. E. and Nassel, D. R. (2000). Expression and functional characterization of a Drosophila neuropeptide precursor with homology to mammalian preprotachykinin A. J Biol Chem *275*, 23273–80.

[Sontheimer, 2005] Sontheimer, E. J. (2005). Assembly and function of RNA silencing complexes. Nat Rev Mol Cell Biol *6*, 127–138.

[Souza-Neto et al., 2009] Souza-Neto, J. A., Sim, S. and Dimopoulos, G. (2009). An evolutionary conserved function of the JAK-STAT pathway in anti-dengue defense. Proc Natl Acad Sci U S A *106*, 17841–6.

[Sreekumar et al., 2009] Sreekumar, A., Poisson, L. M., Rajendiran, T. M., Khan, A. P., Cao, Q., Yu, J., Laxman, B., Mehra, R., Lonigro, R. J., Li, Y., Nyati, M. K., Ahsan, A., Kalyana-Sundaram, S., Han, B., Cao, X., Byun, J., Omenn, G. S., Ghosh, D., Pennathur, S., Alexander, D. C., Berger, A., Shuster, J. R., Wei, J. T., Varambally, S., Beecher, C. and Chinnaiyan, A. M. (2009). Metabolomic profiles delineate potential role for sarcosine in prostate cancer progression. Nature *457*, 910–914.

[Steiner et al., 1981] Steiner, H., Hultmark, D., Engstrom, A., Bennich, H. and Boman, H. G. (1981). Sequence and specificity of two antibacterial proteins involved in insect immunity. Nature *292*, 246–8.

[Stouthamer et al., 1999] Stouthamer, R., Breeuwer, J. A. and Hurst, G. D. (1999). Wolbachia pipientis: microbial manipulator of arthropod reproduction. Annu Rev Microbiol *53*, 71–102.

[Strauss and Strauss, 1994] Strauss, J. H. and Strauss, E. G. (1994). The alphaviruses: gene expression, replication, and evolution. Microbiol Rev *58*, 491–562.

[Teixeira et al., 2008] Teixeira, L., Ferreira, A. and Asburner, M. (2008). The bacterial symbiont Wolbachia induces resistance to RNA viral infections in Drosophila melanogaster. PLoS Biol *6*, 2753–2763.

[Teninges et al., 1979] Teninges, D., Ohanessian, A., Richard-Molard, C. and Contamine, D. (1979). Isolation and biological properties of drosophila X virus. J Gen Virol *42*, 241–254.

[Thorne and Amrein, 2008] Thorne, N. and Amrein, H. (2008). Atypical expression of Drosophila gustatory receptor genes in sensory and central neurons. J Comp Neurol *506*, 548–568.

[Tomari and Zamore, 2005] Tomari, Y. and Zamore, P. D. (2005). Perspective: machines for RNAi. Genes Dev *19*, 517–529.

[Tsai et al., 2008] Tsai, C. W., McGraw, E. A., Ammar, E. D., Dietzgen, R. G. and Hogenhout, S. A. (2008). Drosophila melanogaster mounts a unique immune response to the Rhabdovirus sigma virus. Appl Environ Microbiol *74*, 3251–6.

[van Rij and Berezikov, 2009] van Rij, R. P. and Berezikov, E. (2009). Small RNAs and the control of transposons and viruses in Drosophila. Trends Microbiol *17*, 163–171.

[van Rij et al., 2006] van Rij, R. P., Saleh, M. C., Berry, B., Foo, C., Houk, A., Antoniewski, C. and Andino, R. (2006). The RNA silencing endonuclease Argonaute 2 mediates specific antiviral immunity in Drosophila melanogaster. Genes Dev *20*, 2985–95.

[Vassalli, 1992] Vassalli, P. (1992). The pathophysiology of tumor necrosis factors. Annu Rev Immunol *10*, 411–52.

[Venter and Schneemann, 2008] Venter, P. A. and Schneemann, A. (2008). Recent insights into the biology and biomedical applications of Flock House virus. Cell Mol Life Sci *65*, 2675–87.

[Wang et al., 2006] Wang, X. H., Aliyari, R., Li, W. X., Li, H. W., Kim, K., Carthew, R., Atkinson, P. and Ding, S. W. (2006). RNA interference directs innate immunity against viruses in adult Drosophila. Science *312*, 452–4.

[Wessells et al., 2004] Wessells, R. J., Fitzgerald, E., Cypser, J. R., Tatar, M. and Bodmer, R. (2004). Insulin regulation of heart function in aging fruit flies. Nat Genet *36*, 1275–1281.

[Wu et al., 2010a] Wu, Q., Luo, Y., Lu, R., Lau, N., Lai, E. C., Li, W. X. and Ding, S. W. (2010a). Virus discovery by deep sequencing and assembly of virus-derived small silencing RNAs. Proc Natl Acad Sci U S A *107*, 1606–11.

[Wu et al., 2010b] Wu, Q., Wang, X. and Ding, S. W. (2010b). Viral suppressors of RNA-based viral immunity: host targets. Cell Host Microbe *8*, 12–5.

[Xi et al., 2008] Xi, Z., Ramirez, J. L. and Dimopoulos, G. (2008). The Aedes aegypti toll pathway controls dengue virus infection. PLoS Pathog *4*, e1000098.

[Ye et al., 2011] Ye, J., Chen, S. and Maniatis, T. (2011). Cardiac glycosides are potent inhibitors of interferon-β gene expression. Nat Chem Biol *7*, 25–33.

[Yoon and Stay, 1995] Yoon, J. G. and Stay, B. (1995). Immunocytochemical localization of Diploptera punctata allatostatin-like peptide in Drosophila melanogaster. J Comp Neurol *363*, 475–88.

[Yu et al., 2006] Yu, F., Takahashi, T., Moriya, J., Kawaura, K., Yamakawa, J., Kusaka, K., Itoh, T., Morimoto, S., Yamaguchi, N. and Kanda, T. (2006). Traditional Chinese medicine and Kampo: a review from the distant past for the future. J Int Med Res *34*, 231–239.

[Zambon et al., 2005] Zambon, R. A., Nandakumar, M., Vakharia, V. N. and Wu, L. P. (2005). The Toll pathway is important for an antiviral response in Drosophila. Proc Natl Acad Sci U S A *102*, 7257–62.

[Zambon et al., 2006] Zambon, R. A., Vakharia, V. N. and Wu, L. P. (2006). RNAi is an antiviral immune response against a dsRNA virus in Drosophila melanogaster. Cell Microbiol *8*, 880–9.

[Zamore et al., 2000] Zamore, P. D., Tuschl, T., Sharp, P. A. and Bartel, D. P. (2000). RNAi: double-stranded RNA directs the ATP-dependent cleavage of mRNA at 21 to 23 nucleotide intervals. Cell *101*, 25–33.

List of Figures

List of Tables